Institut für Physik der Universität Potsdam

Linking Structure and Function of Complex Cortical Networks

Dissertation

zur Erlangung des akademischen Grades
"doctor rerum naturalium"
(Dr. rer. nat.)
in der Wissenschaftsdisziplin Nichtlineare Dynamik

Eingereicht an der
Mathematisch–Naturwissenschaftlichen Fakultät
der Universität Potsdam

von
Gorka Zamora-López

Potsdam, den 2. Oktober 2008

To Lucia Zemanová,
for opening our minds to the wonders of cortical networks.

Abstract

The recent discovery of an intricate and nontrivial interaction topology among the elements of a wide range of natural systems has altered the manner we understand complexity. For example, the axonal fibres transmitting electrical information between cortical regions form a network which is neither regular nor completely random. Their structure seems to follow functional principles to balance between segregation (functional specialisation) and integration. Cortical regions are clustered into modules specialised in processing different kinds of information, e.g. visual or auditory. However, in order to generate a global perception of the real world, the brain needs to integrate the distinct types of information. Where this integration happens, nobody knows. We have performed an extensive and detailed graph theoretical analysis of the cortico-cortical organisation in the brain of cats, trying to relate the individual and collective topological properties of the cortical areas to their function. We conclude that the cortex possesses a very rich communication structure, composed of a mixture of parallel and serial processing paths capable of accommodating dynamical processes with a wide variety of time scales. The communication paths between the sensory systems are not random, but largely mediated by a small set of areas. Far from acting as mere transmitters of information, these central areas are densely connected to each other, strongly indicating their functional role as integrators of the multisensory information.

In the quest of uncovering the structure-function relationship of cortical networks, the peculiarities of this network have led us to continuously reconsider the stablished graph measures. For example, a normalised formalism to identify the "functional roles" of vertices in networks with community structure is proposed. The tools developed for this purpose open the door to novel community detection techniques which may also characterise the overlap between modules. The concept of integration has been revisited and adapted to the necessities of the network under study. Additionally, analytical and numerical methods have been introduced to facilitate understanding of the complicated statistical interrelations between the distinct network measures. These methods are helpful to construct new significance tests which may help to discriminate the relevant properties of real networks from side-effects of the evolutionary-growth processes.

Zusammenfassung

Die jüngste Entdeckung einer komplexen und nicht-trivialen Interaktionstopologie zwischen den Elementen einer großen Anzahl natürlicher Systeme hat die Art und Weise verändert, wie wir Komplexität verstehen. So bilden zum Beispiel die Nervenfasern, welche Informationen zwischen Regionen des Kortex übermitteln, ein Netzwerk, das weder vollkommen regelmäßig noch völlig zufällig ist. Die Struktur dieser Netzwerke scheint Funktionsprinzipien zu folgen, die ein Gleichgewicht zwischen Segregation (funktionale Spezialisierung) und Integration (Verarbeitung von Informationen) halten. Die Regionen des Kortex sind in Module gegliedert, welche auf die Verarbeitung unterschiedlicher Arten von Informationen, wie beispielsweise Visuelle oder Auditive, spezialisiert sind. Um eine umfassende Vorstellung von der Realität zu erzeugen, muss das Gehirn verschiedene Informationsarten kombinieren (integrieren). Wo diese Integration jedoch geschieht, ist noch ungeklärt. In dieser Dissertation wurde eine weitreichende und detaillierte graphentheoretische Analyse der kortiko-kortikalen Organisation des Katzengehirns durchgeführt. Dabei wurde der Versuch unternommen, individuelle sowie kollektive topologische Eigenschaften der Kortexareale zu ihrer Funktion in Beziehung zu setzen. Aus der Untersuchung wird geschlussfolgert, dass der Kortex eine äußerst reichhaltige Kommunikationsstruktur aufweist, die aus einer Mischung von parallelen und seriellen übertragungsbahnen besteht, die es ermöglichen dynamische Prozesse auf vielen verschiedenen Zeitskalen zu tragen. Die Kommunikationsbahnen zwischen den sensorischen Systemen sind nicht zufällig verteilt, sondern verlaufen fast alle durch eine geringe Anzahl von Arealen. Diese zentralen Areale agieren nicht allein als übermittler von Informationen. Sie sind dicht untereinander verbunden, was auf ihre Funktion als Integrator hinweist.

Bei der Analyse der Struktur-Funktions-Beziehungen kortikaler Netzwerke wurden unter Berücksichtigung der Besonderheiten des untersuchten Netzwerkes die bisher verwandten Graphenmaße überdacht und zum Teil überarbeitet. So wurde beispielsweise ein normalisierter Formalismus vorgeschlagen, um die funktionalen Rollen der Knoten in Netzwerken mit einer Community-Struktur zu identifizieren. Die für diesen Zweck entwickelten Werkzeuge ermöglichen neue Methoden zur Erkennung dieser Strukturen, die möglicherweise auch die überlappung von Modulen beschreiben. Das Konzept der Integration wurde revidiert und den Bedürfnissen des untersuchten Netzwerkes angepasst. Außerdem wurden analytische und numerische Methoden eingeführt, um das Verständnis des komplizierten statistischen Zusammenhangs zwischen den verschiedenen Netzwerkmaßen zu erleichtern. Diese Methoden sind hilfreich für die Konstruktion neuer Signifikanztests, die relevante Eigenschaften realer Netzwerke von Nebeneffekten ihrer evolutionären Wachstumsprozesse unterscheiden können.

List of Publications

This dissertation is partially based on the following publications:

Papers

I G. Zamora-López, V. Zlatić, C. S. Zhou, H. Štefančić and J. Kurths, *Reciprocity of networks with degree correlations and arbitrary degree distribution.* Phys. Rev. E **77**, 016106 (2008).

II G. Zamora-López, C. S. Zhou, V. Zlatić and J. Kurths, *The generation of random directed networks with prescribed 1-node and 2-node degree correlations.* J. Phys. A **41**, 224006 (2008).

III C. S. Zhou, L. Zemanová, G. Zamora, C.-C. Hilgetag, J. Kurths, *Hierarchical organization unveiled by functional connectivity in complex brain networks.* Phys. Rev. Lett. **97**, 238103 (2006).

IV C. S. Zhou, L. Zemanová, G. Zamora-López, C.-C. Hilgetag, J. Kurths, *Structure-function relationship in complex brain networks expressed by hierarchical synchronization.* New J. Phys. **9**, 178 (2007).

V G. Schmidt, G. Zamora-López et al., *Simulation of large scale cortical networks by use of individual neuron dynamics.* Submitted to Int. J. Bif. Chaos.

Book Chapters

1. G. Zamora-López, C. S. Zhou and J. Kurths, *Structural characterisation of networks.* In "Lectures in Supercomputational Neuroscience: Dynamics in Complex Brain Networks." Edited by P. beim Graben, C. S. Zhou, M. Thiel and J. Kurths. Springer, Berlin (2008) Series: Understanding Complex Systems. ISBN: 978-3-540-73158-0.

2. M. Barbosa et al. *Parallel computation of large neuronal networks with structured connectivity.* In "Lectures in Supercomputational Neuroscience: Dynamics in Complex Brain Networks." Edited by P. beim Graben, C.S. Zhou, M. Thiel and J. Kurths. Springer, Berlin (2008) Series: Understanding Complex Systems. ISBN: 978-3-540-73158-0.

3. R. Steuer and G. Zamora-López, *Global properties of networks.* In "Analysis of Biological Networks." Edited by B. H. Junker and F. Schreiber. Wiley series on Bioniformatics, Computational Techniques and Engineering. ISBN: 978-0-470-04144-4.

Contents

Preface

The irruption of complex networks in the natural sciences has altered the manner we understand complexity. Traditionally, a system has been classified as *complex* when it comprised of many elements (degrees of freedom) which interact in a nonlinear fashion. The recent discovery of an intricate and nontrivial interaction topology among the elements in a wide range of natural systems introduces a new dimension in the spectrum of complexity.

Graph theory, as a branch of combinatorial mathematics, is a discipline with a long tradition. Its origins go back to the 18th century when the swiss mathematician Leonhard Euler introduced the very first theorem of graph theory in order to solve the problem of "the 7 bridges of Königsberg", which consisted in finding a round trip that traversed each of the bridges of the prussian city of Königsberg exactly once. Graph theory has typically dwelled with combinatorial problems such as the graph colouring problem, e.g., what is the minimum number of colours needed to paint a political map such that no neighbouring country has the same colour. The analysis of random graphs has been especially productive, giving rise to analytical formulae for the expectation values of graph measures, easy to compare with real data for significance testing.

From the practical point of view, graph theory has largely benefited from several applications, but it is worth giving a special mention to the social sciences. Acquaintance networks such as friendships or professional collaboration have interested sociologists for almost a century. Indeed, many of the nowadays popular graph measures such as the clustering coefficient and the centralities, are direct inheritance from the social network analysis [147]. Furthermore, most of our current knowledge about significance testing and random networks with a given degree distribution arises from the social network analysis [69, 76, 81, 123]. Despite its traditional roots, it was not until the decade of the 1990s that applications of graph theory became popular and invaded almost every field of the natural sciences. This outbreak was, no question, facilitated by the advances in computer power, when systematic analysis of large networks from different disciplines became possible and several common mechanisms and properties were discovered.

In autumn of 2004 I joined the group of Prof. Jürgen Kurths with the intention of applying the complete toolbox of graph theory to the cortico-cortical connectivity network of the cat. Looking back in time, I could hardly imagine those days that this small network would become the *source* of my work rather than its *target*. Because, if I have to summarise the thesis you are about to read in few words, this is a story of a bidirectional interaction and mutually feeding motivation. On the one hand, I believe that graph theoretical tools did help gaining insights in the organisation of the mammalian cortex and its functionality. On the other hand, the peculiarities of this network continuously

challenged the existing literature, forcing me to reconsider established concepts and to reformulate several measures. The majority of works published during the "early years" of complex network research $(1998 - 2004)$, although extremely relevant, committed several common "excesses", sometimes due to analytical simplicity, often just by the inertia generated by previous works. First, the directionality of the connections present in most real systems was often deliberately ignored and the networks would be *symmetrised* by adding the necessary links. Second, the analysis typically restricted to few global statistics, for example, the degree distribution. However, global averages and the degree distribution provide only limited information of the rich internal structure of a network. And third, due to analytical simplicity, the majority of network models presented focused in the thermodynamical limit, say, large and sparsely connected networks.

The goal of my work was to study the different scales of organisation in the mammalian cortex and try to relate the individual and collective topological characteristics of cortical areas to their functionality. From the biological point of view, we might have uncovered the structural organisation substrate (at the level of the cortex) which permits the integration of the multisensory information towards a comprehensive and unified understanding of the environment. Few cortical areas, which are spatially distant from each other, are found to be hubs of the network. Furthermore, these hubs are found to be very densely connected among them forming a *spatially segregated cluster* of areas where multisensory information is integrated. Technically, we have contributed to the significance testing in real complex networks by the introduction of analytical and numerical methods for the computation of expectation values. We have focused in a null model of *maximally random networks* conditional on the degree distributions *and* the degree-degree correlations. Additionally, we have extended a framework to "predict" *functional properties* of individual nodes (and subsets of nodes) from their topological properties. Therefore, necessary conditions for the *capacity of integration* are introduced at both the structural and at the dynamical levels.

The first two chapters are dedicated to introduce the formalism and basic concepts of graph theory, and to briefly explain our contribution to the significance testing of network measures. Our main results in these topics have been published in the papers I and II in detail. Here, summarised explanations will be provided. The rest of the dissertation comprises of unpublished material. Chapter 3 is dedicated to review the established knowledge of large-scale brain connectivity prior to our work. The global classification of cortical networks is also re-analysed towards a more comprehensive understanding of their overall organisation. A detailed and extensive graph theoretical analysis of the cortical network of the cat is presented in Chapter 4. The results of different centrality measures are compared, and a novel formalism to characterise the functional roles of vertices is introduced. While the details of the formalism are left for the Appendix A, its application permits to uncover the hierarchical organisation of the cortical network of the cat. The final chapter is dedicated to our tentative efforts to link the observed structural organisation to its potential function. The concept of *capacity of integration* is introduced in both topological and dynamical terms. The results of this preliminary formulation of integration support the conclusions of Chapter 4, which have been derived from topological observations and justified with neuroscientific facts. Finally, in Chapter 6 the main results of the thesis are summarised and extended in the context of our additional observations published in papers III, IV and V.

CHAPTER 1:

Characterisation of Complex Networks

Complex dynamical systems are characterized by a large number of nonlinearly interacting elements, giving rise to emergent properties that transcend the principle of linear superposition. Classically, science has broken up nature into independent abstract pieces (systems) susceptible of being separately studied, and seeked for holistic solutions by "summing up" the understanding of individual fragments. Even for systems composed of many elements, provided that linear interactions dominate, statistical methods allow their description by means of macroscopic properties. But, what if a system cannot be divided into independent subsystems? Or what if the overall behavior cannot be described in terms of the individual behaviour of its components? Despite its tremendous contribution to science, the principle of linear superposition fails to capture the emergent collective behaviour of many real systems such as synchronisation phenomena [104, 133], the spontaneous formation of human collectives [55, 56, 106], the spontaneous outbreak of epidemies [18, 132] and etc., including examples of nuclear physics, neural organisation and information processing.

In the recent years, yet another ingredient causing the emergence of complex behaviour in nature has received an exceptional attention: *the intricate pattern of interactions among the elements of a system.* But, what makes networks so interesting? Recall that one of the principal enigmas in biology, and the central issue of physiology, is the intrinsic relationship between the physical geometry of biological structures and their function. The relationship between form and function transcends the borders of biology, it extends into science as some philosophical obscure concept which, sometimes unconsciously, plays a relevant role in our quest to understand nature. A network is an abstract manner of representing aspects of a system, so general and flexible that it can be applied to a broad range of real systems. A network representation provides the system with a form (topology) which can be mathematically tractable towards uncovering its functional organisation and the underlying design principles. Indeed, as realised rather recently, many empirically derived complex networks, ranging from technological and sociological to biological examples, share common topological features. The organising principles of empirical networks often reflect crucial system properties, such as robustness, redundancy, or other functional interdependencies between network elements.

Often, the network arises from some trivial physical property. In a map, cities are linked by roads; neurones connect to each other through axons and synapses; the internet is formed by computers and servers connected by cables. Sometimes, networks are con-

3

structed over more abstract interactions, for example the social relationships: friendship, profesional collaboration, sexual contacts, etc.; in ecological food webs the species are linked depending on their trophic relations in a given ecosystem; the World Wide Web is composed by web pages linked by hyperlinks pointing from one web page to another. Yet, more abstract concepts are also plausible for being translated into networks, e.g. protein interaction networks where the proteins in a cell or an organism are assumed to be linked if they participate in the same chemical reaction, or the folding states of a protein; different states are considered to be linked if they are accessible by a direct transition without the need to undergo through an intermediate state.

The reason the term *complex* was coined to name all these examples is that most real systems have neither a regular nor a completely random topology, they survive in some intermediary state, probably governed by underlying rules of self-organisation. The aim of current complex network research is to uncover the relationship between function and structure, however, there is no realistic manner to talk about function of a network in a generic and global manner. We shall never forget that *function* is something inherent to the system itself and, a network, simply is an abstract representation of that system. The emerging structure of a system depends uniquely on the individual necessities of that particular real system. For example, transportation networks such as the railroad, the electrical power-grid and the blood-vessels of an animal are physical constructions for supporting the transit of trains, electricity and blood. Their dominating function is supporting effective internal flows. Very different is the aim of, say, social networks or the World Wide Web.

In the following sections of this chapter, typical measures of graph characterization are introduced, which form the elementary toolbox of the graph analysis. They have been classified as *local, mesoscopic* and *global*, depending on the range of information necessary to derive them.

1.1. Graph Representation and Local Measures

In the classical nomenclature of graph theory, a network is represented as a graph $G = (V, E)$ consisting of a set V of N_V vertices and a set E of N_E edges. We distinguish between undirected graphs, whose vertices are connected by edges without any directional information and directed graphs (digraphs), whose edges, in this case named arcs, possess directional information. Additionally, the edges might be associated with a scalar value quantifying a possible interaction strength, a cost, or a flow capacity giving rise to weighted graphs. Self-loops are edges connecting a node to itself.

Due to the multiple and interdisciplinary applications of graph theory, the nomenclature has become confusing. To keep consistency with the already published papers I and II, we will refer to the size of the network (number of vertices) as N and the number of links as L. A network is mathematically represented by an adjacency matrix $\mathbf{A}$, with entries $A_{ij} = 1$ when there is a link from vertex i to vertex j, and $A_{ij} = 0$ otherwise. For undirected networks, the adjacency matrix is symmetric $A_{ij} = A_{ji}$, and for weighted networks, the elements A_{ij} are replaced by non-binary scalar values W_{ij}. The adjacency matrix can sometimes become computationaly inefficient, particularly in the case of sparse networks, i.e. networks where the number of edges is much smaller than the number of

possible links, $L \ll N^2$. Alternatively, the network can be specified by a set of **adjacency lists**, consisting of N lists enumerating the direct neighbours of each vertex.

The presence of directed links modifies the graph measures. For example, the maximum number of edges in a digraph is $L_{max} = N(N-1)$ (if no self-loops are considered the N diagonal entries are ignored) while a graph can have only up to $\frac{1}{2}N(N-1)$ edges. The **density** of a network, $\rho(G)$, is the fraction between its number of links L and the maximum possible number of links, L_{max}. In a graph, the **degree** of a vertex v is the number of its first neighbours $k(v) = \sum_{j=1}^{N} A_{vj}$. In digraphs the number of connections entering to, and leaving from v are not necessarily equal. The **output degree** is the number vertices leaving from v and is computed as the row sum of the adjacency matrix $k_o(v) = \sum_{j=1}^{N} A_{vj}$. The **input degree** is the number of links received by v and equals the column sum $k_i(v) = \sum_{j=1}^{N} A_{jv}$. In the context of weighted graphs, the natural extension of the degree is the **vertex intensity**, defined as $S(v) = \sum_{j=1}^{N} W_{vj}$, where $\mathbf{W}$ is the weighted adjacency matrix.

1.1.1. Degree distribution

A first statistical information that can be computed from a network is its **degree distribution**, i.e. the probability $p(k)$ that a randomly chosen node has a given degree k. One of the key discoveries that triggered a renewed interest in complex network theory was that the distribution $p(k)$ of many empirical networks approximately follows a power-law $p(k) \sim k^{-\gamma}$ [95], where γ is the **degree exponent**. The relevance of this discovery is twofold. On the one hand, it largely contrasts the until then prevailing picture that real networks undergo a purely random process of formation and, as a consequence, all nodes have a similar degree. However, many empirical networks are largely inhomogeneous: while the vast majority of vertices only possess a small number of neighbours, a small number of vertices (the **hubs**) are highly connected. On the other hand, power-laws play a special role in statistical physics where phase transitions between ordered and random states are typically characterised by power-law distributions. At the transition point, the system has self-similar (scale-free) properties, i.e. the system looks qualitatively the same at all scales.

Though one of the most basic characteristics of network architecture, a statistically stringent numerical estimation of the degree distribution is far from trivial [54]. In the simplest case $p(k)$ can be straightforwardly estimated from a (usually binned) histogram of degrees. However, for many real networks with strongly inhomogeneous degree distributions, the simple histogram approach provides insufficient statistics at high degree vertices and is a notorious source of misinterpretations [54]. More reliable in terms of numerical estimation is the **cumulative degree distribution**, $p_c(k)$, defined as the probability that a randomly chosen vertex has a degree larger than k. The distribution $p_c(k)$ is a monotonously decreasing function of k and its estimation requires no binning. For a power-law distribution $p(k) \sim k^{-\gamma}$, the cumulative degree distribution is of the form $p_c(k) \sim k^{-(\gamma-1)}$. An exponential distribution $p(k) \sim e^{(-k)}$ corresponds to an invariant cumulative distribution $p_c(k) \sim e^{(-k)}$.

It should be noted that all empirical networks necessarily show deviations from a strict mathematical scale-free degree distribution and the formula $p \sim k^{-\gamma}$ often only applies to an intermediate region of the empirical degree distribution and has to be adjusted with an

exponential cut-off at high degrees. Reality imposes many restrictions to the capacity of networks to become fully scale-free even if self-organisation processes are the underlying construction motors, as nicely stated in [70]:

> ...the examples of social networks with a good fit to a power-law must probably have an upper cut-off of the degree distribution if the network was extended to the whole population of the Earth: If the network of sexual contacts (a year back in time) had a $p(k) \sim k^{-3.5}$ as reported in ref. [85] then, assuming $N = 6.4 \times 10^9$ the most active person would have around $N^{1/2.5}(year)^{-1} \approx 23$ new sexual contacts per day [28]. If the number of phone-calls per person and day is distributed as $p(k) \sim k^{-2.1}$ as reported in ref. [2] the person calling most would dial $\sim 5 \times 10^5$ phone-calls a second, 24 hours a day (...) In the spirit of keeping a model simple one does not need to make it realistic in every detail.

Although every system may have its particular restrictions, two general phenomena have been proposed for the emergence of cut-offs [5]: the *limited capacity* of a vertex to make connections and their *aging* [5, 82]. After some time the vertices stop playing an active role and stop making new connections. For example, the actor-collaboration network is constructed by linking any two actors who have ever co-worked in one film. As actors retire at some time of their lives, they receive no more links but they are still part of the network.

More intriguingly is the effect of the network size itself on the distribution. As shown in the recent literature, the reported degree exponent of many empirical networks correlates with network size and thus might not reflect the actual exponent of the underlying networks [24, 37, 38]. Nevertheless, for most of the real problems, it is more important to know that the degree distribution is highly inhomogeneous and broad (sometimes informally referred as *fat-tailed*), as opposed to the question whether it fits a power-law in a strict statistical sense or not.

1.1.2. Degree correlations and reciprocity in digraphs

Despite its statistical and historical importance, the degree distribution provides only little information about the internal structure and organisation of the network. The analytical toolbox of graph theory contains numerous measures which cover different scales of the topology, from very local vertex measures to measures depending on the structure of the whole network. Among them, there are several local correlation quantities.

When a network is composed of directed interactions, the input and the output degrees of a vertex are not necessarily equal; moreover, the statistical distributions of the k_i and of k_o may be different. This imposes very relevant consequences for the expectation of the measured quantities and is the central issue of our papers I and II. A thorough discussion is left for Chapter 2. For the moment, lets only mention that the 1-node degree correlation between the input degree k_i and the output degree k_o of individual vertices is an indicator for potential functionality. A vertex with $k_i \gg k_o$ might be considered as some sort of *integrator* which is accumulating information and putting it together, while another vertex with $k_i \ll k_o$ might be some sort of *distributor*, passing copies of the same information to many other vertices. At this point it is necessary to pay attention to the reciprocal links, i.e. a link $v \to v'$ for which the counterpart $v \leftarrow v'$ exists. Therefore, the complete degree

characterisation consists of a **degree vector** $\mathbf{k}(v) = (k_o(v), k_i(v), k_r(v))$ where k_r denotes the **reciprocal degree**, or equivalently, $\widetilde{\mathbf{k}}(v) = (k^+(v), k^-(v), k_r(v))$, where $k^+ = k_o - k_r$ and $k^- = k_i - k_r$ are the **excess degrees**.

It is also interesting to look for correlations between the degrees of adjacent vertices. The **2-node degree correlation** is formally expressed by the joint probability $P(k, k')$ that the two vertices at the ends of a randomly chosen link have degrees k and k' respectively. In the case of digraphs, the 2-node degree correlations become splitted into different subclasses. Often, a crude measure of the degree-degree correlations in terms of the probability $p(k, k')$ is not suitable because of poor statistics at the high degrees. Alternatively, the **average nearest-neighbour's degree**, $\langle k_{nn}(k) \rangle$, has been proposed [102]. For each vertex v of degree k' the average degree of its neighbours is computed, $k_{nn,v}$, and then the k_{nn} of all vertices with same k' is averaged. A network is called *assortative* if nodes of similar degree preferentially connect to each other ($\langle k_{nn}(k) \rangle$ is thus an increasing function of k), and *disassortative* if high degree vertices preferentially connect to low degree vertices ($\langle k_{nn}(k) \rangle$ is a decreasing function of k). As pointed out in [95], social networks tend to be assortative while technological and biological networks are disassortative.

In papers I and II we have demonstrated that there exist a very close statistical relationship between the 1-node, the 2-node degree correlations and the reciprocity. Our work is a first step towards understanding the statistical inter-dependencies between graph measures, which is still a poorly studied question but a key point for the identification of the relevant properties governing the organisation principles of real networks. Chapter 2 is dedicated to review this problem and to summarise our related work.

1.2. Mesoscopic Graph Measures

While local graph measures include the properties of individual nodes and the relationship with their neighbours, global properties take into account the structural features of the whole network. However, there exists a large gap between the local and the global organisation levels. These intermediate scales ranging from few nodes to large communities are the most interesting and relevant features of the topology, but they are often difficult to define and quantify.

1.2.1. Matching Index

The **matching index** estimates the topological similarity between two vertices by quantifying the overlap of their neighbourhood spaces. The **neighbourhood** of a vertex v is defined as the set of its direct neighbours, $\Gamma(v) = \{j : A_{vj} = 1\}$. Note that in graphs without multiple links, the size of the neighbourhood, $|\Gamma(v)|$, equals the degree of v. Thus, the matching index of two vertices v and v' is the number of common neighbours that they have: $MI(v, v') = |\Gamma(v) \cap \Gamma(v')|$. Defined in this manner $MI(v, v')$ depends on the degrees of v and v', so a normalisation is desired. By counting the total number of distinct vertices to which v and v' connect, $|\Gamma(v) \cup \Gamma(v')| = k(v) + k(v') - |\Gamma(v) \cap \Gamma(v')|$, the matching index can be re-defined as:

$$MI(v, v') = \frac{|\Gamma(v) \cap \Gamma(v')|}{|\Gamma(v) \cup \Gamma(v')|} = \frac{\sum_{i,j=1}^{N} A_{vi} A_{v'j}}{k(v) + k(v') - \sum_{i,j=1}^{N} A_{vi} A_{v'j}} \tag{1.1}$$
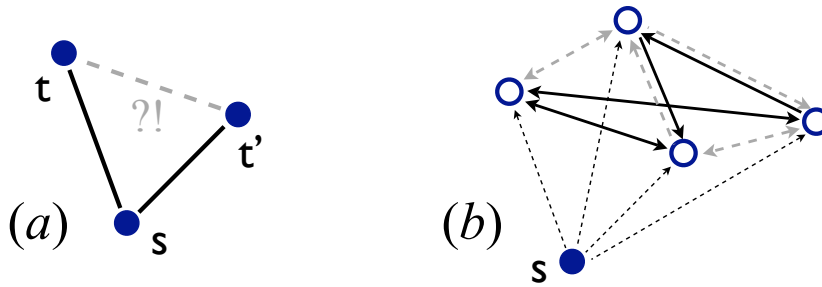
Figure 1.1: Illustration of clustering coefficient. (a) Clustering quantifies the conditional probability of two vertices to be connected provided they share a common neighbour. (b) Local $C(s)$ measure as used in directed networks: the fraction of existing connections between neighbours of s to all the possible connections between them.

Now, $MI(v, v') = 1$ if all neighbours of v and v' are the same, $\Gamma(v) = \Gamma(v')$, and $MI(v, v') = 0$ if they have no common neighbours at all. In the case of *digraphs* the matching may be computed taking into account only the output neighbours $\Gamma^+(v)$, only the input neighbours $\Gamma^-(v)$ or both, depending on the kind of information we are interested in. Additionally, pairwise matching index can be represented into a matrix for further statistical analysis.

1.2.2. Clustering coefficient

There is a well known aspect of social behaviour, as stated in the following dictum: *"The friends of my friends, are also my friends."* Persons are more likely to become acquainted when they have at least one common friend. People use to meet each other by attending the same social events, which happens more likely if they have common friends. Thus, the clustering coefficient, C, of a network is formally defined as the overall conditional probability that any two vertices, chosen at random, to be connected provided they share a common neighbour. Most of the real networks possess a large clustering, despite the fact that they are often very sparsely connected.

Given a graph, the most popular way of measuring C is by counting the number of triangles within the network, $N(\triangledown)$,

$$C = 3 \times \frac{N(\triangledown)}{N(\vee)} \tag{1.2}$$

where $N(\vee)$ is the number of paths of length 2, i.e. the number of times that two distinct vertices t and t' have a common neighbour. The weight 3 is introduced only to account for the fact that, within a single triangle, there exist 3 paths of length 2. In digraphs, however, it is not clear how to define a triangle due to the directions of the links. Alternatively, the local clustering coefficient, $C(v)$, is defined as the local density of links among the neighbours of v. If v has out-degree k_o, then there is a maximum of $L_{max} = k_o(k_o - 1)$ directed links between its k_o neighbours (self-loops are discarded). The actual number of links between the out-neighbours of v, $L(\Gamma^+(v))$, can be computed in terms of the
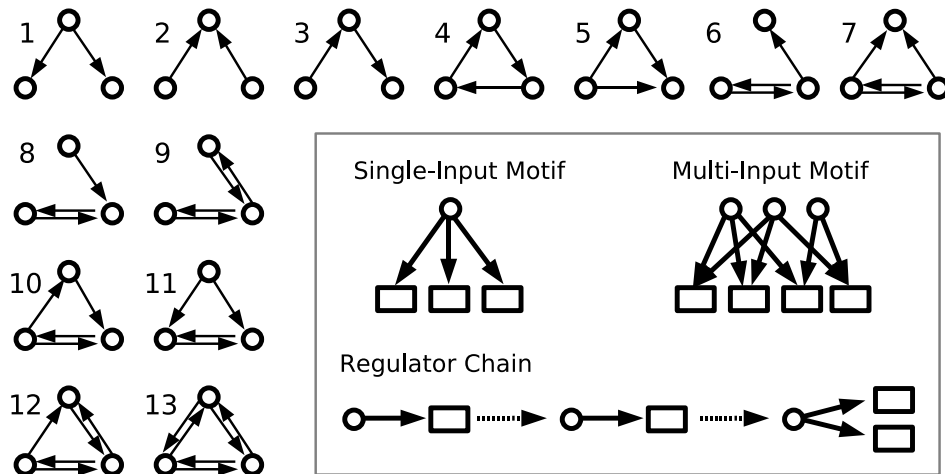
Figure 1.2: All 13 possible three-vertex motifs, according to [90, 120]. *Inset:* The concept of motifs can be generalized to account for specific repeated subgraphs within a complex network. Shown are possible motifs of the yeast transcription regulatory network, with circles denoting regulators and rectangles denoting gene promoters, according to [84].

adjacency matrix:

$$C(v) = \frac{L(\Gamma^+(v))}{L_{max}} = \frac{\sum_{i,j}^{N} A_{vi} A_{vj}(A_{ij} + A_{ji})}{k_o \, (k_o - 1)}. \tag{1.3}$$

Note that the local clustering coefficient can be alternatively computed for the in-neighbourhood of v, or, for its **complete neighbourhood** by considering all neighbours of v whether they are in- or out-neighbours, $\Gamma(v) = \Gamma^+(v) \cup \Gamma^-(v)$. In Chapter 4 we choose the latter option to avoid problems of data limitations in the cortical networks. Then, C is calculated as the average of the local clustering of all the vertices. It is important to stress that, as pointed out in [95], the average of the local clustering is not exactly a measure of the conditional probability defined above because it tends to overestimate the contribution of low-degree vertices due to smaller denominator.

1.2.3. Subgraphs and motifs

Providing a bridge between local, vertex-related, properties and global functional properties of networks, the basic idea behind motif analysis is that large complex networks may be composed of small subgraphs [75, 84, 90, 120]. In Figure 1.2 all the possible subgraphs (motifs) of size 3 are depicted. Some motifs are considered to play a certain specific function, e.g. the subgraph number 4 clearly is a feedback-loop. In general, the concept of motifs is not restricted to subgraphs with a fixed number of vertices. Rather, it allows to look for any re-occuring patterns, including more complicated topological structures, such as multi-input motifs, regulator chains, or dense overlapping regulons (DORs) [84, 120]. Motif analysis has received much attention under the belief that, from the specific motifs present in a network one could "uncover" its functional building blocks. However, there are several issues indicating that a careful interpretation is required. First, we might

recall that *function* is a property inherent to the real system itself, not to its network representation. Therefore, the functional role of the motifs needs to be properly interpreted in terms of the functional purposes (if any) of the underlying real system, not in terms of its graph representation. Second, after the work by Milo and collaborators [90], it is typical to compare the motif counts in real networks to the counts in randomised networks with the original degrees preserved. Although this is a very respectable null-model (see further discussion in Chapter 2), interpretation pitfalls are still possible. For example, in a comment [12] submitted to [90], the authors demonstrated that taking into account the spatial restrictions of the neural system of the *C. Elegans* mnematode, the motifs previously thought to be relevant became statistically insignificant.

1.2.4. Community and hierarchical structure

One of the most relevant organisation properties of networks (and one of its most challenging features to characterise) is the agglomeration of vertices into *modules* or *communities* and their hierarchical interrelationships. There is no generally accepted definition of what constitutes a module. As a working definition, modules are understood as subsets of vertices which are densely connected among each other, but only sparsely connected to other vertices outside the community. In these terms, the problem of community detection consists in identifying the densely connected subgraphs, i.e. to find a partition such that the number of internal links within the modules is maximised and the number of inter-module links is minimised.

In the recent years a myriad of methods have been proposed based on local and global topological properties (many of them have been compared in [31]), as well as based on dynamical properties [8, 23][1]. The question now is, once a method has separated the vertices into a partition of n modules, *how good* is that partition? how can the results from different methods be compared? For that, Newman and Girvan proposed a cost function, called the **modularity** [96], which evaluates how successful the maximisation / minimisation process has been as compared to the expected result in a random network with the same degree distribution. The modularity is formally defined as:

$$Q = \sum_{s=1}^{n} \left[\frac{L_s}{L} - \left(\frac{d_s}{2L} \right)^2 \right] \tag{1.4}$$

where L_s is the number of links inside the module S, and d_s is the sum of the degrees of the vertices in S. Thus, the left term is the density of links of module s, and the right term is the expected link density of S in the case of a random network of the same size and degree distribution.

A key question related to the community structure is that, often, the modules overlap each other [99] and transcend different scales of organisation. Recent advances suggest an optimistic future in this direction [9, 48, 114]. Critical questions are still to be answered, for example, there is still no common agreement on how to define a hierarchy. For the moment, two classes of hierarchies are present in the literature. In the model proposed by

---

[1]However, a recent study [62, 63] demonstrates that standard ways of clustering data, for example, based on k-means or hierarchical clustering, often outperform newer methods.
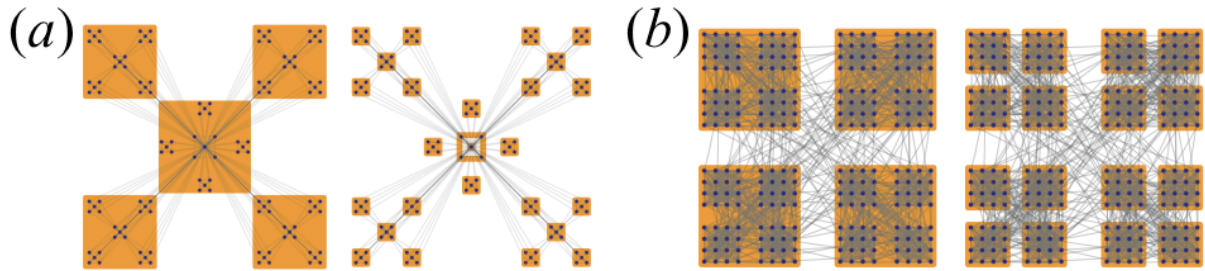
Figure 1.3: Hierarchical structure of complex networks. (a) Centralised hierarchy. (b) Hierarchies as agglomeration of modules. Figures reprinted with permission from Arenas et al. [10].

Ravasz and coauthors [105] (Figure 1.3(a)) modules are organised in a tree-like structure. In a different approach by Arenas *et al.* (Figure 1.3(b)), a group of communities agglomerate together to form larger communities, what is regarded as a higher order in the hierarchy [8]. In this dissertation, we will present yet another class of hierarchy, observed in the organisation of the mammalian brain, which might be regarded as a mixture of both definitions. Besides, the novel graph theoretical tools proposed in the Appendix A are useful to characterise and classify different types of hierarchies.

1.3. Global Graph Measures

In this section few graph measures are presented which make use of the global topology of a network. Even if some of these measures are assigned to individual vertices, their derivation requires taking into account the topology of the whole network. Towards deducing funtional roles of vertices, some of these measures permit a first classification of individual vertices in terms of their global importance.

1.3.1. Distance and closeness centrality

The topological distance, d_{st}, between two vertices s and t is the length of the shortest path between them, i.e. the minimal number of edges crossed to travel from s to t. If there is a direct link $s \rightarrow t$, then $d_{st} = 1$. If there is no shorter path than going from s to some other node t' and from here to t, then $d_{st} = 2$, and so on. Note that, in digraphs, the distance is usually not symmetric $d_{st} \neq d_{ts}$. The shortest path between two vertices is usually not unique, often there are several alternative "parallel" shortest paths. This path multiplicity is very relevant for the flow dynamics and information redundancy in networks. When there exist no possible path from s to t then $d_{st} = \infty$, so s and t are disconnected. Sometimes, a graph is broken into several sets of vertices, called connected components, which are internally connected but no path exist between the sets.

The average or characteristic pathlength, l, is the average distance between all pairs of vertices. Real networks, even if they can be very large, typically have a very short average pathlength, what is known as the small-world property. As l depends on both the size N and the density of links, a network is said to be small-world when $l \leq \log(N)$.

When weighted links are present, the concept of distance can be adapted. For example,

within a network of train connections, the shortest path (distance) between two stations can be defined according to the physical distance between them, or, by taking travel time into account. Often, it happens that travelling between two cities following a longer path is faster because of several factors, e.g. faster trains, less stops, etc. Indeed, web-based travel organisers tend to provide search results which minimise time travel. Other search options are usually offered, for example, a search based on cheaper connections, or based on the minimum number of times that the traveller needs to change to a new train.

Once the distance between all pairs has been calculated, a classification of vertices is possible in terms of their average distance to the rest of the network, known as the closeness centrality:

$$C_c(v) = \frac{1}{N-1} \sum_{i=1, i \neq v}^{N} d_{vi} \tag{1.5}$$

Again, in directed networks closeness centrality is splitted into the output centrality measuring how fast the network can be searched starting from v, and the input centrality quantifying how fast can be v accessed.

1.3.2. Betweenness centrality

In order to characterise the influence of a vertex on the flow and the spread of information through a network, the betweenness centrality, $BC(v)$ [6, 49], measures the number of shortest paths going through v. An exact quantification requires to find *all* possible shortest paths in the network, what is often computationally impracticable and approximative methods are required [14, 26]. There are different manners of normalising the betweenness centrality. For example:

$$BC(v) = \frac{\sum_{i,j \neq v}^{N} \sigma_{ij}(v)}{\sum_{i,j=1}^{N} \sigma_{ij}} \tag{1.6}$$

where $\sigma_{ij}(v)$ are all shortest paths starting from i, going through v and finishing in j. The condition $i, j \neq s$ avoids counting paths starting from or finishing into v. The denominator, σ_{ij}, is the total number of shortest paths in the network.

Equivalently, the centrality of links can be characterised as the fraction of all shortest paths going through a given link $v \to v'$. Notice that BC is only an approximate measure of flow centrality because it assumes that all information travels uniquely through shortest paths, which is not necessarily true.

Typically, both the vertex degree, the closeness and the betweenness centralities are considered as the basic centrality measures. They are all useful to classify vertices in terms of their relevance, but they provide different kind of information. First of all, $k(v)$ is based in local information while the $C_c(v)$ and $BC(v)$ make use of global information to classify the vertex. Second, although they tend to be correlated they are not necessarily equivalent, e.g. a large degree is no warranty for large $C_c(v)$ or $BC(v)$.

1.4. Summary

The recent discovery of a complex pattern of interactions between the elements of many real systems, has shifted the attention of scientists into the study of the relationship between form and function. However, there is no unique observable that would completely determine the structure of a network. The graph theoretical toolbox comprises of many different measures, each providing information about specific details of the topological organisation. Understanding the precise structure of one network is similar to building a puzzle, whose pieces are the outcome of the different graph measures. In this chapter the basic measures have been reviewed and summarised. All of them will be used in the following chapters to characterise the connectional organisation of the mammalian brain. According to the topological scale of information required to compute them, the graph measures have been presented as *local, mesoscopic,* or *global*.

CHAPTER 2:

Network Models, Null-models and Significance Testing

The word 'model' is almost omnipresent in natural and social sciences, however, it is also a major source of misunderstanding between theoretical and applied scientists. Back in my times as an undergraduate student, a professor would tell us: *"Physics is the art of making approximations. The work of a theoretical physicist consists in trying to get rid of the overwhelming complexity of nature by uncovering only the few, most relevant, parameters and variables."* In the eyes of a theoretical scientist, a model is an abstract construction (mathematical, computational, etc.) which aims to explain natural phenomena by capturing the main principles behind them. The source of a model is not necessarily data, very often qualitative observations are all to start with[1]. Such a model is considered valid only if, appart from explaining known phenomena, it also has the power to make *predictions* which can be corroborated *later* by experimental observations[2].

On the contrary, an applied scientist needs to deal with data and find generalised manners to fit it into some analytical model. For an experimentalist a model is typically a mathematical formula which fits a set of data and predicts the outcome of similar experiments in the future. Obviously, experimentalists also want to uncover the main principles governing the natural phenoma, and in order to extract the most relevant observables from the data *statistical (or significance) testing* is used.

No question, graph theory is a data analysis toolkit, and as such, the experimentalist approach is necessary. This doesn't mean that there is no benefit from the minimalistic and intuitive approaches of the theoretical approach to modeling. Unfortunately, due to the interdisciplinary nature of the field of complex networks, there is some confusion. Sometimes null-models are treated as models, and models presented as null-models. In my opinion, part of this problem arises from the fact that we still have a poor understanding of the complicated statistical interdependencies between the different graph measures, so understanding which are the true *driving forces* in the development, growth and evolution of a given real network is difficult. Modelling in the theoretical sense still requires excessive *guessing*, and there is a considerable danger of misinterpreting non-relevant variables as

---

[1]We shall remind here that Newton and Einstein derived their gravitational models based mainly in qualitative observations.

[2]Such is the case with Einstein's theory of general relativity. From its equations tens of predictions were derived which have been corroborated only *a posteriori*, as the technology for experimental observations advanced and permitted to test the validity of those predictions.

fundamental, and the other way around.

This chapter is dedicated to summarise our efforts to bring some order to this confusion and to present the tools we have proposed to continue working in this direction. In Sections 2.1 and 2.2, a brief historical review of popular network models and null-models is presented, and in Sections 2.3 and 2.4, our papers I and II are summarised.

2.1. Prototypical Graph Models

In order to understand and elucidate whether an estimated value corresponds to nontrivial structure requires to consider basic prototype models of complex networks. None of the models described below aims to mimic the detailed features of any real network. Rather they represent minimal models, each invented to exhibit distinct generic features observed in empirical networks.

2.1.1. Random Graphs

The random graph is probably the most studied network model ever. Introduced by Solomonoff and Rapoport [124], it consists of an initially *empty network* of N unconnected nodes, whose pairs of vertices receive an edge between them with probability p. Erdős and Rényi later proposed an equivalent model where L edges are introduced one-by-one at random [43]. In both models the probability of having a link between two randomly chosen vertices equals the density of links: $p = \rho = \frac{2L}{N(N-1)}$.

The properties of a random graph largely depend on the parameter p. Its degree distribution follows a *binomial distribution*, approximating a *poissonian* in the thermodynamical limit ($N \to \infty$ and $p \to 0$),

$$P(k) = \binom{N}{k} p^k (1-p)^{N-k} \; \to \; \frac{z^k e^{-z}}{k!}, \tag{2.1}$$

meaning that most of the vertices have a very similar degree, fluctuating around the mean degree $z = \langle k \rangle = L/N = p\,(N-1)/2$ (Figure 2.1). Since the 1960s this model received considerable s attention for several reasons. Its most prominent statistical characteristic is a percolation phenomena, equivalent to continuous phase transitions studied in statistical physics and thermodynamics. In Chapter 1, a network was formally defined as *small-world* if its average pathlength is much smaller than the number of vertices: $l < \log(N)$. This means that all vertices remain "close" to each other. For decades social networks were known to be small-world, as popularised by a famous experiment of Milgram [89, 142] based on spreading of letters among randomly chosen citizens in the United States. As the *random graph* model obeys the small-world property (for p above the precolation threshold) it was long time considered as a *model* for real networks.

2.1.2. The small-world model of Watts and Strogatz

For the major part of the 20th century, graph theory developed with little help of computers and typically only small networks were analysed. The increase and accesibility to computer power during the 1990s permitted a systematic analysis of real (and large)
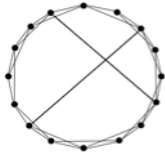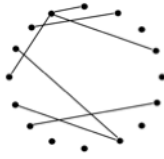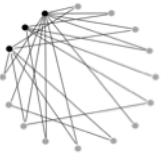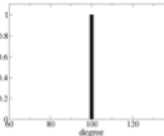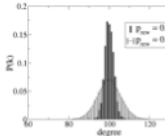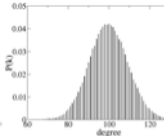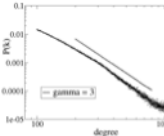
	Lattice	W-S	E-R	B-A
Structure				
k-distribution	dirac-δ, P(k) = δ(k-z)	Binomial (Poisson : $p_{rew} \to 1$)	Poisson : N $\to \infty$	Scale-free; P(k) ~ k$^{-\gamma}$
distance	$l \approx \dfrac{N}{4z}$	no analytical estimation	$l \sim \dfrac{\ln N}{\ln z}$	$l \sim \dfrac{\ln N}{\ln(\ln N)}$
clustering	$C = \dfrac{3}{4}\dfrac{z-1}{2z-1}$	$C \sim \dfrac{3}{4}\dfrac{z/2-1}{2z-1}(1-p_{rew})^3$	$C = p$	$C \sim \dfrac{(\ln N)^2}{N}$
k-correlation	P(k | k') = z for all k.	depends on p_{rew}	none	none

Figure 2.1: Comparison of random graph models.

networks for the first time. While the small-world property was confirmed as a universal characteristic, two new general properties were discovered. One of them is a large clustering coefficient, indicating that real systems are very cohesive due to local structure. The random graph model correctly reproduces the *small-world* property, but it fails to account for the clustering observed in real networks (usually by orders of magnitude), and therefore, it cannot be considered as a *model* anymore. However, random graphs play a crucial role as the most elementary null-model in network analysis.

In 1998, Watts and Strogatz proposed a model which simultaneously accounts for large clustering and small average pathlength [148]. Their model is a transition between regular lattices and random graphs. In a regular lattice vertices are only connected to their spatial neighbours (see Figure 2.1). Such local structure gives rise to a large clustering coefficient. As all vertices have the same number of neighbours, the degree distribution is a Dirac-δ: $p(k) = 1$ when $k = z$, and $p(k) = 0$ otherwise. But, the spread of information is slow because traveling between physically distant vertices requires to cross many connections. By modifying a regular lattice and introducing shortcuts (by randomly rewiring the links), the average pathlength decreases very rapidly. For small rewiring probabilities ($p_{rew} < 0.1$) it conserves much of the clustering of the original lattice and, simultaneously, gains a small pathlength. For large rewiring probabilities ($p_{rew} \to 1$) the model is equivalent to the random graph.

2.1.3. Scale-free models

The second novel property discovered during the 1990s is that right-skewed degree distributions with a high-degree tail (decaying slower than exponential) are abundant in real-world networks. But why should real networks possess such unexpected degree distributions? Scale-free (SF) distributions are typical of self-organised systems, explaining the large attention that complex networks received by physicists afterwards. Two main ingredients for the emergence of power-laws have been debated. Contrary to the classical perspective, a real network is usually an object *growing* in time. Additionally, if the growing process is governed by some sort of *preferential attachment* mechanism, the vertices with many neihgbours tend to accumulate more and more links as time goes by.

In 1965 de Solla Price presented a network model intended to describe the emergence of power-law degree distributions of citation networks [32, 33]. A citation network is described as a directed network, where a link $s \rightarrow t$ means that the paper s cites the paper t. The out-degree of a paper is the number of other papers it cites and thus, never changes after publication. The in-degree, however, increases in time. As popular papers (highly cited) become known to more scientists, they gain a larger probability of being cited. De Solla Price modeled this preferential probability as proportional to its current input degree, k_i:

$$p(t) = \frac{k_i(t)}{\sum_{j=1}^{N} k_i(j)} \tag{2.2}$$

After many iterations, the model returns an in-degree distribution of $p(k_i) \sim k_i^{-(2+1/m)}$ where m is the output degree of a newly published paper (assuming that all papers intoduce the same number of citations).

In 1999 Barabási and Albert (BA) presented a simplified model [16] (for undirected graphs) which could be regarded as a rediscovery of de Solla Price's model. The BA model exhibits a scale-free degree distribution $p(k) \sim k^{-\gamma}$ with exponent $\gamma = 3$ (Figure 2.1). These SF network models capture the small world property observed in real networks (small average pathlength), as well as a "fat tail" degree distributions. However, stated as they are, they lack of the assortivity (degree-degree correlation) observed in many real networks, and more importantly, they generate networks of very small clustering coefficient. Nevertheless, they provide a possible mechanism to explain the evolution of real networks and they have motivated a myriad of new, modified models which additionally capture degree correlations [102], large clustering coefficient [71, 82] and the cut-offs in the degree distribution of many empirical networks [5, 24].

2.2. Statistical Testing of Network Properties

Graph theoretical measures help understand the topological organisation of networks. Once the structure has become clear, the second goal is to construct adequate models. For that, it is necessary to uncover the features which are characteristic to the underlying system and the fundamental properties of its development. In this sense, the question is not whether a graph measure takes a specific numerical value, but rather whether this value distinguishes the network from others of similar characteristics. But how should

such a deviation be detected or quantified? An answer to these questions lies in the formulation of appropriate null-hypotheses. Let us illustrate this with an example.

Imagine we have to analyse a given real network G' of size N', L' links and certain degree distribution $p'(k)$ which is fat-tailed. After measuring its clustering coefficient we obtain $C_{G'} = 0.41$. Clustering values lie between 0 and 1 and, in principle 0.41 is quite a large value. Now, it is well known that C depends on the density of links (indeed, $C = 1$ only in the case of a **complete graph**, a graph with $\rho = 1$). We should then ask whether $C_{G'}$ is expected, or otherwise, significant. Imagine now that the clustering coefficient of random graphs of size N' and L' links is $\langle C \rangle_{rand} = 0.12 \pm 0.02$. Compared to $\langle C \rangle_{rand}$, $C_{G'} = 0.41$ is very large and it can be regarded as a characteristic feature of the real system under study.

So far so good, but, G' was assumed to have a fat-tailed degree distribution (as is typical of real networks). Random graphs, on the contrary, posses Poissonian distributions. The question is now: *being $p(k)$ a basic statistical feature of graphs, and being $p(k)$ of real networks so distinct from that of random graphs, how meaningful is it to use the random graph as a null-model?* How meaningful is the value $\langle C \rangle_{rand} = 0.12$ as an expectation value for G'? Definitely, the random graph is always a valid null-model, this is no question. However, we would prefer to compare $C_{G'}$ to the expected value using a null-model which, while preserving the same degree distribution as G', it is *maximally random*.

For practical applications, how are the expected values and the deviations calculated out of a null-model? In the ideal case, analytical formulae are available as happens for many expectations of the random graph model. Unfortunately, this is rarely the case with more complicated null-models and the expectations have to be computed after numerical experiments; an ensemble of random graphs is generated and the ensemble average of the desired measure is computed.

2.2.1. Generation of random graph ensembles

There are different manners of generating an ensemble of random surrogate networks with preserved degree distribution. The **configuration model** consist of constructing a network with a previously specified degree distribution [20, 91, 97]. Starting from an empty set of N vertices, each vertex is assigned a degree $k(v)$ that can be visually regarded as *free stubs* (Figure 2.2(a)). Subsequently, pairs of stubs are randomly chosen and connected. The configuration model has several limitations and it is often difficult (if not impossible) to generate networks without introducing self-loops or multiple links. In paper II we have extended the configuration model to include also prescribed degree correlations and a mechanism to overcome this problem is proposed, see Section 2.4.

Alternatively, random networks with given degree sequence can be obtained by iteratively swapping randomly selected edges [69, 76, 81, 107] as schematically depicted in Figure 2.2(b). Given a real network, at each iteration two links are chosen at random $(s_1 \rightarrow t_1)$ and $(s_2 \rightarrow t_2)$, and rewired as $(s_1 \rightarrow t_2)$ and $(s_2 \rightarrow t_1)$ provided that the respective new links do not already exist nor introduce self-loops. Repeating the process "sufficient" times the resulting network conserves the initial degree distribution but any other internal structure of the empirical network is destroyed. This is usually the method of choice for significance testing of graph measures, basically, because it works without the problems of the configuration model. However, this method is slower and there is no

(a)

(b)
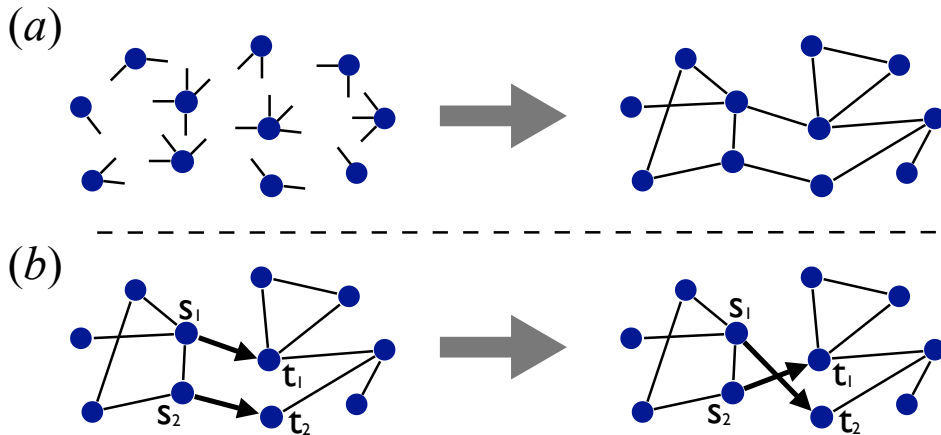
Figure 2.2: Generating random networks with preserved degree distribution. (a) Schematic representation of the configuration model. Each vertex is assigned a fixed number of 'stubs' (degree) which are then joined at random. (b) Link switching method. Two edges are selected at random and switched, provided that the new edges do not already exist neither become self-loops.

proof of how many iterations are *sufficient* to destroy the internal structure. In order to establish a solid estimation, we have performed a series of numerical experiments.

Initial switches randomise the internal structure of the real network. There should be a point in the process when the network is already maximally random so that subsequent rewirings give rise to just another maximally random network, statistically equivalent to the one before. An indirect manner to detect this *critical point* is to look at how macroscopic observables evolve during the rewiring process. In the Figure 2.3, we show the evolution of average pathlength and clustering coefficient of the cortico-cortical connectivity network of the cat. Once the rewiring process has been *successfully* repeated $1 \times L$ times ($2 \times L$ links have been rewired), the network reaches its maximally random state and therefore both measures reach a stable value. Further iterations do not alter them because the macroscopic statistical state of the network does not change. Exactly the same behaviour has been observed for all the 14 real networks analysed in papers I and II, and for all graph measures tested (average pathlength, clustering coefficient and reciprocity). With these results, we numerically assure that rewiring a network $1 \times L$ times is the minimal number of iterations acceptable. For safety, we would suggest to perform the rewiring at least $2 \times L$ times.

Returning to the previous example, imagine now that the clustering coefficient from the ensemble of randomised networks is measured and it gives $\langle C \rangle_{1n} = 0.39 \pm 0.05$. Compared to this value, $C_{G'}$ is not anymore significant. This implies that, compared to a complete random process, the network has (at least) two properties which are significant (the degree distribution and the clustering), but which are statistically related to each other. The main problem now is that towards building a proper model, statistically speaking, we cannot discern which of the two properties is a leading factor of the system, and which of them is simply a by-product of the other. Did the system evolve to favour a certain degree distribution and the observed clustering coefficient is a by-product of that process? or is it the other way around? In general, this sort of questions are very difficult to answer
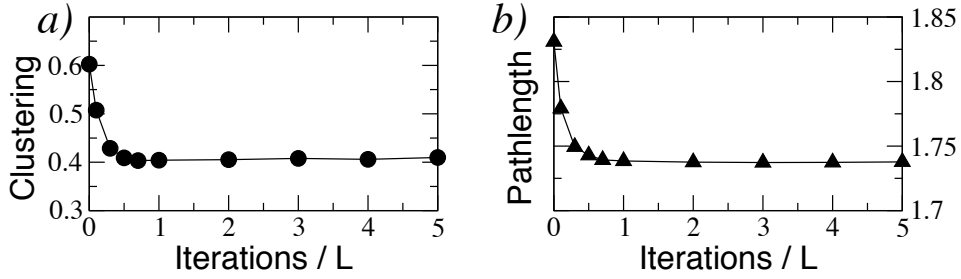
Figure 2.3: Stability of the link switching method to generate random networks with desired degree distribution. After L succesfull iterations have been completed (so $2 \times L$ edges have been rewired) the network reaches its *maximally random state*, as shown by macroscopic measures reaching a stable value. Further switches simply lead to another random network, statistically equivalent to its parent.

because we still have a limited understanding of the statistical interdependence between the different graph measures. Our paper I, summarised below, is an step in this direction, aiming to understand the interrelation between the local graph measures (k-distribution, k-correlations and reciprocity) and to create statistical tools useful for further work.

2.3. Summary of Paper I

The reciprocity r of a directed graph is classically defined as $r = \frac{L^{\leftrightarrow}}{L}$ [147] where $L^{\leftrightarrow}$ is the number of directed links $s \to t$ that also have a reciprocal (bidirectional) counterpart $s \leftarrow t$, and L is the total number of directed links. Statistically speaking, r is the probability that, for a randomly chosen link $s \to t$, the opposite link $s \leftarrow t$ also exists. In the case of a *random digraph*, the probability of a link joining a pair of nodes equals the density of links ρ. As $p(s \to t)$ and $p(s \leftarrow t)$ are independent of each other, it is a well known result that $r_{rand} = \rho$ [52, 147, 153]. In a few words, r linearly depends on the number of links L. However, we expect that the 1-node ($1n$) degree correlations should affect r. Intuitively, a vertex with large input degree k_i *and* large output degree k_o has a higher tendency to form reciprocal links than another vertex with any of k_i or k_o small. Furthermore, as r involves the pairwise connectivity of vertices, the 2-node ($2n$) degree correlations should also be relevant. For example, given the link $s \to t$, the probability that $s \leftarrow t$ exists should strongly depend on $k_i(s)$ and $k_o(t)$. If s has input and output degrees $\boldsymbol{k} = (k_i, k_o)$, and t has degrees $\boldsymbol{q} = (q_i, q_o)$, there exist 4 different subclasses of 2-node, 2-degree correlations ($2n2d$) as depicted in Figure 2.4. When all the four values (k_i, k_o, q_i, q_o) are correlated, then both the 1-node and the 2-node correlations are present.

In paper I we have studied the expected reciprocity $\langle r \rangle$ of networks with *prescribed degree sequences* and *arbitrary 2-node degree correlations.* We consider the complex networks as members of the statistical ensemble with given node degree sequence and degree correlations, and we calculate the expected reciprocity of such ensembles in the thermodynamical limit. In order to analytically estimate $\langle r \rangle$ under different correlation structures, we propose the following characterisation of the network correlations. Given a network with N vertices and links L,

- $N(k_i, k_o) = N(\boldsymbol{k})$ is the number of vertices having in-degree k_i *and* out-degree k_o,
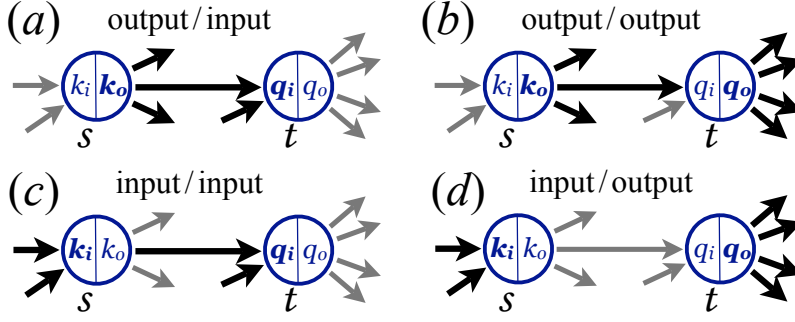
Figure 2.4: 2-node 2-degree correlations ($2n2d$) of *neighbouring nodes* in directed networks. Links corresponding to correlated degrees are colored black.

- $L(\boldsymbol{k} \rightarrow \boldsymbol{q})$ is the number of directed links pointing from nodes with degrees (k_i, k_o) to nodes with degrees (q_i, q_o).

These properties are easy to extract from real networks and contain all the relevant information about the degree correlations. We use frequencies of these properties as their probabilities and calculate the expected number of reciprocal links $\langle L^{\leftrightarrow} \rangle$. Remind that by definition, $\langle r \rangle$ is related to $\langle L^{\leftrightarrow} \rangle$ by $\langle r \rangle = \langle L^{\leftrightarrow} \rangle / L$.

Under the class of 1-node and 2-node degree correlations assumed here, a network is considered as maximally random when *any of the nodes with degrees $\boldsymbol{k}$ is equally likely connected to any of the nodes with degrees $\boldsymbol{q}$*. If a network contains $L(\boldsymbol{k} \rightarrow \boldsymbol{q})$ links of the type $\boldsymbol{k} \rightarrow \boldsymbol{q}$, this probability is, in the thermodynamical limit:

$$p(\boldsymbol{k} \rightarrow \boldsymbol{q}) = \frac{L(\boldsymbol{k} \rightarrow \boldsymbol{q})}{N(\boldsymbol{k})N(\boldsymbol{q})}. \tag{2.3}$$

The denominator $N(\boldsymbol{k})N(\boldsymbol{q})$ is the number of all possible connections between nodes with degrees $\boldsymbol{k}$ and nodes with degrees $\boldsymbol{q}$.

Having established the statistical framework, we derive our most general result, the expected reciprocity of a network conditional on its 1-node *and* its 2-node degree correlations:

$$r_{1n2n} = \frac{1}{L} \sum_{\boldsymbol{k},\boldsymbol{q}} \frac{L(\boldsymbol{k} \rightarrow \boldsymbol{q}) \, L(\boldsymbol{k} \leftarrow \boldsymbol{q})}{N(\boldsymbol{k}) \, N(\boldsymbol{q})} = \frac{L}{N^2} \sum_{\boldsymbol{k},\boldsymbol{q}} \frac{\mathcal{P}(\boldsymbol{k} \rightarrow \boldsymbol{q}) \, \mathcal{P}(\boldsymbol{k} \leftarrow \boldsymbol{q})}{P(\boldsymbol{k}) \, P(\boldsymbol{q})}. \tag{2.4}$$

where the node frequency $P(\boldsymbol{k}) = N(\boldsymbol{k})/N$ and the link frequencies $\mathcal{P}(\boldsymbol{k} \rightarrow \boldsymbol{q}) = L(\boldsymbol{k} \rightarrow \boldsymbol{q})/L$ are considered as the probabilities in the thermodynamical limit. When all four degrees are independent, then r_{1n2n} reduces to the previously known result for the special case of uncorrelated random networks, $r = L/N^2$, which equals the density of links.

2.3.1. Results and discussion

From the general result r_{1n2n}, formulae for the expected reciprocity in all the 10 combinations of $1n$ and $2n2d$ correlations are derived. The results are applied to 14 different real networks of various classes and we find that the $1n2n$ degree correlations alone "explain" the observed reciprocity r_{real} of many real networks. In others, while r_{1n2n} accounts for
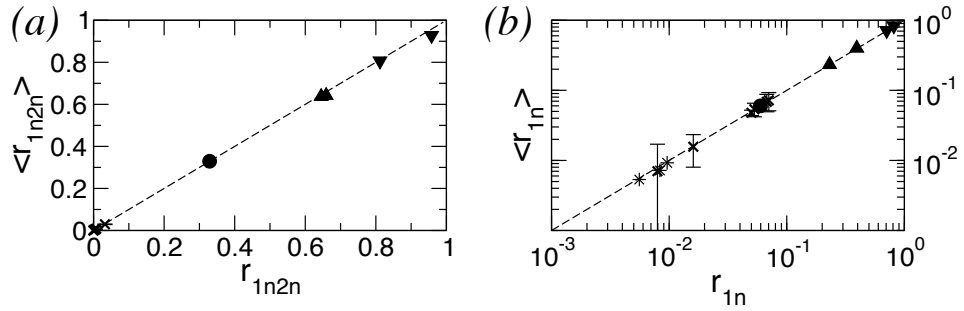
Figure 2.5: Numerical corroboration of theoretical estimations of the expected reciprocity. Experimentally measured reciprocities (vertical axes) and theoretical estimations (horizontal axes). (a) All 1-node and 2-node correlations conserved. (b) 1-node correlations. All data points are averages of 100 realizations. Food webs ($\times$), C. Elegans ($\bullet$), World-trade-web ($\blacktriangledown$), cortical networks ($\blacktriangle$) and Wikipedias ($*$). Dashed lines are references of perfect coincidence.

a large part of r_{real}, the difference between expected and measured values suggests the presence of further internal structure, e.g. community and hierarchical organisation might be a good explanation for this differences.

Finally, in order to numerically corroborate our analytical results, we have invented and presented novel algorithms to obtain *maximally* random networks with desired special classes of 2-node degree correlations preserved. The comparison of numerical and theoretical results shows an excellent agreement in all cases (Figure 2.5 shows only few examples).

2.3.2. Practical applications

To illustrate the usefulness of our proposed statistical formulation, I now show how it can reproduce a very well-known and established result. The modularity Q is commonly used to quantify the validity of a partition of a network into communities (see Chapter 1). Given a graph (undirected) with N vertices and L edges, and a partition of its nodes into n communities $\mathcal{P} = \{S_1, S_2, \dots S_n\}$, the modularity for this partition is defined as:

$$Q_{Newman} = \sum_{s=1}^{n} \left[\frac{L_s}{L} - \left(\frac{d_s}{2L} \right)^2 \right], \tag{2.5}$$

where d_s is the total degree of the nodes in the community S. Clearly, Q is the difference between the number of links inside a community (L_s), and the expected number of links that the same community should have in a random network with the same degree distribution. Denoting the expected number of links as $\langle L_s \rangle$, we re-write:

$$Q = \sum_{s=1}^{n} \left[\frac{L_s}{L} - \frac{\langle L_s \rangle}{L} \right]. \tag{2.6}$$

Now, the statistical framework in paper I can be used to analytically obtain $\langle L_s \rangle$. In a random network with degree distribution $N(\boldsymbol{k})$, the probability (frequency) that one of

the nodes with degrees $\boldsymbol{k} = (k_i, k_o)$ has a link pointing to one of the nodes with degrees $\boldsymbol{q} = (q_i, q_o)$ is:

$$\mathcal{P}(\boldsymbol{k} \to \boldsymbol{q}) = \frac{k_o N(k_o)}{L} \frac{q_i N(q_i)}{L}.$$

Taking only the degree distribution inside the community $N_s(\boldsymbol{k})$, then $\langle L_s(\boldsymbol{k} \to \boldsymbol{q}) \rangle_{1n} = L \, \mathcal{P}_s(\boldsymbol{k} \to \boldsymbol{q}) = L \, \frac{k_o N_s(\boldsymbol{k})}{L} \frac{q_i N_s(\boldsymbol{q})}{L}$, leading to the following expression for the modularity:

$$Q_{1n} = \sum_{s=1}^{n} \left[\frac{L_s}{L} - \sum_{k,q} \frac{k_o \, q_i \, N_s(\boldsymbol{k}) N_s(\boldsymbol{q})}{L^2} \right]. \tag{2.7}$$

Considering the cat cortical network and the anatomical partition into four communities (visual, auditory, somato-motor and frontolimbic systems), we obtain that:

$$Q_{Newman} = Q_{1n} = 0.2403.$$

The numerical match is perfect down to 8 decimals.

2.4. Summary of Paper II

In paper I the statistical relationship between the local graph measures (degree, reciprocity and k-correlations) has been studied. In order to numerically corroborate those analytical results, a few novel randomisation and random network generators were invented. In paper II, we have introduced a unified and universal framework for the generation of random digraphs with desired degree correlation structure. This general algorithm is a *generation method*, e.g. as the configuration model in Section 2.2.1. Starting from an empty set of N vertices, L links are introduced one-by-one following certain restrictions. As in the configuration model, a fixed input and output degrees $\boldsymbol{k} = (k_i, k_o)$ is assigned to each vertex. Additionally, the 2-node correlations are specified in the form of the quantities $L(\boldsymbol{k} \to \boldsymbol{q})$. The L links are introduced in the following manner:

1) One vertex is chosen at random, s.

2) as s has been assigned degrees $\boldsymbol{k}'$, to conserve the correlations s can only project into nodes with degrees $\boldsymbol{q}'$ for which $L(\boldsymbol{k}' \to \boldsymbol{q}') > 0$. Hence, a list containing only the possible target vertices is created, `tlist`.

3) From `tlist` another node is chosen at random, t, and the link is introduced, $s \to t$.

By properly updating the degrees of s and t, and the quantities $L(\boldsymbol{k}' \to \boldsymbol{q}')$, the algorithm finishes the random network in only L iterations.

Several optimisations are also included. On the one hand, we have found that real networks contain large number of **deterministic links**, say, links which cannot be randomised without modifying the correlation structure. On the other hand, our general algorithm suffers from similar problems as the configuration model, it often gets trapped into states in which the only possibility to advance is by introducing either a self-loop or a multiple link. We have proposed and positively tested a mechanism (we name it as the **force-and-drop method**) to overcome such blocked states.

2.5. Summary and Discussion

One of the main goals of complex network research is to understand the relationship between structure, function and dynamics [7, 15, 27, 57, 87, 94, 95, 113, 128, 157]. Personally, I think that we are still far away because we don't properly understand the statistical interdependence between the graph measures. Only to mention an example, the synchronisability in networks of coupled oscillators has been reported to depend on the degree homogeneity [93, 98, 155, 156], clustering coefficient [150], degree correlations [34], betweenness centrality [27], degree distributions and so on [73]. Besides, some of the reported results seem to contradict each other. As wisely pointed out by Atay and collaborators [13], many statistical network properties do not suffice to determine synchronisability because the spectral properties of networks are simply not derivable from them. In the light of this confusion, it seems that graph theory still lacks of a solid foundation on which theories and models can be *safely* constructed. Only when the complicated statistical interrelation between the graph measures is well understood, will we be able to infer with certainty the causal relations governing the interplay between structure, function and dynamics. The work presented in the papers I and II represents a step in this direction.

For decades, this problem has been in the agenda of graph theory. Due to several experimental limitations, sociologists have been interested in understanding the expected graph measures conditional on different classes of degree distributions [147]. However, it seems that the efforts have not been completely satisfactory. In 1991 the mathematician T. A. B. Snijders made the following statement in his famous paper [123]:

> The uniform distribution conditional on both the out- and the in-degrees, defined in (1) and denoted $\mathcal{U}|\{X_{i+}\}, \{X_{+j}\}$ is a relevant null distribution in many applications (. . .) We indicated in the introductory section that the derivation of exact or approximative formulas for distributional properties of statistics like M under this digraph distribution is very difficult and may be considered impossible. The enumeration and simulation methods presented below provide a method to carry out an exact test of M under $\mathcal{U}|\{X_{i+}\}, \{X_{+j}\}$ that circumvents the need for exact (or approximative) formulas.

Following a classical nomenclature, Snijders refers to the number of dyads M as what we call the number of reciprocal links $L^{\leftrightarrow}$ (exactly, $L^{\leftrightarrow} = 2M$). At that time Snijders considered it *impossible* to find formulae to estimate the expected number of dyads in a network with fixed degree distribution ($\mathcal{U}|\{X_{i+}\}, \{X_{+j}\}$) and therefore he proposes a numerical approach as the *only* solution. The analytical results that we have presented in paper I largely overcome this problem to include also the effect of the 2-node degree correlations. Precisely, the equation (6) of paper I, $r_{1n} = \frac{L}{N^2} \frac{\langle k_i k_o \rangle^2}{\langle k \rangle^4}$, is the "impossible" result that Snijders mentions, and it arises just as a special reduction of the general result r_{1n2n} which is conditional on all 1-node and 2-node degree correlations.

Some recent works have also tried to uncover the statistical interdependencies between several graph measures. In [35, 72] the statistical interplay between 2-node degree correlations and the clustering coefficient has been studied, but restricted to the special case of undirected graphs. Very recently, the expected number of cycles (closed paths) of arbitrary length [21] has also been computed conditional on the 1-node degree correlations.

Further work in this direction is desirable and the analytical tools presented in paper I can be extended to study other network measures such as the clustering coefficient and motif profiles. Using modularity as an example, we have shown the flexibility of our formalism. When analytical studies become impracticable, the numerical methods proposed in paper II open the door for a new generation of faster algorithms to create ensembles of random networks conditional on degree correlations. No doubt, both theoretical and experimental applications will significantly benefit from the advances in this direction.

CHAPTER 3:

Large-Scale Connectivity of the Mammalian Brain

> *. . . in an abiotic world, information plays no role; physical interactions just happen, they are driven by energy exchange between the interacting parts and do not require any operations of information processing (. . .) But for living organisms, information is the very essence of their existence: to maintain a long-term state of stable thermodynamic non-equilibrium with its surroundings, consistently increase its organisation and reproduce (. . .) This, comprises both* **biomolecular information** *processes controlling the metabolism, growth, multiplication and differentiation of cells, and* **neural information** *processes controlling animal behavior and intelligence.*

> Juan G. Röderer [110]

Life has managed to conquer the oceans and the surface of our planet, succeeding even in remote and extreme environments to our surprise and joy. Yet, living organisms are fragile entities which struggle to survive by continuously feeding their internal state of non-equilibrium with energy. While the ability to consume and transform energy and matter makes life possible, it is the capacity of collecting and processing information that makes life *stable.* In an constantly changing environment, the "knowledge" of the internal and the external states is a necessary condition for the control of a stable existence.

Unicellular organisms mainly rely in *bio-molecular* information. Proteins anchored in the cell membrane "smell" the environment triggering internal cascades of chemical reactions. New information and responses leading to a sucessful existence is stored as genetic information in the course of evolution. For multicellular organisms, the simple difussion of molecules is not always fast enough to evoke a response to sudden changes. At early stages of the evolution the nervous system merely served as a "high speed" information transmission device. Environmental signals, transduced into electrical pulses, may be conveyed into distant parts of the body and, for example, activate a muscle to trigger an escape response. Such "action-reaction" paths are known as *reflex arcs*, and take place at the lowest levels of information processing in the nervous system of any animal species. These basic circuits evolved into *neural networks* capable of discriminating

different signals and causing specialised responses. Finally, *memory circuits* emerged to store relevant information for later use.

Composed of an estimated number of 10^{10} neurones, the mammalian nervous system (NS) is the responsible for collecting information, generating satisfactory interpretation (perception) of the world and providing adaptive responses in a constantly changing environment. The five senses commonly attributed to the nervous system (sight, hearing, smell, taste and touch), underestimate its real complexity. Just imagine, at the root of every hair in our body there is a sensory neuron transducing the movements of the hair into electrical signals. Muscles and joints are populated by *proprioceptors*, neurones sensing the stretching of muscles and the position of body parts. The *thermoreceptors* located inside the body and at the skin respond to temperature changes. A subclass of *chemoreceptors* fire electrical impulses when they detect high concentrations of carbon dioxide in the blood, triggering an increase in the breath and heart rates. Even physical pain is often the consequence of stimulation of specialised neurones which detect chemical, thermal or mechanical events which have the potential to damage the body tissue [19, 80].

As responsible for the global coordination of the organism, the NS is in continuous communication with all other organs, for example, the endocrine system. The finding only few years ago of synaptic communication between lymphocytes of the immune system and neurones [61, 86, 134, 140, 141] is a beautiful evidence of something we all suspect by common experience: that mind and health go hand-in-hand together. Towards a holistic understanding of the brain and its function, we should not forget the fundamental role of the **neurochemistry** and its interplay with the ongoing electrical activity. Good examples are learning and synaptic depression processes. Electrical activity may cause permanent chemical changes at the synapses, and reciprocally, drug intake can alter the electrical activity, e.g. leading to a temporal loss of awareness under anaesthesia. Furthermore, the neurochemistry plays a fundamental role as the intermediary between the genetic information and the electrical activity, i.e. the ultimate interplay between the memory of the species and the current experiences of the individual.

In this chapter a necessarily brief and incomplete review of the organisation and the information processing in the nervous system is provided. Our goal is to motivate the relevance of the topological/structural organisation of the nervous system before shifting into a detailed analysis of its connectivity. For that, we will focus on the anatomical connectivity between cortical areas in the brain of cats.

3.1. Processing of Information in the Mammalian Nervous System

Despite the large number of neurones and their different forms, they only collect and transmit two kinds of electrical signals: graded potentials and action potentials (spikes). Hence, the capacity of the nervous system to simultaneously process different kinds of information relies, to a large extent, on the circuitry where the stimulus is received and processed, not only on the specific temporal code.

3.1.1. Processing of sensory information

The sensory system, also known as the peripheral nervous system, is responsible for collecting the sensory information and converting it into electrical signals. Far from being mere transducers, sensory neurones play a fundamental role in the pre-processing and organisation of information, and their adequate functioning is fundamental for a proper perception of the reality. We distinguish some general features:

Modality: every sensory cell is destined to collect and transduce one, and only one, kind of sensory stimulus. Consequently, information from different modalites remains separated for most of the processing path.

Location of the stimulus: the information from sensory cells located close to each other in the body is transmitted together and projected into topologic maps in the brain for processing.

Intensity: the strength of the stimulus is coded as the firing frequency of action potentials.

Duration of the stimulus: Phasic receptors respond only to the sudden onset or termination of an stimulus. Tonic receptors are constantly active as long as the stimulus is present.

Once the signals have been transduced, the information travels through the different hierarchical levels of the NS. At every stage of the propagation, information is "filtered" and the necessity for a special response is evaluated. Such is the case of scape reflexes, 'hard-wired' security mechanisms which are automatically activated in extreme situations, when life or integrity are in danger. We all experience situations in which our body reacts to a stimulus far before we become consciously aware of the danger. While reflexes are necessary for survival, they are extremely simple and imprecise responses. More intricated neural networks have evolved to analyse and discriminate types of input signals and produce specific and refined responses. Every sensory signal, regardless whether it causes a reflex response or not, propagates towards upper levels in the hierarchy of the nervous system and every level leaves its "imprint" on it, including emotions [92].

Despite the fact that the separation of modally different information paths is a relevant characteristic of organisation in the NS, at the highest levels this separation seems to fade away [50, 146]. In order to achieve a coherent and unified perception of the reality, sensory information needs to be integrated together at some point [108] and at some time [42, 45, 122]. For that, the paths of information need to converge somewhere. Even monosensory perception, like vision or audition, has become so complex that sensory information arriving at the cortex is first segregated and individual characteristics are analysed separately. Visual information arriving into the primary visual cortex is forwarded to different visual regions, each specialised in detecting different features, e.g. orientation, movement direction and speed, distance, contrast, color, etc. But to create a comprehensive visual perception, those elements of information need to be integrated together [44, 112]. This process is also known as the binding problem [19, 80, 108, 122].

3.1.2. Binding, integration and high level processing

So far, we may emphasise two mayor aspects of sensory perception:

Bottom-up information flow: Starting at the sensory neurones, the information flows in an ascending manner towards higher processing levels, where neuronal networks and their capacity of processing grow in complexity.

Modular organisation: Information paths for signals of the same modality traverse the body together, separated from the other modalities. Even in the cortex, the regions processing different aspects of the same modality are spatially located close to each other.

The intimate relationship between the organisation architecture of the nervous system and the steps of sensory processing has been extensively documented in the literature. However, these organisational principles seem to fail to explain higher order processing like cognition. While sensory perception is dominated by the characteristics of the input, higher level cortical networks are not necessarily influenced by sensory input. Attention, imagination and voluntary actions are the result of self-generated percepts influencing the information processing in a top-down manner.

Up to date, there is nothing we could identify as the cortical region specialised in mathematical calculus or in socio-political opinions. Cognitive information seems to be represented over wide, overlapping and interactive neuronal networks in the cerebral cortex. Even if we would regard consciousness as the result of a global integrative process of the multisensory information to create a comprehensive perception of reality [108, 121, 135], there is no evidence for a unique brain region performing such a task. In the words of J. M. Fuster [50]:

> ...because only the sensory aspects of perception and memory can be mapped, it is becoming increasingly evident that cognitive information transcends any of the traditional subdvisions of the cortex by structural or functional criteria (...) Thus, whereas the modular paradigm has been most helpful to clarify the neural basis of sensations, it is inadequate to clarify the central substrates of perception or memory. Simply extrapolating principles of modular representation to larger modules does not lead to the identification of those substrates.

3.2. Topological Organisation of the Mammalian Cortex

In the previous section, the relevance of the connectional organisation of the nervous system has been emphasised. Unfortunately, a detailed description of the neuronal connectivity is still far from satisfactory and only some reliable data is known at the large scale of few mammalian species. Three main scales of connectivity are distinguished:

3.2.1. Scales of connectivity

Microscopic connectivity: It is estimated that each neuron receives approximately 10^4 synapses from other neurones, the majority of them being from local neighbours.

Usually, each neuron makes contact to its closest neighbours by only one synapse or none at all [25, 111]. Collection of detailed neuron to neuron connectivity is almost impossible for several reasons and for the moment, only qualitative conclusions can be derived.

Mesoscopic connectivity: In the cortex, the dynamics of neuron populations is more relevant than the firing patterns of individual neurones, what is reflected by the agglomeration of neurones at different scales. Assemblies of $80 - 100$ neurones align vertically across cortical layers II and IV, forming *columns* and *microcolumns* [22, 109, 111]. Such modules are considered as the basic functional units in the cortex.

Macroscopic connectivity: In the cerebral cortex, extense regions can also be found which differ from each other in cytoarchitecture and function. Originally defined and listed by Brodmann at the beginning of the 20th century [25], the architecture and function of cortical areas has been the subject of intensive investigation and debate: 1) their precise function and borders can differ from subject to subject, 2) cortical neurones are typically involved in more than one functional circuit, and 3) high level functions rely in vast territories of cortex that extend beyond the specialised and localised areas [50].

Despite the lack of detailed information, some common qualitative features are observed across scales. Neural connectivity is neither random nor fully regular and neurones possessing similar function tend to form assemblies. The best example of microscopic connectivity is the nervous system of the mnematode *Caenorhabditis Elegans* which has been reported to possess small-world[1] characteristics [148] and modular structure [11]. At the intermediate scales, neurones of the cerebral cortex are aligned forming microcolumns, which group together into columns [127, 129]. This kind of organisation remembers the hierarchical topology discussed in Chapter 2 and illustrated in Figure 1.3(b), in which groups of densely connected vertices interlink to form larger assemblies.

3.2.2. Modular and hierarchical organisation

At the level consisting of cortical areas connected by long-range fibers, small-world properties have also been found for the macaque and the cat [64, 125, 126]. For example, clusters or streams of visual cortical areas have been identified that are segregated both functionally [143] and in terms of their inputs, outputs and mutual interconnections [151]. To identify the clusters of cortical networks, a stochastic optimisation method applied to the cortical networks [64] detected a small number of distinctive clusters in global cortical networks of cat and macaque [65]. These clusters contain areas which are more frequently linked with each other than with areas in the remainder of the network. Additionally, the obtained clusters follow functional subdivisions, e.g. they contain predominantly visual areas. Hierarchies of cortical areas can also be constructed based on the laminar origin and termination patterns of interconnections [47, 68].

The ubiquitous feature of the segregation of cortical networks into multiple, interconnected network clusters and their capacity to share multimodal information is the central

---

[1]By small-world architecture we mean that the networks have large clustering coeffient and their vertices lie at a short topological distance from each other.

issue of this dissertation. Many previous works have stressed the necessity of a balance between segregation (specialisation) and integration (binding) in cortical processing. Using graph selection methods for computationally generated networks, the emergence of connectivity patterns giving rise to small-world networks composed of interconnected clusters have been found [128]. The algorithm favoured for graphs maximising a particular measure of global *complexity* defined for the whole network[2]. In Chapter 5 we will further discuss these topics from an information theoretical perspective.

3.3. Cortico-Cortical Connectivity of the Cat

Currently, several neural connectivity databases exist from which a network can be extracted. At the microscopic level, the nervous system of the mnematode *Caenorhabditis Elegans* has been completely mapped [41, 149]. At the macroscopic level, cortico-cortical connectivities have been obtained for three animal models: cat, macaque and rat (partially). The invasive and toxic nature of the experimental techniques does not permit a systematic description of the connectivity of the human cortex. Non-invasive imaging techniques such as Diffusive Tensor Imaging (DTI) offer a future perspective for collecting human anatomical data. In this dissertation, we concentrate uniquely on the cortico-cortical connectivity of the cat brain for the following reasons:

a) Macroscopic analysis: Experimental neuroscience has been very succesful in describing the electro-chemical principles of neural excitation and the mechanisms of transduction of sensory information into electrical pulses. Techniques like *in-vivo* microelectrode recording have permitted the investigation of more complex organisation and function of the brain, e.g. recording the brain activity of animals while performing sensory or behavioural tasks. But, if we want to understand cognitive functions and consciousness, it is necessary to understand how information from different modalities and parts of the brain are integrated.

b) Statistical reliability: Among the three available cortical connectivity datasets, the one of the macaque monkey is the most interesting to analyse because there exists a rich literature reporting task-dependent experiments in macaques. A comparison between the experimental and the graph theoretical results should be highly desirable. Unfortunately, this data is not yet complete enough[3] while the connectivity data of the cat offers the possibility of deriving detailed and statistically reliable graph theoretical results.

The database of the cortical connectivity of the cat was created by Jack W. Scannell after a collation of an extensive literature reporting anatomical tract-tracing experiments [115, 117]. It consists of a parcellation into 53 cortical areas and 826 fibers of axons between them as summarised in Figure 3.1. The connections are weighted according to the axonal density of the projections between areas. Scannell et *al.* classified the connections originally reported as *weak* or *sparse* with 1 and, the connections originally

---

[2]This particular measure of complexity aims to capture the complex characteristic of networks (neither randomly nor regularly connected) by analysing the dynamical dependence among the vertices at all scales of organisation.

[3]The CoCoMac project [1, 130] opens a promising possibility for the near future.
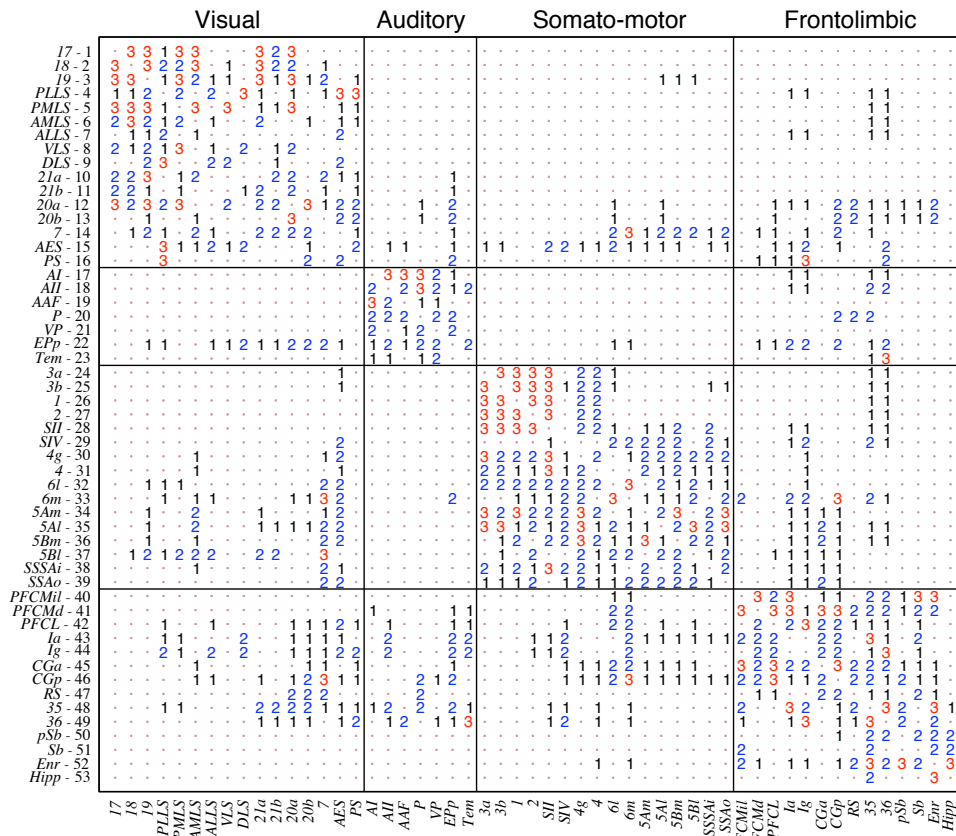
Figure 3.1: Adjacency matrix of the cortico-cortical connectivity of the cat comprising of 826 directed connections between 53 cortical areas. In the vertical axis the names of the areas have been numbered to simplify the interpretation of plots afterwards. More information about the cortical areas is summarised in Appendix B. The connections are classified as weak (1, black), intermediate (2, blue) and dense (3, red) according to the axonal densities in the projections between two areas. For visualisation purpouses, the non-existing connections (0) have been replaced by dots.

reported as *strong* or *dense* with 3. The connections reported as *intermediate*, as well as those connections for which no strength information was available, were weighted with 2.

A common source of misinterpretation is the fact that the cases in which a connection was explicitly reported as absent, and those connections which no experiment ever attempted to detect, were treated equally and weighted with 0. It is expected that further experiments may detect new connections which are still missing in the database. Being aware of this and other limitations, we have established the following criteria for the graph theoretical analysis of the network, in order to provide *fair statistical results* and interpretations:

a) Communities: Using data mining techniques, the connectivity data of the cat has been found to be organised into four communities [64, 115, 117], whose composition is similar to the functional divisions: visual, auditory, somato-motor and frontolimbic (see Figure 3.1). Current community detection methods based on the maximisation of the

modularity function detect an optimal partition which is slightly different. However, we believe that the result of more sensitive community detection methods is not necessary because the known imperfections of the data. Therefore, the communities established in the literature have been adopted as valid a working partition.

b) Reciprocal connections: The reciprocity coefficient of the network is $r = 0.73$, meaning that most of the links have a reciprocal counterpart and only 27% of the connections are unidirectional. Because of the missing links, it is difficult to evaluate the reliability of the nonreciprocal links and to provide a functional interpretation. On the other hand, there is an increasing evidence that all cortico-cortical connections are reciprocal [3, 51]. In the *complex networks* literature it is common to find directed networks which have been symmetrised "by hand" for convenience[4]. We do not agree with this kind of data manipulation. Instead, graph measures are flexible enough to find proper compromises without a need for altering the data. For example, as the input and output degrees of the cortical areas are correlated (not shown), the degree can be computed as their average: $k(v) = 0.5(k_i(v) + k_o(v))$. Throughout the Chapter 4, additional criteria are adopted for each of the graph measures.

c) Thalamo-cortical connections: The cortico-cortical connectivity is a subset of a larger dataset comprising also the thalamic regions and the thalamo-cortical connections [116]. Two special features of this extended data are: 1) all thalamo-cortical connections are reciprocal, and 2) no connections exist between thalamic regions. Here, as in many works [64, 83, 115, 129], the thalamic areas and their projections have been ommited. However, the thalamus is typically considered the *gate* of sensory information to the cortex and thus a brief justification follows. First, while the thalamic inputs are relevant for understanding the function of primary sensory cortical areas, they have very little influence on the cortex of association, where most of the cognitive functions happen [50]. Second, thalamic projections represent only a very small percentage of the inputs that a cortical area receives. Even in the primary visual cortex, whose function mainly depends on sensory input, only 5% of its terminal axons is of thalamic origin. Most of the other inputs are of cortical origin [103].

3.4. Classification of Cortical Networks

The cortico-cortical networks of cat and macaque have been classified as small-world networks due to their large clustering coefficient C and their small average pathlength l. On the other hand, robustness of cortical networks reveal similarity to scale-free (SF) networks [79]. Damage profiles after intentional attack on the highest degree nodes, or attack on randomly chosen areas, display similar robustness profiles to those of SF networks. To bring some order into this apparently contradictory classification, ensembles of 100 random networks of different classes have been generated for comparison. The network models and the methods to generate them are described in Chapter 2:

1. Random graphs of size $N = 53$ and with $L = 413$ undirected links (the connectivity of the cat contains 826 directed links).

---

[4]The symmetrisation is typically done by adding the necessary links. If $A_{ij} = 1$ and $A_{ji} = 0$, then A_{ji} is set to one.

	Cat cortex	Random Graph	Cat Rewired	Watts-Strogatz	Scale-free
C	0.55	0.30 ± 0.01	0.396 ± 0.005	0.56 ± 0.01	0.37 ± 0.01
l	1.83	1.673 ± 0.003	1.735 ± 0.004	1.77 ± 0.02	1.686 ± 0.004

Table 3.1: Comparison of average clustering and average shortest path between the cat cortical network and equivalent random networks. 'Rewired Cat' also possess the same degree sequence. Each value is the average over 100 realizations.

2. Random rewired digraphs of same size N, number of links L and degree distribution $N(\mathbf{k})$ as the connectivity of the cat. The set was generated by application of typical rewiring algorithms which conserve the input and the output degrees of every vertex.

3. Small-world networks after the model of Watts and Strogatz (W-S). Starting from a regular ring-lattice of size $N = 53$, each vertex is connected to its 8 closest neighbours and then links are rewired with probability $p_{rew} = 0.1$. The resulting networks have 424 undirected links.

4. Scale-free (SF) networks with exponent $\gamma = 1.5$ have been generated following the method in [53], which consists of a modification of the configuration model. Certainly, with only 53 nodes the obtained networks cannot achieve a SF distribution, nevertheless, they display a broad distribution, see Figure 3.2.

The results are summarised in Table 3.1 and Figure 3.2. With respect to the *small-world* characteristics, the cortico-cortical network of the cat clearly lies close to the W-S networks, Figure 3.2(a). However, even if the global average C and l are very similar, the W-S model cannot be considered as a plausible model to explain the cortical organisation because: 1) W-S networks do not display community organisation, and more relevant 2) the vertices of W-S networks have similar degree. On the contrary, the network of the cat cortex possesses a very wide degree distribution, i.e. few areas connect up to 60% of all other areas. As shown in Figure 3.2(b), the difference in the cumulative degree distributions is prominent.

The cumulative degree distribution of SF graphs with $N = 53$ and $L = 423$ (solid line of Figure 3.2(b)) closely follows the real distribution of the cat cortex, what explains the similar attack tolerance behaviour [79]. But, as expected, the clustering coefficient of SF networks is very small (Table 3.1). Hence, the random SF graph is not a suitable model for cortical networks either. The W-S and SF random models are only minimal models intended to capture *certain* global properties observed in real systems, and cortical networks have a very rich internal organisation.

It has been previously stressed that the balance between segregation and integration is a relevant feature of the nervous system. On the one hand, the modular structure of the cortex, divided into few subsystems, provides the structural support for specialised information processing. Similar to the W-S model, few connections between the communities permit that all information remains accessible everywhere. But, what about the *integration*? are the shortcuts between communities enough for supporting the integrative capacity of the brain? if so, why should the network possess such broad degree distribution? These are the main questions that we try to answer in the following chapters.
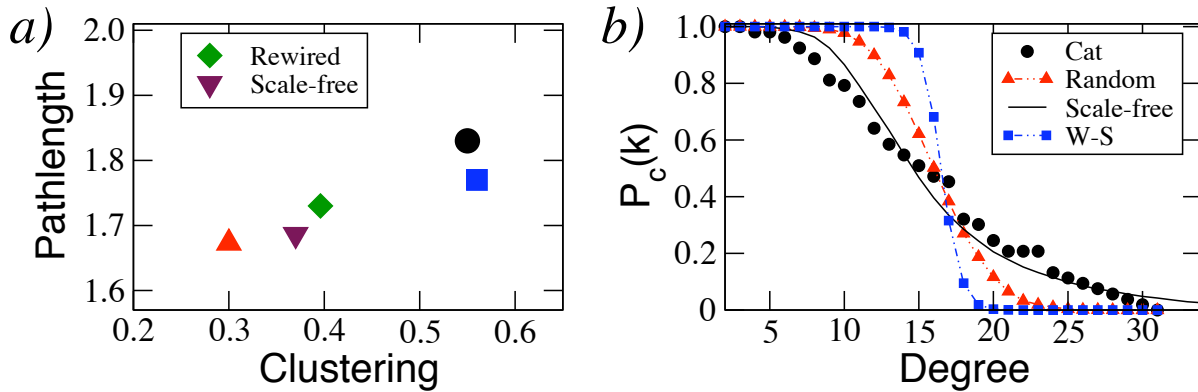
Figure 3.2: Classification of the cat cortical network. Comparison to ensembles of random null-models and generic models. (a) comparison of the *small-world* characteristics, and (b) cumulative degree distributions. Cat cortex (●), random graphs (▲), rewired (♦), scale-free (▼) and Watts–Strogatz networks (■).

3.5. Organisation of the Multisensory Connectivity

We finish this chapter with a rough analysis of the connectivity and a preliminary classification of the cortical areas in terms of their multimodal interactions. Next chapters will deepen this classification using more sophisticated statistical tools. So far, two relevant features of the organisation of the cat cortex have been stressed: its modular organisation and the presence of largely connected areas. A simple visual inspection of the adjacency matrix reveals a clue to understand the apparent contradiction of simultaneous similarity to the W-S model and to the SF networks: *the inter-community links are not randomly distributed, but some cortical areas accumulate most of them.* Internal links are defined as connections between two areas in the same comunity, and external links as connections between two areas in different communities. Out of the 826 axonal connections in the dataset 470 of them (57%) are internal, and 356 are external (43%). This tight ratio of internal to external links gives a rough idea of how fragile the community structure is and of the multiplicity of communication paths between modalities.

	V	A	SM	FL
V	**0.583**	0.098	0.109	0.201
A	0.098	**0.81**	0.018	0.204
SM	0.199	0.089	**0.742**	0.241
FL	0.237	0.276	0.237	**0.648**

Table 3.2: Inter-community connection densities. Diagonal elements represent the internal density of links within the communities, and extradiagonal elements are the fraction of existing links from one community to another (out of all possible links between them). The frontolimbic system is the most connected to the others, in accordance to its presumed functional role in association.
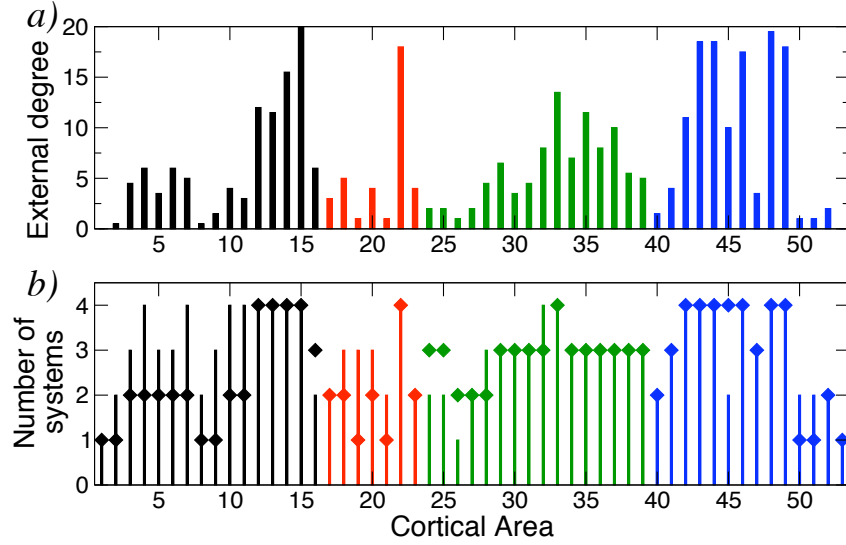
Figure 3.3: Multisensory nature of cortical areas. Modal systems are represented by: black (visual), red (auditory), green (somato-motor) and blue (frontolimbic). (a) The number of external connections that each cortical area makes to areas in other systems. Within each system, only few areas are the main responsibles of multimodal communications. (b) Number of modal systems to which cortical areas are connected. In (b) bars represent the output connections and ◆ the inputs. Almost all cortical areas make multimodal connections, although only few ones connect to the four systems.

3.5.1. Large-scale overview

In Table 3.2 the connection densities within and between the communities is summarised. Density is defined as the fraction of exisiting links to the number of all possible links[5]. The diagonal values of Table 3.2 represent the internal densities of connections within the systems being the auditory and the somato-motor systems the densest of all. The extradiagonal values are the inter-community connection densities. Due to the directed nature of the dataset, the inter-community densities are not symmetric. The most relevant observation is that the frontolimbic system is the most connected to all other systems. This feature is probably one of the largest obstacles for a clean partition into communities. Nevertheless, from a functional point of view this is expected because of the important role of the frontolimbic cortex for associations and high level processing. On the contrary, the auditory system is the most independent of all, a fact which has been confirmed in dynamical simulations [154, 157, 158].

---

[5]For internal connections $\rho_{int}(I) = \frac{L_I}{N_I(N_I-1)}$ and for the external connections from system I to system J, this is $\rho_{ext}(I \to J) = \frac{L_{I \to J}}{N_I N_J}$, where $N_I N_J$ is the number of all possible connections from areas in system I to areas in J.

	V	A	SM	FL
Supramodal Hub	20a, 20b, 7	EPp	6m, 6l	Ia, Ig, CGp
	AES			35,36
Multimodal area	PLLS, PMLS	AI, AII	SII, SIV, 4g, 5Al	PFCMd, PFCL
	AMLS, ALLS	P, Tem	5Am, 5Bl, 5Bm	CGa, RS
	19, 21a, 21b		SSSAi, SSSAo	
Unimodal area	17, 18	AAF, VP	1, 2, 3a, 3b	PFCMil, pSb, Sb
	VLS, DLS			Enr, Hipp

Table 3.3: Tentative classification of cortical areas according to their multimodal connectivity. *Supramodal hubs* are cortical areas with many external connections in all the four systems, and *unimodal (specialised) areas* are those linked almost uniquely within their community. Other areas have several connections to one or two external systems and have been classified as *multimodal areas*.

3.5.2. Multimodal and unimodal areas

Let us define the internal degree, $k^{int}(v)$, as the number of neighbours that vertex v has within its own community, and the external degree, $k^{ext}(v)$, as the number of neighbours of v in other communities. In order to derive a preliminary classification of cortical areas, in Figure 3.3 their multisensory connectivity is illustrated. An interesting observation out of Figure 3.3(a) is that, within each system, few areas are largely connected to other systems. This observation indicates that the multisensory communications between the systems might be mediated by few areas. Except for the primary visual cortex (area 17) and Hippocampus in the FL cortex, all other cortical areas have connections to at least one external system (Figure 3.3(b)). Further details are summarised in the following:

Visual system: Visual areas 20a, 20b, 7 and AES alone make 60% of all the external connections, all of them spanning their connections into the four systems. On the contrary, the primary and secondary visual cortices, areas 17 and 18, together with VLS and DLS, have almost no multimodal connections, indicating a purely specialised function in visual processing. The rest of visual areas, while highly specialised, make several connetions to other systems, mainly to the auditory hub, area EPp, and to different motor areas. These latter links might indicate the connectivity substrate for the control of visual attention.
Auditory system: Only area EPp can be considered as a hub, while the rest of areas have poor external connectivity, with the exception of some sparse links with the frontolimbic system and the visual hub, area AES.
Somato-motor system: Areas 6m and 6l are the best candidates to be considered as hubs. Areas 5Al, 5Bm and 5Bl also have many external connections but none of them connects to the auditory system. A characteristic feature of the SM system is that most of its areas make few multisensory connections to areas in the frontolimbic and in the visual systems. All these areas span their links over three systems (see Figure 3.3(b)). Only the somatosensory areas 1, 2, 3a, 3b, have sparse external connectivity (see Figure 3.3(a)).
Frontolimbic cortex: The associative nature of the frontolimbic cortex is captured by its large number of multisensory hubs. Areas Ia, Ig, CGp, 35 and 36 have each over 17

external connections spanning among all the systems. Only a small part of the prefrontal cortex (PFCMil), the subicullum (Sb, pSb) and the entorhinal cortex (Enr) could be classiffied as purely unimodal areas.

In the light of these observations, we propose a preliminary, tentative classification of cortical areas into three categories as summarised in Table 3.3. Areas making uniquely (or almost uniquely) internal connections to other areas in their community are classified as unimodal. The areas which, belonging to one community, sparsely connect to areas in one or two external communities are named multimodal. Finally, as supramodal hubs are considered the areas with large degree, which also span their connections over the four systems. In the following chapters more reliable classification schemes will be presented. Even if this classification is based uniquely on the internal and external connectivities of areas, it coincides with known biological features. Cortical areas involved in low level (specialised) sensory processing typically exhibit additional internal organisation. Early visual cortical areas have layered *retinotopic maps* such that information conveyed by contiguous retinal neurones is processed by adjacent neurones in the cortex. Regions of the somatosensory cortex are arranged into *somatotopic maps* of the body. Neurones of the auditory cortex form *tonotopic maps*, i.e. they are ordered according to the frequency to which they respond. This kind of internal organisation is not observed in cortical areas involved in higher processes such as binding and association [50]. According to the descriptions in [115], *none* of the areas classified above as multimodal hubs, have a mapped internal organisation. On the contrary, primary and secondary visual cortices (areas 17 and 18), as well as areas 19, 20a, 20b and PS are known to be retinotopically organised; primary auditory cortex AI as well as AAF, P and VP have tonotopic maps; somatosensory areas 1, 2 and 3b contain somatotopic maps of cells responsive to cutaneous estimulation and SIV has an orderly topographic representation of the body surface. Most of these areas have been classified as unimodal and few of them in the intermediate category.

3.6. Summary and Discussion

The mammalian nervous system (NS) is a complex system par excellence. Composed of over 10^{10} neurones, it is the responsible for collecting and processing information, and for providing adaptive responses which permit the organism to survive in an ever changing environment. The sensory information is processed in a bottom-up manner. Environmental information is transduced into electrical signals by the sensory neurones and ascends through distinct hierarchies of increasing complexity.

In this chapter, the interest of understanding the large-scale connectivity of the NS has been motivated. The main reason is the belief that, comprehension of the topological substrate in which the processing of information happens, should uncover relevant aspects of brain function. While sensory information of different modalities follows particular paths of processing, the emergence of a general state of awareness requires that the multisensory information converges in space and time [108, 121, 135]. How and where this happens is still a subject of debate. There is, however, increasing evidence that cognitive information is represented over wide, overlapping, and interactive neuronal networks in the cerebral cortex [50, 51, 146].

As a working database, the cortico-cortical connectivity network of the cat has been

chosen because it is, up to date, the most complete of its kind. Therefore, it is the most suitable for a detailed (and statistically reliable) graph theoretical analysis. Nevertheless, the data contains several limitations and future experiments may reveal new connections which are currently missing. In order to overcome these and other limitations, several criteria for the analysis have been established. For example, even if there are strong indications that all cortico-cortical connections might be reciprocal [3, 51], the network has not been symmetrised. It is common to find in the complex networks literature that networks have been symmetrised for analytical or computational convenience. We believe that the graph theoretical measures are flexible enough to find proper compromises without the need to alter the data.

Finally, the basic characteristics of cortical networks have been revisited. Cortical networks are organised into modules [64, 115, 116] which closely follow the functional subsystems: visual, auditory, somato-motor and frontolimbic. Cortical networks have also been classified as *small-world*, meaning that cortical areas are at a short topological distance of each other, and that they are very cohesive due to internal organisation [64, 65, 129]. A recent study showed that the robustness properties of cortical networks are similar to those of scale-free (SF) networks. To bring some light into this classification scheme, a comparison to several random network models has been presented. Our conclusions are that, while the cortical network of the cat has large clustering coefficient (probably due to the modular organisation) it also has a broad degree distribution and contains several hubs. The multisensory connectivity of the cortical areas has been analysed. We find that every system (visual, auditory, etc.) contains at least one hub which might be responsible for the multisensory communication between the systems. These reasults have led us to a preliminary classification of cortical areas in terms of their multisensory connectivity as: supramodal hubs and unimodal (sensory specialied) areas. Other areas lie in an intermediate class between the two extremes, which has been named multimodal.

CHAPTER 4:

Detailed Graph Theoretical Analysis of the Cat Cortex

By the date I joined the group of Jürgen Kurths, the analysis of cortical networks had mainly focused on their modular and hierarchical organisation [64, 115, 126] and on the characterisation of a few average measures such as clustering coefficient (C) and average pathlength (l). As explained in the previous chapter, this characterisation led to a classification of the cortical connectivities as small-world networks [127, 129]. In general, complex networks possess a rich internal structure and average measures are not sufficient to understand their structure. Therefore, I started working together with Changsong Zhou and Lucia Zemanová with a clear goal in mind: *to perform an extensive graph theoretical analysis of cortical networks, aiming to relate the topological properties of individual areas to their specific function.*

In this chapter a detailed graph theoretical analysis of the cat cortex is presented in order to go beyond average graph measures. First, the properties already presented in Chapter 3, the degree distribution, the clustering coefficient and the distance will be re-analysed in more detail. Then, cortical areas will be classified in terms of their centrality properties and finally, a shift from invidual to collective behaviour is introduced.

In order to perform a significance test for the graph measures, an ensemble of 1000 surrogate networks has been created following the *link switching method* explained in Chapter 2. All the resulting networks have the same size N, the same number of links L and the same degree distribution, $N(k_i, k_o)$, as the cortico-cortical network of the cat. To assure that any further internal structure is destroyed, every randomised network is the product of $10 \times L$ iterations (see Chapter 2). In the following, we refer to this set of randomised networks as the rewired ensemble, $\{G_{1n}\}$, and the original cortico-cortical network of the cat is denoted as G_{cat}. The ensemble average results of applying graph measures to the set of surrogate networks $\{G_{1n}\}$ are considered as the expected values.

4.1. Classification of the Cat Cortex Revisited

In the previous chapter, G_{cat} was shown to have a clustering coefficient significantly larger than expected (as compared to random and rewired networks). Furthermore, C and l of the cat cortex are very close to the values expected according to the model by Watts and Strogatz (WS). However, its broad degree distribution is similar to that of scale-free
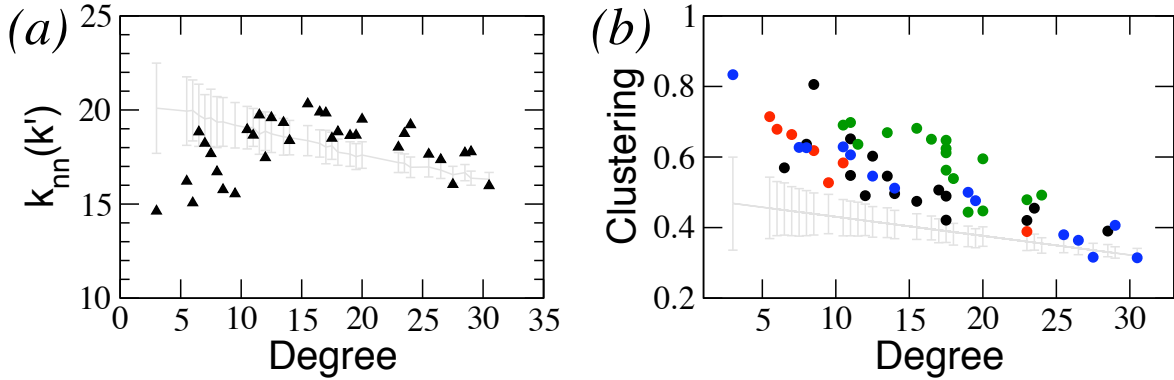
Figure 4.1: (a) Degree-degree correlations computed as the average nearest-neighbour's degree. Cat cortex (▲) and ensemble average of $\{G_{1n}\}$ (grey line). The expected $k_{nn}(k')$ is slightly disassortative as a consequence of the broad degree distribution $p(k')$. (b) Dependence of the local clustering coefficient $C(v)$ on the degree $k(v)$. Cortical areas are displayed in terms of their anatomical communities: V (black), A (red), SM (green) and FL (blue).

(SF) networks (although strictly speaking, with only 53 vertices it is unsuitable to name it scale-free).

4.1.1. Degree-degree correlations

We first re-analyse the local properties. A network is called **assortative** when the vertices of similar degree are connected together and **disassortative** if large degree vertices preferentially connect to low degree vertices. As G_{cat} has only 53 vertices, a crude measure of the degree-degree correlations in terms of the probability $p(k|k')$ of adjacent vertices is not suitable. Alternatively, we compute the **average nearest-neighbour's degree**, $\langle k_{nn}(k) \rangle$ [102]. We remind that, in order to overcome the limitations of the data due to missing links, the degree of an area is computed as the average between its input and output degrees: $k(v) = \frac{1}{2}(k_i(v) + k_o(v))$. Unless otherwise specified, this criterion will be used from now on (see Section 3.3 for more details). In Figure 4.1(a) triangles represent the $k_{nn}(k')$ of the cat cortex and the grey line in the background is the expected neighbour's degree as computed out of the rewired ensemble $\{G_{1n}\}$. Clearly, the cat cortex is neither assortative nor disassortative.

Due to the broad degree distribution, the rewired ensemble displays a slightly disassortative behaviour. The only remarkable feature is that for low degrees ($k < 10$), $k_{nn}(k')$ of G_{cat} is significantly below the expectation. The explanation lies in the modular organisation of the network, i.e. cortical areas with small degree preferentially connect to other areas in their community.

4.1.2. Clustering coefficient

The clustering coefficient C is an average measure providing an indication of global cohesiveness in the network. A more detailed analysis shows that the local clustering of
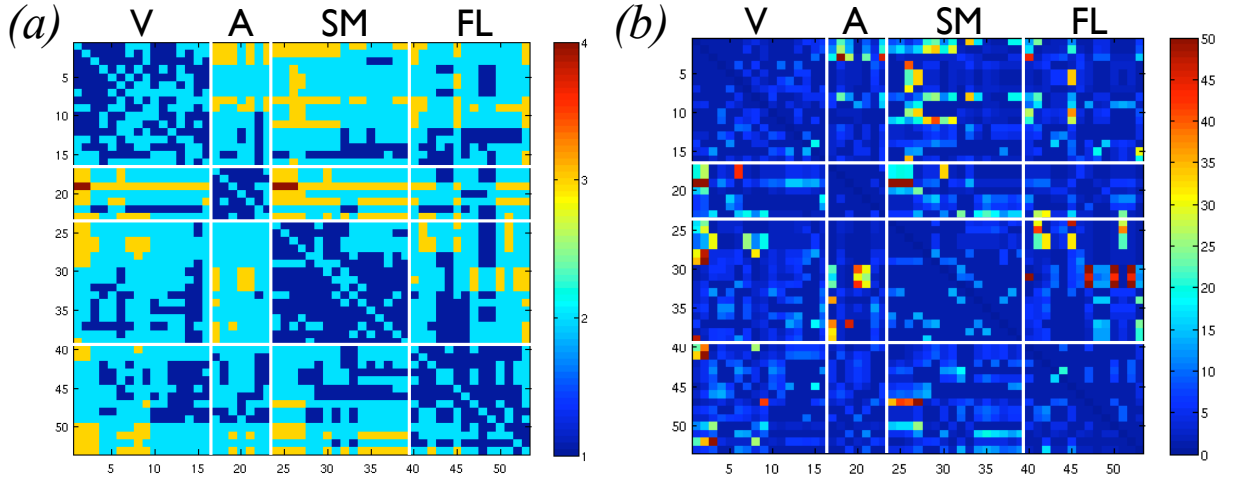
Figure 4.2: (a) Distance matrix D_{ij} of the cortico-cortical network of the cat. The network has a very small average pathlength of $l = 1.83$. The most distant cortical areas are separated by only 4 steps. (b) Path multiplicity matrix M_{ij} representing the number of "parallel" shortest paths (of length D_{ij}) from area i to area j. We find that, on average, there exist 5.2 "parallel" paths between every pair of areas.

the areas $C(v)$ is very inhomogeneous[1], ranging from 0.3 to 0.8. Furthermore, $C(v)$ anticorrelates with the degree of the areas (Figure 4.1(b)), which is a sign of hierarchical and modular networks [82, 95]. Low degree areas typically connect to other areas within their community so their neighbours usually "know" each other. On the contrary, the hubs necessarily span their connections over different communities. Note that the largest community consists of only 16 areas and the hubs have degree of up to $k = 31$. The neighbours of a hub, which belong to different communities, are not usually connected causing a low value for the $C(v)$ of the hub.

The expected local clustering, computed out of the rewired ensemble (grey line in Figure 4.1(b)), displays also a slight anticorrelation with the degree. This effect does not arise from degree-degree correlation (as G_{cat} lacks it), but from the mathematical characterisation of $C(v)$ itself (Chapter 1). Nevertheless, the local clustering of the low degree areas is still significant while $C(v)$ of the hubs have the values expected from the null-model.

4.1.3. Distance and path multiplicity

The cortico-cortical connectivity of the cat is characterised by a very short average pathlength: $l = 1.83$. Taking a look at the pairwise distance matrix $\boldsymbol{D}$ (Figure 4.2(a)), one finds that the network is dominated by direct connections (826) and by paths of length 2 (Table 4.1). Indeed, 87.4% of all the pairs are connected by paths of $d_{ij} = 1$ or 2. The

---

[1]$C(v)$ is computed as the density of links among the nearest neighbours of the vertex v, $C(v) = \frac{L(\Gamma(v))}{k(k-1)}$. Our network is directed, and one could a priori compute $C(v)$ considering only the output neighbours $\Gamma^+(v)$ or the input neighbours $\Gamma^-(v)$. To overcome the data limitations due to missing connections, we consider all neighbours of the cortical area, $\Gamma(v) = \Gamma^+(v) \cup \Gamma^-(v)$, and the density of links among them.

	$d = 1$	$d = 2$	$d = 3$	$d = 4$
All connections	826	1584	341	5
Internal	470	232	2	0
External	356	1352	339	5

Table 4.1: Distribution of the pairwise cortico-cortical distances. Out of the distance matrix D (Figure 4.2(a)), the number of pairs at distance $d = 1 - 4$ are counted. 87.4% of all pairs are separated by only one or two steps. The internal connectivity within the communities is dominated by direct connections ($d = 1$) between the cortical areas, and the external connectivity by paths of length $d = 2$, meaning that most of the paths joining areas in different communities require an intermediate vertex.

diameter of a network is defined as the longest distance between any two vertices, which in this case is $d_{ij} = 4$. Only five pairs (all starting from auditory area VP) have $d_{ij} = 4$. The internal connectivity within the clusters is dominated by direct connections (66.8% of the cases), and the rest are at distance 2. The external connectivity is then clearly dominated by paths of $d_{ij} = 2$ (66.0% of the cases), and there are almost as many pairs separated at a distance $d_{ij} = 3$ and at $d_{ij} = 1$.

These characteristics imply extraordinary functional implications to understand cortical information processing. First, as all cortical areas are highly accessible to each other, information can be shared easily regardless of the sensory origin of the information. Second, as recently shown by Kaiser and Hilgetag [66, 77, 78], neural organisation might favour short information processing paths rather than short physical connections. Instead, the traditional belief is that the nervous system tends to minimise the wiring length because of the energetic benefits of propagating electrical impulses through shorter axons. And third, it is a strong indication that direct connections are the most fundamental processing paths in brain activity.

If we just mentioned that serial information processing might be reduced to a few steps, the computational power of short paths cannot be underestimated. In general, there is more than one path linking two vertices. Even if we assume that information only flows through shortest paths, there is a considerable amount of **path multiplicity** in G_{cat}, what might foster rich and flexible computation capabilities. The number of shortest paths between every pair of cortical areas has been counted and summarised into the **path multiplicity matrix**, $\mathbf{M}$ (Figure 4.2(b)) for statistical analysis. The elements M_{ij} are the number of shortest paths (of length d_{ij}) starting from area i and finishing in area j. There is a total of 14301 shortest paths including the 826 direct links. Due to its combinatorial nature, the multiplicity of paths increases with the length of the path as observed in Table 4.2. The average number of the shortest paths of pairs separated by a given distance d is displayed in brackets. For example, even if there are only five pairs of areas with distance $d = 4$ (Table 4.1), for every pair there is an average of 61.4 "parallel" shortest paths. Another example of the relevance of path multiplicity is described later in terms of the **betweenness centrality** of the areas.

	$d = 1$	$d = 2$	$d = 3$	$d = 4$
All connections	826 (1)	6648 (4.20)	6520 (19.12)	307 (61.4)
Internal	470 (1)	1384 (5.97)	28 (14)	—
External	356 (1)	5264 (3.89)	6492 (19.15)	307 (61.4)

Table 4.2: Multiplicity of shortest paths. Out of the path multiplicity matrix M (Figure 4.2(b)), the total number of shortest paths of length $d = 1$ to 4 is summarised. The values in parenthesis are the average number of shortest paths per pair of vertices at the given distance which, for combinatorial reasons, increases with d.

4.2. Centrality of Cortical Areas

The computation of pair-wise distances and the analysis of path multiplicity permits to additionally classify the vertices in terms of their *accessibility* and relevance in information *transmission*. The closeness centrality $C_c(v)$ is the average distance between v and the rest of the vertices (see Chapter 1). Changes in central vertices (or information leaving from them) propagate very fast and affect the entire network. Moreover, central nodes can also rapidly *sense* global changes. The betweenness centrality $BC(v)$ is the number of shortest paths in which v takes part as an intermediate vertex, say, it quantifies the relevance of v for the transmission of information in the network. This involves finding *all* shortest paths of length $l \geq 3$. A common criticism to $BC(v)$ is the underlying assumption that all information travels uniquely following shortest paths. The predomination of very short paths uncovered in the previous section, suggests that this assumption is a reasonable approximation for cortical networks.

4.2.1. Closeness centrality

The cortico-cortical network of the cat G_{cat} is directed and, in principle, one could compute both the input and output closeness. Following the data analysis criteria discussed in Chapter 3, we define the closeness of a cortical area as the average between its input and output closeness: $C_c(v) = 0.5 \left(C_c^{in}(v) + C_c^{out}(v) \right)$. As it could be expected, highly connected areas are more central, while areas with few connections have larger $C_c(v)$. This is captured by the anticorrelation between C_c and the degree, Figure 4.3(a). Furthermore, C_c of the cortical areas follows almost exactly the expected closeness centrality as computed from the rewired ensemble $\{G_{1n}\}$ (grey line in Figure 4.3(a)). There is only some deviation observed for few, low k, areas. Again, this is caused by the modular organisation of the network. The areas with the largest significant $C_c(v)$ are the visual 17, 18 and VLS; the auditory AAF and VP; and somato-motor areas 1 and 2. All of them were classified as *unimodal* areas. Indeed, areas 17 and 18 are the primary and secondary visual cortex, and areas 1 and 2 are the primary and secondary somatosensory areas respectively. This observation manifests how the modular organisation keeps highly specialised sensory (unimodal) areas slightly "isolated".

In Figure 4.4(top), the cortical areas are ordered from the most central (left) to the most peripheral (right). The centre of the network is dominated by frontolimbic (FL)
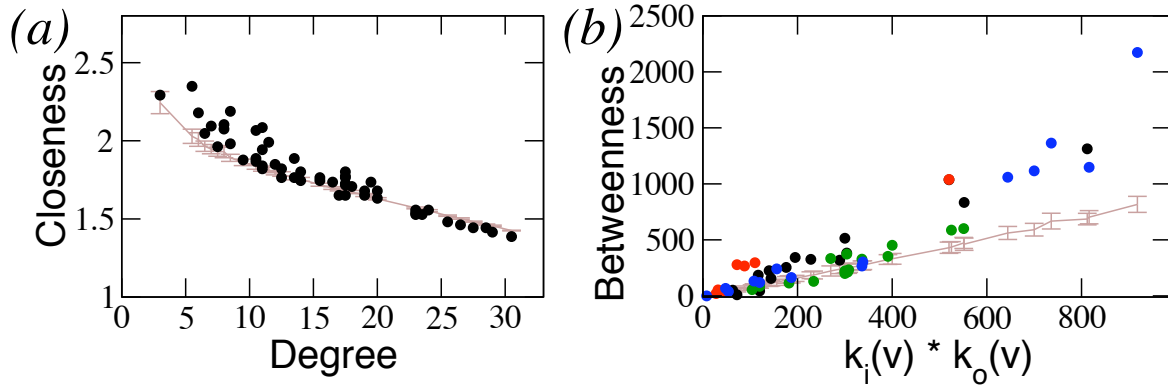
Figure 4.3: Centrality measures of the cortical areas in the cat (•) and their expected values in rewired networks (grey lines). (a) Closeness centrality. $C_c(v)$ of the areas follows the expectation values very closely. (b) Betweenness centrality. BC of the hubs is significantly larger than expected. Colours represent: Visual areas (black), auditory (red), somato-motor (green) and frontolimbic (blue).

areas, precisely those classified as *supramodal hubs* (35, CGp, 36, Ia, Ig). Only the visual area AES is infiltrated among them in third place. The FL areas are followed by the visual hubs 7 and 20a, and by the auditory hub EPp. Finally, the somato-motor hubs 6m and 5Al come in 10th and 11th position, followed by another SM area, 5Bm, although there is a small shift in the value of C_c.

4.2.2. Betweenness centrality

The precise dependency of C_c and BC on the degree of the vertices can be very complicated and is unknown yet. In the previous section, C_c has been compared to the degree of the areas but to represent $BC(v)$ we find the comparison to $k_i(v)\,k_o(v)$, the multiplication between the input and the output degrees of v more suitable. The reason is that $BC(v)$ is the number of shortest paths going through the vertex v and for each path entering v there are $k_o(v)$ possible output paths. The grey line in Figure 4.3(b) is the expected BC as computed from the $\{G_{1n}\}$ ensemble and grows linearly with $k_i k_o^2$.

While most of the cortical areas follow closely the betweenness expected from the null-model, the ensemble $\{G_{1n}\}$, the hubs deviate significantly from expectation, a feature not observed before. Both for the local clustering (Figure 4.1(b)) and, to a lower extent, for the closeness centrality (Figure 4.3(a)) the low degree vertices deviated from expectation while the hubs did not. It has been argued that those deviations were caused by the modular structure of the network. A consequence of this organisation is that the paths between unimodal areas in different communities largely depend on using the supramodal hubs as mediators, e.g. from primary visual cortex (area 17) to visual hub 20a, to auditory hub EPp and finally to primary auditory cortex AI.

The classification of cortical areas in terms of BC (Figure 4.4, bottom) again shows a domination of frontolimbic hubs followed by the visual, auditory and somato-motor hubs.

---

[2]We don't claim that this is the ultimate dependence of BC on the degree, further work is still required. However, in our case most of the shortest paths have length $l = 2$ so $BC(v) \propto k_i(v)k_o(v)$ makes a reasonable approximation. Note that the 826 direct links do not contribute to BC.
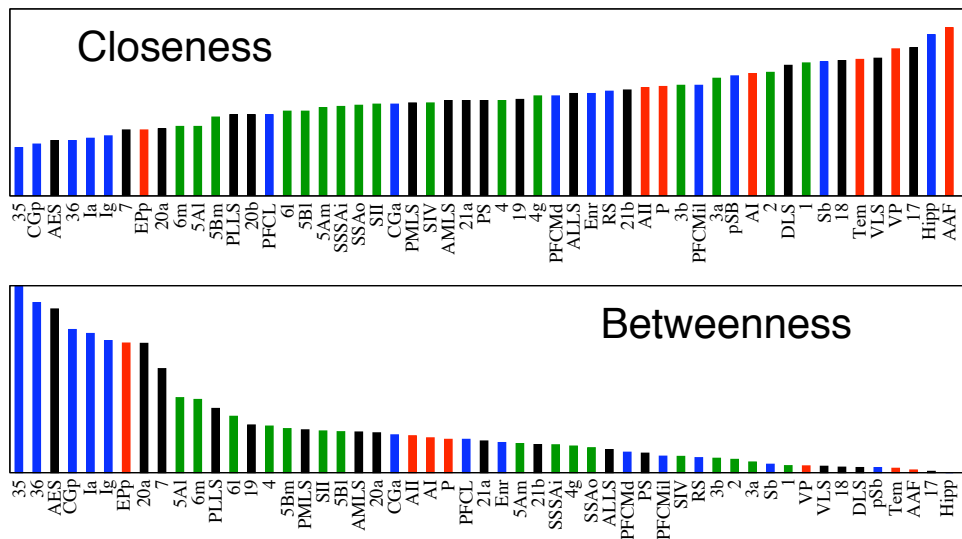
Figure 4.4: Classification of cortical areas from *central* to *peripheral* in terms of: (top) closeness centrality and, (bottom) betweenness centrality. Colours represent: Visual areas (black), auditory (red), somato-motor (green) and frontolimbic (blue).

In this case, however, the absolute differences in BC between the central and non-central areas are very pronounced, reflecting the different function between areas of the association cortex and areas specialised in the early stages of sensory processing.

In summary, even if the precise order slightly differs depending on closeness or betweenness (Figure 4.4), the centrality analysis largely confirms our preliminary classification of cortical areas from Chapter 3. The centre of the network (low C_c or large BC) is formed by the areas classified as *supramodal hubs*. Those areas classified as *multimodal* have medium values of centrality (and lie in the middle of both Figures 4.4(top) and (bottom)), and the periphery of the network (right-most areas in Figure 4.4), is composed of the areas classified as *unimodal*.

4.3. Topological Roles of Cortical Areas

Typical community detection methods partition the vertices of a network into separated modules, but except for trivial cases such a division is never clean. In reality vertices have a probability to participate in more than one community and thus, the modules overlap each other [99, 114]. Up to now, we have implicitly made use of this concept by classifying the cortical areas as unimodal, multimodal and supramodal hubs as a sign of their level of overlap. The connections have also been termed as internal when the link happens between two areas of the same community, and external when areas of two different communities are linked[3]. In general terms, a vertex shall be named as peripheral

---

[3]Although an intuitive concept, the problem of overlap is a very difficult challenge. If defining a *community* in mathematical terms is already controversial, dealing with the diffuse borders between communities (the overlap) is even more difficult.
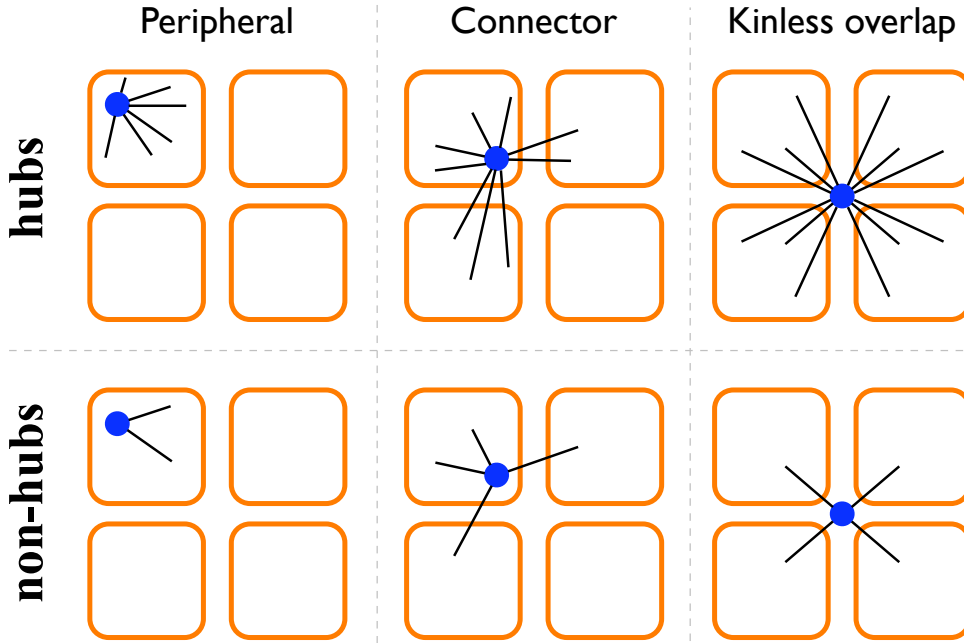
Figure 4.5: Illustration of the *topological positions* that a vertex might occupy within the modular division of a network.

when it preferentially connects to neighbours inside the community, **connector** when it belongs to a community but also participates in some other community, and as **kinnless** when the vertex similarly overlaps between all the communities and it cannot be assigned to any of them with certainty. See Figure 4.5 for illustrative examples.

In order to classify vertices after the topological position they occupy within the community structure, Guimerà and Amaral (GA) proposed a quantitative framework consisting of two parameters. One evaluates the internal position of the vertex and the other its external connectivity [58, 59]. Assume a network of size N and a partition into n communities. Within a community S of size N_S, its vertices have internal degree κ_i. The internal parameter, named as **within-module degree** of a vertex is then defined as the z-score of its internal degree:

$$z_i = \frac{\kappa_i - \langle \kappa \rangle}{\sigma} \tag{4.1}$$

where $\langle \kappa \rangle = \frac{1}{N_S} \sum_{j \in S} \kappa_j$ is the average internal degree within the community, and σ its standard deviation. When $z_i > 2.5$ the node is classified as a hub of the network[4]. The external parameter, named as the **participation coefficient**, quantifies how distributed the links of a node are among all the communities:

$$P_i = 1 - \sum_{s=1}^{n} \left(\frac{k_{i,s}}{k_i} \right)^2 \tag{4.2}$$

where k_i is the degree of the node and $k_{i,s}$ the number of links that i makes with nodes of community S. If $i \in S'$ and has only internal links then, $k_{i,s'} = 1$ and $k_{i,s} = 0$ for

---

[4]While the division of regions in terms of the participation index have been validated by a simulated annealing analysis of real and artificial networks, the choice of $z = 2.5$ as a valid delimiter between hubs and non-hubs is not justified in any of the references [58, 59, 60].
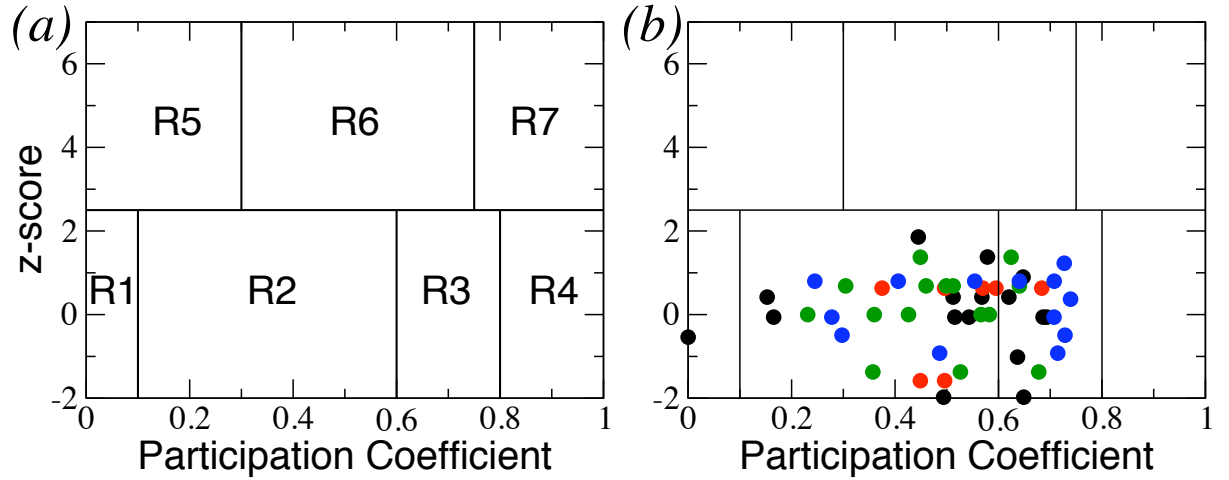
Figure 4.6: (a) Two dimensional diagram of Guimerà and Amaral to classify the position of the nodes according to a partition into communities. The diagram is the result of two parameters, one describing the internal position of the node within its community, and a external parameter capturing the overlap of the node with other communities. Different regions are defined to help in the interpretation of results. (b) Application of the measures to G_{cat} and its anatomical partition into four anatomical communities (V, A, SM and FL), gives rise to counter-intuitive results.

any $s \neq s'$, hence $P_i = 0$. On the contrary, if the node has its links equally distributed between all the communities, $P_i \to 1$. A Combination of z_i and P_i leads to a diagram of the type shown in Figure 4.6(a). Additionally seven regions have been defined to simplify the orientation and interpretation of the classification: R1, ultra-peripheral nodes; R2, peripheral nodes; R3, non-hub connectors; R4, non-hub kinless nodes; R5, peripheral hubs; R6, connector hubs; R7, kinless hubs. The illustrations in Figure 4.5 have been ordered similarly to the GA space for clarity.

4.3.1. Limitations of the GA framework

When applying GA's method to different real networks, we observed some counterintuitive results. For example, the GA diagram for the cortical network of the cat (G_{cat}) in Figure 4.6(b) does not display any hub (R5, R6 and R7 are empty) even if we know that it contains several. It does neither display kinless nodes (R4 and R7), while some areas heavily connect to all the four communities. A close inspection of z_i and P_i revealed several limitations of the formalism which seems correct in the thermodynamical limit (large size and sparse connectivity), with many communities of similar size. But for networks of limited size and inhomogeneous communities, a normalised formulation is required. Conceptually speaking, it should be noted that a vertex which is a local hub within its community, is not necessarily a global hub of the network. Neither is it in the opposite case. To illustrate this point, we have compared the 'within-module degree' (z-local) to the z-global[5] of the cortical areas in G_{cat}. The result shown in Figure 4.7(a) evidences the

---

[5]z-global is computed using the degree of i, k_i, and the average degree of the network $\langle k \rangle = L/N$.

point here raised, otherwise, a linear relationship should be observed. Some cortical areas play a central role within their community (z_i-local is large) but are globaly irrelevant (z_i-global ≈ 0).

While the original and general idea of GA remains valid, understanding of its limitations led us to an extension of the formalism and its conceptual interpretation towards a normalised framework in which networks of different characteristics can be compared under universal criteria. A detailed argumentation and description of the proposed formulation is explained in the Appendix A. We found it suitable to normalise the z-score function of the degree in the following manner:

$$z_i' = \frac{z_i}{z_1^*} = \frac{z_i}{\sqrt{N-1}}, \tag{4.3}$$

where N can be either the size of the network (if the z-global is being computed), or the size of a community N_S (if the within-module degree is desired). With such a normalisation a node has $z_i' \to 1$ when it is the only hub of a very sparse network, $z_i' \approx 0$ when the node has an average degree, and $z_i' \to -1$ when i has small degree in a very dense (sub)network.

The normalisation of the participation index is more elaborated since a new tool is introduced. Given a partition into n modules, every vertex is assigned a **participation vector** $\overrightarrow{P_i}$ (of n dimensions) whose elements $P_i(s)$ represent the probability that i belongs to the community S. We found suitable to define $P_i(s) = \frac{k_{i,s}}{N_S}$, meaning that, out of all possible neighbours that i could have in S, in reality i has $k_{i,s}$. To be more precise, if $i \in S'$, then $P_i(s') = \frac{k_{i,s'}}{(N_{s'}-1)}$. In order to reduce the information of the vector into a single scalar, the standard deviation of its n elements, σ_i, is computed and the **participation index** is defined as:

$$P_i = 1 - \frac{\sigma_i}{\sigma_{max}(n)} = 1 - \frac{n}{\sqrt{n-1}}\,\sigma_i, \quad \text{where} \quad \sigma_i = StdDev\left(\overrightarrow{P_i}(s)\right). \tag{4.4}$$

Note that, for the moment, we avoid providing further delimiters as the regions R1, R2, etc. in GA's diagram. This question requires further conceptual and technical considerations which are to some extent debated in the Appendix A. Now that an alternative and (hopefully) universal formalism has been introduced for the topological roles of vertices, we return to the analysis of cat cortex.

4.3.2. Topological roles of cortical areas

From the result displayed in Figure 4.7(a), it is evident that in G_{cat} local hubs are not always global hubs, neither the other way around. Otherwise the plot would display a linear relation. To mention only an example, in previous chapters the auditory area EPp has been classified as a supramodal hub and, primary and secondary auditory areas AI and AII as unimodal. When computing the (normalised) local z-scores we obtain the following results: $z_{AI}' = 0.315$, $z_{AII}' = 0.315$ and $z_{EPp}' = 0.070$. Internally, AI and AII are the hubs of the auditory system. Only after computing the global z-scores it can be realised that EPp is a hub of the network: $z_{AI}' = -0.146$, $z_{AII}' = -0.105$ and $z_{EPp}' = 0.153$. Indeed, AI and AII obtain negative values meaning that globally, they are peripheral areas.

In the GA framework P_i is plotted against z_i. After proving that z-local and z-global are not necessarily correlated, the question remains whether P_i should be represented
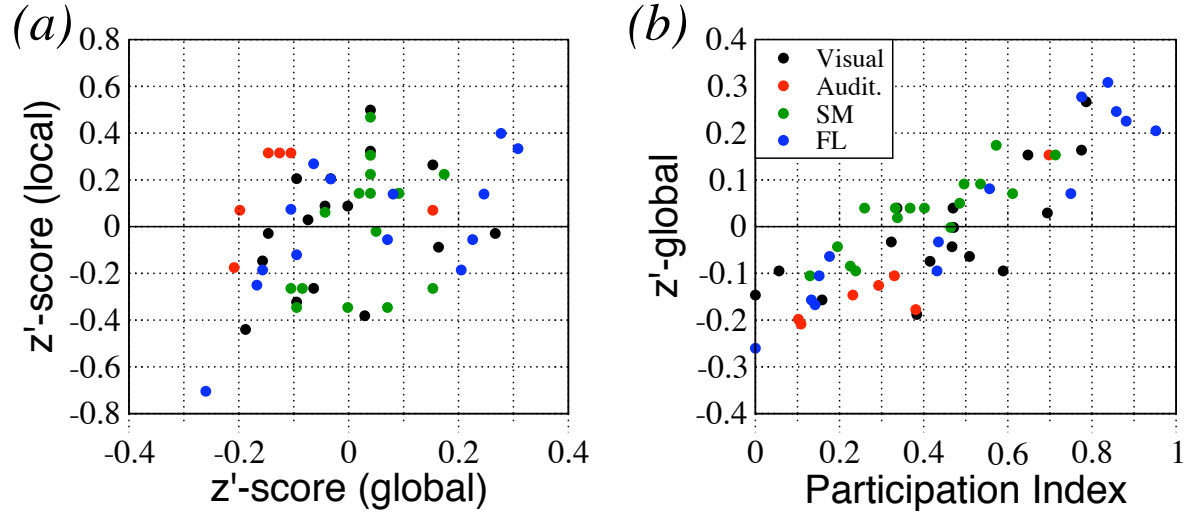
Figure 4.7: (a) Illustration using the G_{cat} network that local hubs within the communities are not necessarily hubs of the network. Neither the other way around. Some cortical areas display large z-local, but z-global ≈ 0. (b) Result for G_{cat} of the normalised classification diagram. Participation index of the cortical areas is plotted against their global z-score. In the cat cortical network it happens that only the areas with high degree overlap over the four systems, while low degree areas preferentially make internal connections. Therefore the ascending trend. Such a trend is not necessarily expected in other networks.

against z-local or z-global. In Figure 4.7 z-global is shown because it follows the original idea of Guimerà and Amaral to classify vertices as hubs or non-hubs. First, a prominent linear trend exists between z_i-global and P_i. It should be stressed, that such a linear trend is a special characteristic of G_{cat} and its particular hierarchical organisation. In general, the low degree kinless vertices (see Figures 4.5 and 4.6) would populate the lower/right part of the plot, equivalently to the R4 region of the GA diagram. In the previous sections the impact of the community structure on the outcome of graph measures has been observed indirectly. Only the hubs, or only the peripheral (unimodal) areas would deviate from the expectation. As an explanation, it was argued that low degree areas preferentially connect to areas within their community, while the hubs largely overlap between the communities. The linear relation between z_i-global and P_i is the evidence of that organisation. Moreover, note that the hierarchical division as supramodal hubs or unimodal is not perfect. The intermediate region is highly populated, indicating a gradual hierarchical ordering of the areas. These observations are consistent with the initial classification proposed in Chapter 3 as supramodal hubs, unimodal areas and, a diffuse intermediate region between them.

In agreement with the centrality measures, the upper right corner of Figure 4.7(b) is dominated by five frontolimbic areas {Ia, Ig, CGp, 35, 36} and the visual area AES. Following them, visual areas 20a and 7, the auditory hub EPp and the somato-motor area 6m could also be considered as supramodal hubs, however their P_i and z_i'-global are slightly lower, and maybe, they might be classified as *connector hubs* rather than *kinless hubs*. In the opposite corner of the diagram, considering all areas with z_i'-global < -0.1

and $P_i < 0.3$ we find: {17, 18, VLS; AI, AAF, P, VP; 1; PFCMil, pSb, Sb, Hipp}, being visual primary cortex 17 and the Hippocampus the only areas with $P_i = 0$. Most of these areas were classified as unimodal, which is now confirmed. As a last remark, it might be pointed out that the somato-motor areas mainly occupy the middle of the diagram. Apart from 6m, no other SM area could be considered as a supramodal hub, and apart from the primary somatosensory area 1, no other SM area is clearly unimodal. It seems that SM cortex plays a general role as an intermediate hierarchy. We might speculate that this seems reasonable according to its function because movement may arise either as the consequence of (bottom-up) sensory input, e.g. a reflex response, or as the result of a voluntary and planned action (top-down).

4.4. From Individual to Collective Organisation

The analysis perfomed so far has exposed various characteristics of the organisation of cortical networks: 1) the short average pathlength between cortical areas (emphasising the importance of direct connections), 2) the richness of parallel and serial information paths, and 3) the topologically measurable separation between association cortex and sensory cortex. supramodal hubs lie at the *topological centre* of the network while unimodal areas are at the *periphery*.

Thanks to experimental techniques such as microelectrode recordings under controled visual or auditory stimulation, a good knowledge has been achieved about the organisation and information processing at the sensory cortex. The localisationist school, postulating that every function happens at certain localised place in the brain, has been quite successful at the level of the sensory cortex, where refined characteristics of the sensory stimuli are recognised by highly specialised groups of neurones. The spatial location of those neurones is, to a good approximation, the same for every individual. However, little is known about the anatomical substrate permitting higher level, more complex, processing such as cognitive processes and the emergence of consciousness. The localisationist perspective seems to fail at this higher level [50]. At least, no cortical area has been found whose lesion completely destroys consciousness.

The supramodal hubs found here seem to be serious candidates to perform such high level integration because they all have very fast access to information of different modalities. However, as previously pointed out, the closeness centrality of the hubs is not distinct from the value expected out of randomised networks, while their BC was significantly larger than expected. At this point, we have to admit that the accessibility of those hubs to global information is not a sufficient warranty to deduce that they really perform relevant multisensory information processing, nor integration. With the current results we can only affirm that the supramodal hubs are useful for the *transmission* of information from one modality to another. Where does the integration and processing happen, we cannot tell with certainty yet, because information *transmission* is not information *processing*. Another relevant question to answer at this point is, even if we assume that the supramodal hubs are responsible for the processing of multisensory information, why are there so many of them? is each of the hubs specialised in one and only one sort of multisensory processing *independent* of the other hubs? For the rest of this dissertation, we will try to answer these questions by focusing on the characterisation of the hubs and
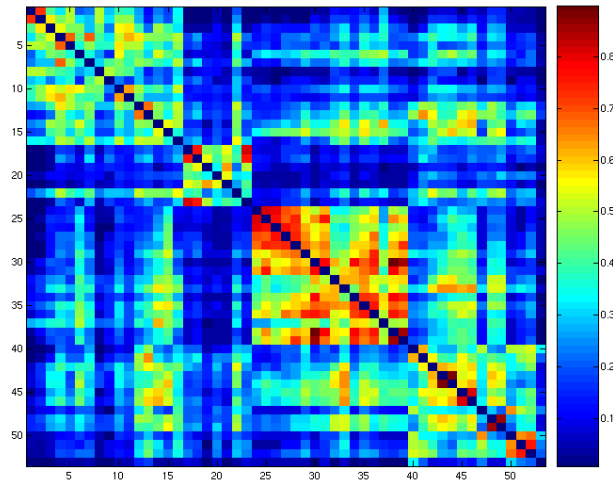
Figure 4.8: Pairwise matching index (normalised) of G_{cat}. The clustered organisation is unveiled by the topological similarity of the cortical areas.

their potential function.

4.4.1. Functional similarity: matching index

The matching index $MI(v, v')$ quantifies the pairwise similarity of areas in terms of their common afferents (inputs) and efferents (outputs). Following one of the central assumptions of systems neuroscience, that the functional roles of brain regions are specified by their inputs and outputs [101], we can safely refer to MI as a measure of *functional similarity* between cortical areas. Indeed, previous studies have successfully attempted a community analysis of cortical networks by grouping together areas with high MI [67].

In Figure 4.8 the MI matrix of G_{cat} is shown, where the four anatomical communities are easily distinguished. In order to investigate whether the supramodal hubs are functionally independent of each other, their average MI has been computed. Considering the set of supramodal hubs {20a, 20b, 7, AES, EPp, 6m, 6l, Ia, Ig, CGp, 35, 36} we obtain an average value of $MI(hubs) = 0.5013$. Compared to the averages of the anatomical communities $MI(V) = 0.3916$, $MI(A) = 0.4713$, $MI(SM) = 0.5811$ and $MI(FL) = 0.3509$, the functional similarity between the hubs is large, only exceeded by $MI(SM)$. This observation strongly indicates that the supramodal hubs are *not* functionally independent of each other, discarding the localisationist perspective as a valid organisation principle at the highest hierarchical levels of the cortex. Alternatively, it seems plausible to postulate that the supramodal hubs form a functional community and therefore, highest level processing and integration emerges as the functional *cooperation* between them. Certainly, this is a very strong statement and requires further analysis for confirmation.

4.4.2. Layered organisation of the network: k-core decomposition

The *k*-core decomposition [36, 118] is a useful graph analysis tool for visualisation of networks [4] because it "peels" the network into several layers. In the centre, only the most densely connected subgroup remains. It works in the following iterative manner.
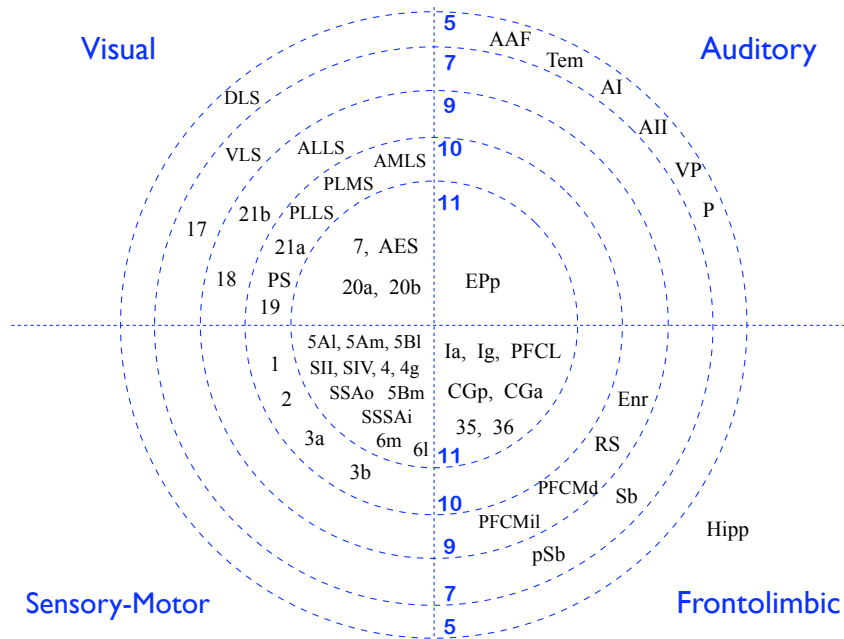
Figure 4.9: k-core decomposition of the cortico-cortical network of the cat. The SM areas dominate the *core* of the decomposition as a result of their dense internal connectivity.

The outermost layer, the **1-shell**, is composed of all the vertices with $k = 1$. They are removed from the network and the degree of the remaining vertices, $k'(v)$, is recomputed. If there are vertices with $k'(v) = 1$, they are also removed from the network and placed in the 1-shell. When no vertex has $k' = 1$, the same procedure is repeated for vertices with degree 2, and so on. At the end, a completely connected core of vertices remains, all having the same degree k'.

In Figure 4.9 the k-core decomposition of the cat cortex is shown. There are several observations to point out, but the most relevant is the dominance of the SM community at the central core. This is not in accordance with the centres and the classification obtained in the previous sections which were dominated by FL areas. A handicap of the k-core decomposition is that it is extremely dependent on local connection densities and therefore the results need to be considered with care. The decomposition cannot be directly regarded as a fair description of the hierarchial structure. The SM community is the densest of all the communities and therefore its dominance. Indeed, the largest complete subgraph[6] within the network consists of 8 areas, most of them somato-motor {6m, 5Am, 5Al, 5Bm, SSSAi, SSAo}, together with visual area AES and frontolimbic areas 35 and 36. The presence of this complete subgraph imposes difficulties for the proper characterisation of the hubs because it biases several observables.

Nevertheless, all areas previously classified as supramodal hubs lie at the core. The areas of V, A and FL are distributed over different shells, the Hippocampus being the most external of all. The V and FL cortices display a stratified arrangement, while all the auditory areas lie at the second most peripheral shell except for the auditory hub EPp, which lies directly at the core. One last observation is that no cortical area has degree

---

[6]A **complete graph** is a graph in which all vertices are linked to all others.
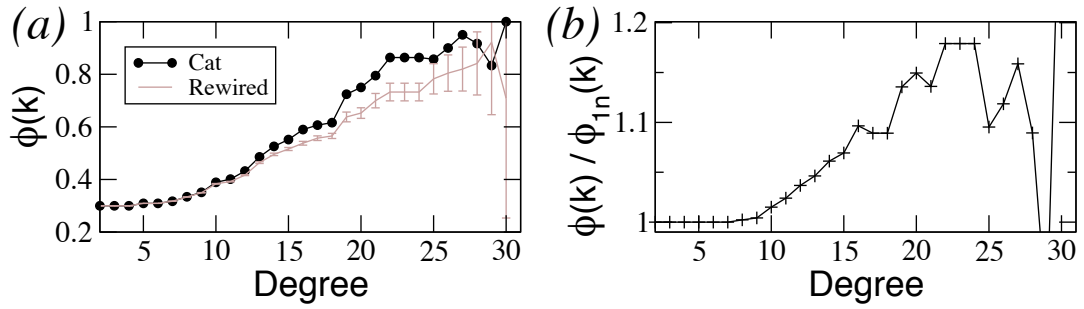
Figure 4.10: Rich club phenomenon in the cortico-cortical network of the cat. (a) Original measure, and (b) Relative difference between the k-density in the cat cortex and its expectation out of the $\{G_{1n}\}$ ensemble.

1 or 2, meaning that the network is very cohesive. Recently the structure of the 1-shell has received much attention because its vertices form tree-like structures "hanging out" of the connected core [145].

4.4.3. Rich-club phenomenon: a community for multisensory integration?

There is yet a similar manner to investigate whether the hubs of a network are topologicaly related, but without the interpretation problems of the k-core decomposition. The rich-club phenomenon happens when the hubs of a network (the "rich" vertices) are densely connected to each other forming a community. Considering only the vertices with degree larger than k', the k-density is defined as:

$$\phi(k') = \frac{L_{k'}}{N_{k'}(N_{k'} - 1)}, \qquad (4.5)$$

where $N_{k'}$ is the number of vertices with $k(v) > k'$ and $L_{k'}$ is the number of links between them. $\phi(k)$ is a monotonous increasing function of k[7]. Only when k' approaches k_{max} a decrease might be observed due to finite size effects. Thus, a plain measure of $\phi(k)$ is not very informative because hubs have a higher intrinsic chance of being connected. A comparison to random networks with the same degree distribution is necessary to investigate whether the increase of $\phi(k)$ with k is significant or not [159].

In Figure 4.10(a) the rich-club phenomenon as computed out of G_{cat} is presented[8], together with the ensemble average $\phi_{1n}(k)$ of $\{G_{1n}\}$. The ratio between the measured $\phi(k)$ and its expected value $\phi_{1n}(k)$ is also shown in Figure 4.10(b). The cat cortex displays a significant rich-club phenomenon. The most relevant k-density occurs for $k = 23$, comprising of a rich-club with of 11 cortical areas, precisely those areas with largest closeness and betweenness centralities {20a, 7, AES; EPp; 6m, 5Al; Ia, Ig, CGp, 35, 36}. This result corroborates that the supramodal hubs do form a tight community, instead of operating independent of each other.

---

[7]Notice that $\phi(0) = \rho(G)$, the density of the network. If the vertices with low degrees are removed, the remaining network contains more links per vertex than the original.

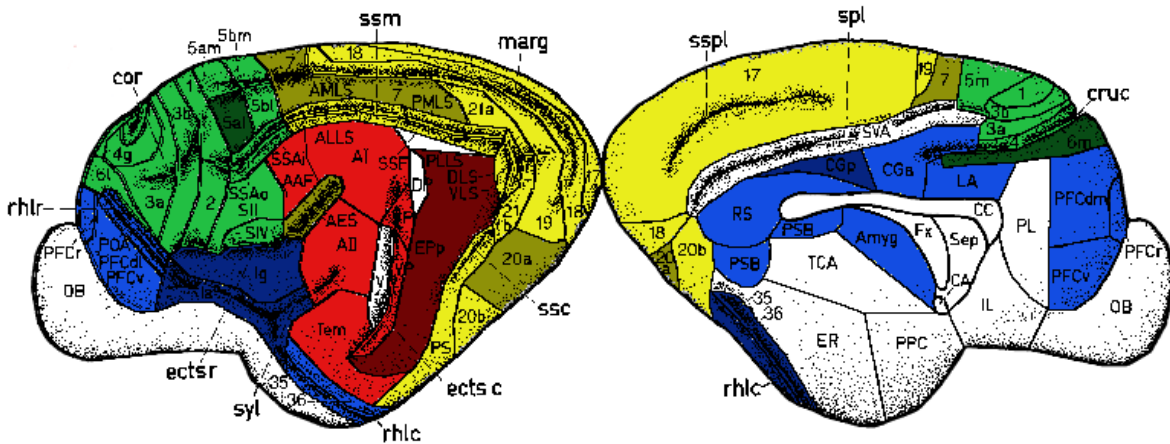[8]Again, we have considered $k(v) = 0.5(k_i(v) + k_o(v))$.

Figure 4.11: Illustration of the spatial location of the areas according to their modality: V (yellow), A (red), SM (green) and FL (blue). The supramodal hubs, coloured darker, form a topological community (densely connected to each other) which is spatially delocalised. Figure adapted from [83].

4.5. Summary and Discussion

In this chapter an extensive graph theoretical analysis of the cortico-cortical network of the cat has been presented, beyond the global and average measures previously studied. From the technical point of view, we have shown that graph theoretical measures can be applied in a flexible manner in order to overcome data limitations, instead of manipulating the data for analytical and computational convenience. Unfortunately, the latter is a common practice in the complex network literature. For example, directed networks are often artificially converted into non-directed ones.

It has been found that inter-area communication is dominated by very short paths; 87% of all areas are separated by a topological distance of only one (direct connections) or two steps. This strongly indicates that the direct connections are the most fundamental information processing paths in cortical communications (although this is not a proof of it). Nevertheless, it has also been stressed that the computation power of short paths should *not* be underestimated. We have detected a large number of "parallel" (alternative) shortest paths in the cortical network of the cat, which represents the anatomical substrate for rich and complex communication processes, i.e. a mixture of alternative and serial information processing.

The modular organisation of the cortex into the V, A, SM and FL communities plays a major role in the topology of the network, affecting all the graph measures applied. Low degree areas are predominantly connected to areas in their own community, while the hubs necessarily span their connections over more than one community. Notice that the largest community consists of only 16 areas and the hubs have degree up to $k = 31$. As a result, biases from expectation are observed in the outcome of graph measures, which permits to topologically distinguish the specialised cortical areas from those involved in higher level processes.

The evaluation of different graph measures leads to a consistent classification of the
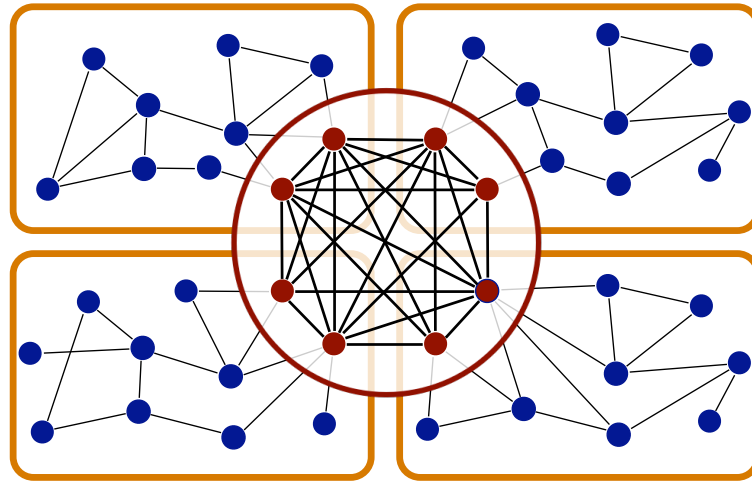
Figure 4.12: Illustrative representation of a novel hierarchical structure observed in the cortico-cortical connectivity of the cat. Every community contains few hubs which connect to the hubs of the other communities. Therefore, the highest hierarchical level is formed by a densely interconnected overlap of the communities. Such an overlap has the capacity of sharing and processing information of different character.

cortical areas, which largely coincides with the preliminary (tentative) categorisation proposed in Chapter 3 in terms of supramodal hubs, multimodal areas and unimodal areas. Particularly interesting is that each of the functional communities V, A, SM and FL contains at least one hub. Nevertheless, the set of hubs is dominated by FL areas, a fact that can be expected from neuroscientific knowledge, since the frontolimbic cortex is related to high order cognitive processes and association [50].

Moreover, we have found that the supramodal hubs are not topologically independent of each other but they are very tightly connected forming a community on their own. From the functional point of view, we now have a strong topological argument to envision large-scale processing and multisensory integration as the result of the collaborative function of the supramodal hubs, in a similar manner in which the cooperative processing of information by the visual areas gives rise to visual perception [44, 108]. There is yet a remarkable difference. While sensory areas of one modality lie physically close to each other, the supramodal hubs are spatially separated but densely connected through the long-range fibers via the white matter, and thus forming a *spatially delocalised* community. Figure 4.11 is an illustration of the cat cortex where areas are coloured according to the four anatomical subsystems: V (yellow), A (red), SM (green) and FL (blue). The regional distribution of the functional modules is evident, apart from the multimodal area AES. In contrast, the supramodal hubs, represented in darker colours, lie spatially separated from each other.

Finally, we have to reconsider the established overall organisation of the cortical network. A relevant question is that, if the hubs form such a densely connected subgroup, why the community detection algorithms do not find it? Actually, $\phi(k) > 0.8$ for the subset composed of all areas with $k > 21$, while the internal densities of the four com-

munities are $\rho(V) = 0.58$, $\rho(A) = 0.81$, $\rho(SM) = 0.74$ and $\rho(FL) = 0.65$. This does not mean that the current partition into four communities is wrong. Community detection algorithms do not simply favour the formation of densely connected subgroups. The cost function used to evaluate the validity of a partition, the modularity function Q, favours subgroups which are internally *denser than expected*, as computed from random networks with the same degree distribution (for example, the $\{G_{1n}\}$ ensemble). Since hubs have a high random chance of being connected, Q will not favour to join them together.

Another limitation of typical community detection methods is that they look for partitions, while very often communities tend to overlap each other, i.e. one vertex might participate in more than one community. From this point of view, the organisation characteristics discussed in this chapter do *extend* the current accepted cortical organisation. What we find is that the multisensory hubs form a community which is overlapping the four anatomical communities, and therefore, the rich-club forms a higher hierarchical level. In Chapter 1, two common manners of understanding a hierarchy have been described. One, after Ravasz and Barabási [105], is a tree-like fractal structure. At the top of the hierarchy, there is a community whose central vertex receives connections from the vertices at the top level and from the communities at lower hierarchies. Such centralised patterns of connections is repeated through the different levels (Figure 1.3(a)). The second type of hierarchy, after Arenas et. al [8], considers a hierarchy as the agglomeration of communities, say, small communities join together and form larger communities (Figure 1.3(b)).

The hierarchical organisation that we are describing here is none of these two, but it might be regarded as a mixture of them. In the second type, the small communities are randomly linked to each other, so that their union forms a larger community. In our case, the intercommunity links are not random, but centralised. Every community contains few hubs which connect to the hubs of the other communities. Therefore, the highest hierarchical level is not formed by the union of the whole communities, but is composed by the overlap of a small part of them. In Figure 4.12, a schematic representation of this novel hierarchical organisation is presented. In such a configuration the hubs of each community are not just passive transmitters of information, but form a tight community which has the capacity of sharing the local infomation of different modalities.

CHAPTER 5:

Towards a Formalism to Measure Integration

The term *information processing* is a generic concept which covers different processes like filtering, signal transformations, integration, memory allocation and retrieval, etc. For example, functional magnetic resonance (fMRI) studies reveal patterns of brain *activity* which permit to identify the brain regions *related* with certain cognitive task. Unfortunately, it is very difficult to understand *what* is exactly an activated region doing. Is it filtering a signal? Is it making copies of information and distributing it somewhere else? Does the fMRI detect an activation only because that particluar region contains memories which are being retrieved and passed to other regions for further processing?

This final chapter represents a preliminary effort to translate the relationship between structure and function into more solid and consistent grounds. At least part of it, because only the concept of integration is investigated. The reason is to justify in a more consistent manner the integrative function assigned in the previous chapters to the top hierarchical level detected in the cortical network of the cat. After briefly reviewing fundamental notions of information theory, the concept of *integration* is presented in terms of the *capacity* that a subset of areas have to integrate information. This concept is then translated into measurable properties at the topological and the dynamical levels.

Entropy and Integration

Information theory has been very succesful determining problems of transmission of information, encoding and channel capacity. At the root of this success lies the original idea of Shannon to translate concepts of statistical physics to represent the nature of communication. The Shannon entropy is defined in the following manner. Consider a system A with M possible states. That is, a measurement made on A will yield one of the possible values $a_1, a_2, \ldots a_M$, with a probability $p(a_i)$. The average ammount of information gained from a measurement that specifies one particular value a_i is given by the entropy of the system $H(A)$ [119, 29]:

$$H(A) = -\sum_{i=1}^{M} p(a_i) \log p(a_i). \tag{5.1}$$

As stated by Faser and Swinney [46], the entropy $H(A)$ could be interpreted as the *quantity of surprise one should feel upon reading the result of a measurement.* The entropy vanishes

when the system has only one accessible state, meaning that the value a is obtained with certainty (there is no suprise). $H(A)$ is maximum when all the states are equally likely, $p(a_i) = \frac{1}{M}$ for all $i = 1, 2, \ldots M$. As there are no preferred states, the ammount of uncertainty (surprise) upon measurement is maximum[1].

To quantify the *statistical dependence* between two systems A and B, their mutual information is defined as [131]:

$$MI(A, B) = H(A) + H(B) - H(A, B), \tag{5.2}$$

where $H(A, B)$ is the joint entropy. By definition $H(A, B) \leq H(A) + H(B)$, and the equality is only fulfilled if A and B are statistically *independent*. In this case $MI(A, B) = 0$, and otherwise $MI(A, B) > 0$.

Unfortunately, the problem of *integration* has received little attention. In a series of papers during the 1990s, Tononi and Sporns introduced a measure which aims to characterise and quantify integration [137, 138, 139]. Given a system X composed of N elements (subsystems), the integration of the system is defined as:

$$I(X) = \sum_{i=1}^{N} H(x_i) - H(X) \tag{5.3}$$

where $H(x_i)$ is the entropy of one element and $H(X)$ the entropy of the system considered as a whole. Comparing to Equation (5.2), one realises that $I(X)$ is an extension of the mutual information to account for more than two systems. $I(X) = 0$ only if all the elements $x_i \in X$ are statistically independent of each other, and positive otherwise. In other words, $I(X)$ measures how much is the system X *internally integrated* and, in the case of dynamical systems, it could be considered similar to the total amount of correlation between the elements x_i; only that $I(X)$ might capture nonlinear effects to which correlation is insensitive.

Returning to the cortical network of the cat, this definition of integration is useful, but only to a limited extent. Remind that the gross structural organisation described in the previous chapter consists of a balance between segregation and integration. Each community receives sensory information which is different in character, e.g. visual or auditory, and performs a specialised processing of that input. A higher hierarchical level, composed of the supramodal hubs, might be the responsible for putting that different information together and produce a global, integrated, perception. Naively speaking, the capacity of integration that we are looking for should be defined as something like: *the capacity of one or more nodes to receive information of different character and combine it to obtain new useful information.* Certainly, this involves crucial theoretical problems, e.g. how to define what the *character* of information is, or what does it mean to *combine* information.

---

[1]As $p(a_i) = 1/M$, then $H_{max}(A) = -\sum_{i=1}^{M} \frac{1}{M} \log \frac{1}{M} = -\log \frac{1}{M}$. Now, the entropy can be normalised for comparison of different systems, $H'(A) = \frac{H(A)}{H_{max}(A)} \in [0, 1]$.

5.1. Topological Capacity of Integration

Although fundamental aspects are still unclear, from the topological point of view the capacity of a node (or a set of nodes) to integrate information should depend in few measurable properties. We propose the following conditions:

1. **Accessibility to the information:** In order to perform integration, a node needs access to the information that is being processed in the system. This capacity could be quantified by centrality measures such as betweenness and closeness centralities. In the presence of communities, the participation index might be also a possible indicator.

2. **Segregation of the system after selective damage:** The removal of selected nodes may cause a reduction in the capacity of the network to integrate information. This can be studied by typical percolation and robustness analysis. If there is modular organisation, the segregation may be captured by an increase in the modularity after intentional attack. If the intercommunity links are removed, then the communication between the communities becomes more difficult.

3. **Capacity of sharing information:** If more than one node is considered, it is necessary for them to be densely connected with each other, otherwise, even if they all are central and receive information from everywhere, they cannot combine information.

In the following, a practical implementation of these concepts is introduced in order to corroborate (or negate) the integrative function of the rich-community of the cat cortical network. In accordance to the data analysis criteria established, we pursue for a statistical description rather than for deterministic results which might be biased by the limitations of the data. Thereafter, all cortical areas with output degree $k_o(v) \geq 20$ have been considered as potential members of the integrator community: {20a, 7, AES; EPp; 6l, 6m, 5Am, 5Al, 5Bm, 5Bl, SSSAi, SSAo; PFCL, Ia, Ig, CGa, CGp, 35, 36}. Out of these 19 areas, all their possible combinations have been constructed with sizes ranging from $N_S = 1$ to $N_S = 19$. There is a total of $524,097$ subsets and we refer to them as $\mathcal{S}_{hubs}$. The aim of the analysis is to detect those cortical areas which, grouped together, possess a higher capacity of integration in topological terms.

5.1.1. Characterisation of Accessibility

Among the possible measures one could define to formulate accessibility, a modification of the betweenness centrality has been chosen. In Chapter 1, the betweenness was defined as:

$$BC(v) = \frac{\sum_{i,j \neq v}^{N} \sigma_{i,j}(v)}{\sum_{i,j=1}^{N} \sigma_{i,j}}$$

where $\sigma_{i,j}(v)$ is the number of shortes paths from i to j going through v and $\sigma_{i,j}$, all the shortest paths from i to j. Considering a subset of vertices S of size N_S, the **accessibility**
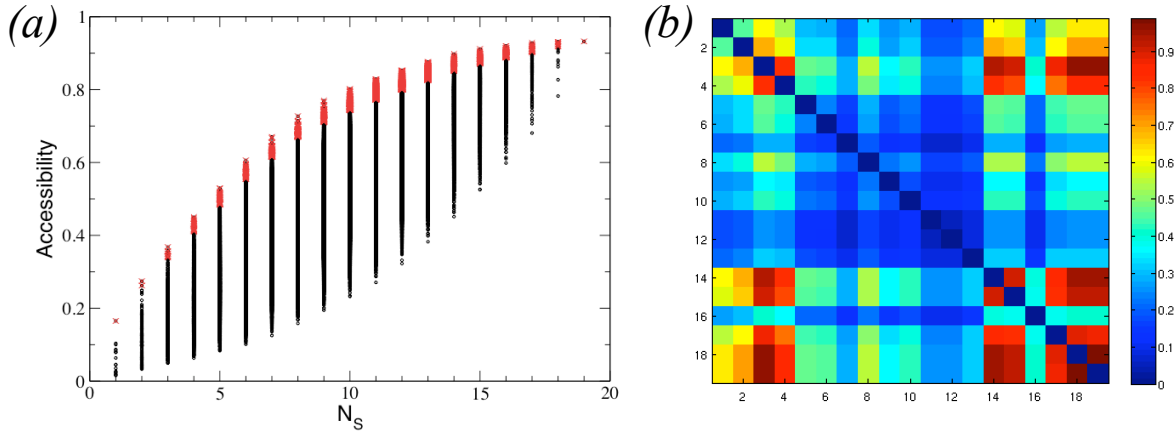
Figure 5.1: Accessibility measure $A(S)$ applied to the $524,097$ combinations of areas with $k_o(v) \geq 20$. (a) The results displayed for combinations of a given size. As expected, $A(S)$ is an icreasing function of N_S, although for the combinations of a given size, there might be large differences. In red, the maximal sets S' for which $A(S') > 0.9\, A_{max}^{N_S}$ are shown. (b) Co-participation matrix representing the fraction of maximal sets in which a pair of areas participate together.

is defined as the fraction of shortest paths between vertices $i, j \notin S$, which go through *at least one* of the vertices in S:

$$A(S) = \frac{\sum_{i,j \notin S} \sigma_{i,j}(S)}{\sum_{i,j \notin S} \sigma_{i,j}} \tag{5.4}$$

For all the $524,097$ subsets $S \in \mathcal{S}_{hubs}$, the accessibility $A(S)$ has been measured and the results are displayed in Figure 5.1(a). As it is expected, $A(S)$ increases with the size of S, i.e., the more vertices in S, the larger is the chance that paths go through at least one of them. However, among the subsets of a fixed size, some achieve very large $A(S)$ while others obtain small values, e.g. for all the subsets of size $N_S = 10$, some absorb up to 80% of the shortest paths between vertices $i, j \notin S$, while other subsets are only used in 20% of the paths. These large differences indicate that the proposed measure permits to discriminate between accessible and non-accessible sets of nodes.

Let $A_{max}^{N_S}$ be the largest accessibility achieved by combinations of size N_S. In order to detect the cortical areas which are most accessible, only the combinations with $A(S) \geq 0.9 A_{max}^{N_S}$ are chosen (red crosses in Figure 5.1(a)). The number of times that two areas simultaneously take part in each of the maximal subsets has been counted and the results summarised into a **co-participation matrix** of size 19×19, shown in Figure 5.1(b). The visual area AES, the auditory area EPp and the frontolimbic areas Ia, Ig, 35 and 36 participate together in over 80% of the maximal subsets. The visual area 7 joins them in 65% of the cases. The most frequent somato-motor area, area 6l, is present in only 50% of all the maximal subsets.

We shall admit that these results are somehow trivial, because the core of accessible areas is composed precisely by those with largest betweenness centrality. Anyway, in general, this might not be always the case. As explained in Chapter 4, the cortico-cortical network of the cat is characterised by a very short average pathlength, 80% of all pairwise communications are done either by direct links or paths of length 2. In this
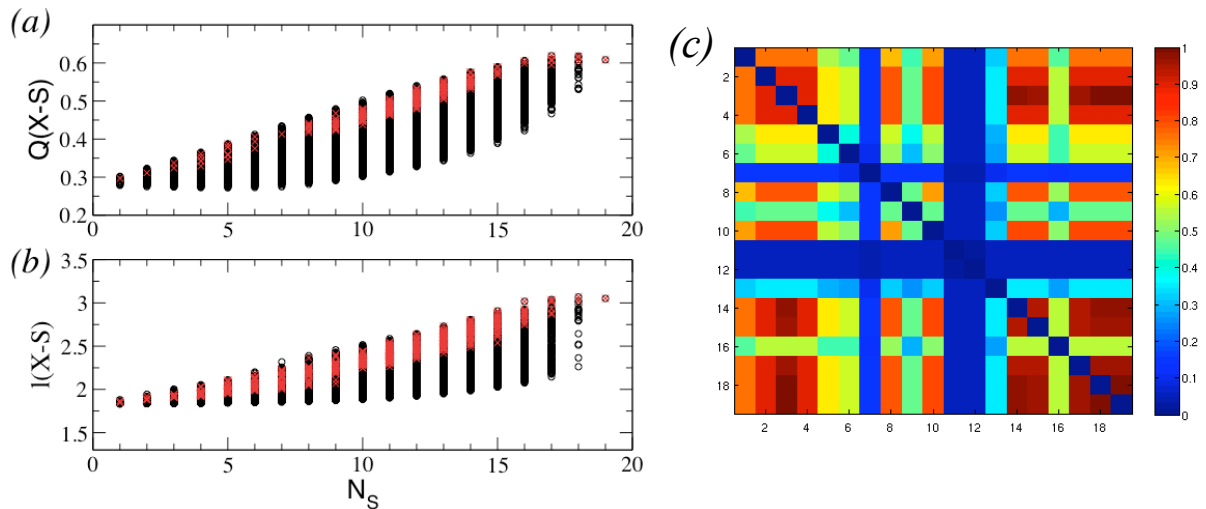
Figure 5.2: Segregation of the network after simultaneous lesion of various cortical areas. (a) Modularity of the lesioned networks, $G_S = X - S$, evaluated on the four anatomical communities V, A, SM and FL. Removal of particular sets increases the modularity as a consequence of the topological separation suffered by the communities. (b) Average pathlength of the lesioned networks, G_S. Even if the lesioned networks are smaller than the original X, the removal of particular combinations leads to a relevant increase of the average pathlength. (c) Co-participation of the cortical areas whose *simulatneous* lesion leads to both large $Q(G_S)$ and large $l(G_S)$.

escenario shortest paths dominate and thus, the individual betweenness of the vertices is very relevant. But in networks with longer paths, the collective accessibility should be less dependent on the betweenness of individual vertices.

5.1.2. Robustness analysis after multiple lesions

For decades, the only manner of inferring the functional characteristics of particular brain regions was through the phsycological study of patients with localised brain lesions. Nowadays, *in-vivo* microelectrode recordings and imaging techniques form the experimental frontline for that quest. Using the cortico-cortical connectivity data of macaque and cat previous works have paid attention to the effects of brain lesions. Young et al. [152] studied the changes in the activity of a simulated cortical networks after removal of individual areas. Recently, robustness of cortical networks against random or selective attack has been found to follow damage profiles similar to those of scale-free networks [79].

In another context, the robustness of metabolic networks has been studied in terms of the modularity of the remaining network after selective removal of the hubs [74]. In this manner, they could identify a set of *currency metabolites* whose removal increases the modularity of the network, i.e., the specialised modules become segregated from each other. In order to analyse the potential collective function of cortical hubs for integration, we adopt here a slightly different robustness analysis, which is based on the *simultaneous* damage of groups of areas rather than one-by-one attacks.

Referring to the original network of the cat as system G_{cat}, when all areas in a subset

S are simultaneously removed, two properties of the lesioned network $G_S = G_{cat} - S$ have been measured to quantify the damage:

1) the modularity $Q(G_S)$ of the lesioned network G_S, considering the four original communities (what remains from the original communities), and

2) the average pathlength of the lesioned network $l(G_S)$.

Note that in [74], the authors recomputed the communities after each attack was performed. In our case, running a community detection algorithm for each of the $524,097$ realisations would have been prohibitive, and therefore the modularity of G_S has been computed on the basis of the four anatomical communities V, A, SM and FL, which loose some areas due to the lesion. The results are shown in Figure 5.2. The red dots in Figure 5.2(a) correspond to the subsets whose lesion gives rise to the largest increases in l, and in Figure 5.2(b), they correspond to the subsets whose lesion gives rise to maximal increase in the modularity. This is only to show that if the lesion of S' leads to a large increase of modularity, then it also triggers a large increase of the average pathlength. The opposite is also true hence, both measures are valid to quantify the segregation, although not completely equivalent. There are yet some small diferences and to get rid of them, we have considered only the subsets whose lesion simultaneously cause a large $Q(G_S)$ and a large $l(G_S)$. The co-participation matrix of cortical areas in those maximal subsets displays again a core of areas participating together in more than 80% of the cases: {7, AES; EPp; 5Al, 5Bl; Ia, Ig, CGp, 35, 36}. The surprise is now the presence of SM areas within this core.

The third condition proposed to support the integrative function of a set of areas, is that they must be densely interconnected between them. Otherwise, they could not possibly share and combine the information that they receive. This condition has been studied in Chapter 4 with the analysis of the rich-club property.

5.2. Dynamical Capacity of Integration

The final section of this dissertation is devoted to translate the concept of *integration capacity* into a dynamical framework. The following shall be considered as an exploratory effort rather than a finished work. The ideas proposed here will be most useful if they could be formulated for application in time series analysis of networked dynamical systems, e.g., the signals out of electroencephalograms (EEG). The Equation (5.3) provides a measure to quantify integration in dynamical systems. For the exploratory purpouses of this section, we consider an extremely simple dynamical model which has the benefit of being analytically solvable. If the elements of a linear system are assumed to be driven by a Gaussian noise ξ_i, the system at the *steady-state* is described by $x_i = g \sum_j A_{ij}^t x_j + \xi_i$, where g is the coupling strength and A_{ij}^t the *transpose* of the adjacency matrix[2]. Written in matrix form:

$$\mathbf{x} = g\mathbf{A^t}\mathbf{x} + \boldsymbol{\xi}. \tag{5.5}$$

---

[2]otherwise the dynamics of x_i would be characterised by its own outputs, not by the inputs from other elements.

Similar approaches have already been used for cortical models [83, 152] in which the variable x_i is regarded as the **activity level** of the cortical area. Another possibility is to interpret x_i as a **mean firing rate** (MFR) of the neurones in the area [17]. The entropy of such a multivariate Gaussian system X can be analytically estimated from its covariance matrix [100, 138]: $H(X) = \frac{1}{2}\log\left[(2\pi e)^N|COV(X)|\right]$, where $|COV|$ stands for the determinant. The entropy of an individual Gaussian process is $\frac{1}{2}\log(2\pi e\nu_i)$, where ν_i is the variance of x_i, i.e., the ith diagonal element of the matrix $COV(X)$. Replacing in Equation (5.3), the integration of such a multivariate Gaussian system is given by:

$$I(X) = \frac{1}{2}\sum_{i=1}^{N}\log(2\pi e\nu_i) - \frac{1}{2}\log\left[(2\pi e)^N|COV(X)|\right] \tag{5.6}$$

Written in this form, $I(X)$ seems to depend on the system size N. We find however that the measure is properly normalised. By using logarithm algebra, the first term of Equation (5.6) can be expanded as:

$$\sum_{i=1}^{N} H(x_i) = \frac{1}{2}\log\left[\prod_{i=1}^{N}(2\pi e)\nu_i\right] = \frac{1}{2}\log(2\pi e)^N + \frac{1}{2}\log\left[\prod_{i=1}^{N}\nu_i\right].$$

The second term of Equation (5.6) is trivially expanded into a sum and this allows the annulation of the terms containing $\log(2\pi e)^N$. Therefore the expresion for the integration can be simplified:

$$I(X) = \frac{1}{2}\sum_{i=1}^{N}\log(\nu_i) - \frac{1}{2}\log|COV(X)| = \frac{1}{2}\ \log\left[\frac{\prod_{i=1}^{N}\nu_i}{|COV(X)|}\right] \tag{5.7}$$

According to [100, 138], the covariance matrix can be analytically computed by solving the system such that:

$$\mathbf{x} = \frac{1}{\mathbf{1} - g\mathbf{A^t}} \cdot \boldsymbol{\xi} = Q \cdot \boldsymbol{\xi}.$$

Averaging over the states produced by successive values of $\boldsymbol{\xi}$, the covariance matrix is obtained: $COV(X) = \langle \mathbf{x}\cdot\mathbf{x}^t\rangle = \langle(Q\cdot\boldsymbol{\xi})\cdot(\boldsymbol{\xi}^t\cdot Q^t)\rangle = Q\cdot Q^t$ [100, 138].

There is still a technical problem which has been poorly addressed in [137, 138, 139]: the system has several poles depending on the coupling strength g. The first pole is given by $g_1 = \frac{1}{\lambda_{max}}$ where λ_{max} is the largest eigenvalue of the adjacency matrix $\mathbf{A^t}$. In principle, the solutions of system (5.5) only have physical meaning for $g < g_1$, otherwise the stationarity condition does not hold. The weighted cortico-cortical network of the cat has $\lambda_{max} = 29.02732$ and thus, it has a first pole at $g_1 = 0.03445$. To compare the dynamics of different networks, from now on the normalised matrix $\hat{\mathbf{A}} = g_1\mathbf{A^t}$ is considered. In this manner, the system has its first pole for $g = 1$ as displayed in Figure 5.3, regardless of the precise adjacency matrix.

Finally, a proper coupling strength g needs to be chosen. For that, the analytically estimated covariance matrices of the cat cortical network have been computed for different couplings, see Figure 5.4. The results are similar to the simulations presented in papers III and IV by using a multilevel model, where each cortical area has been simulated by a
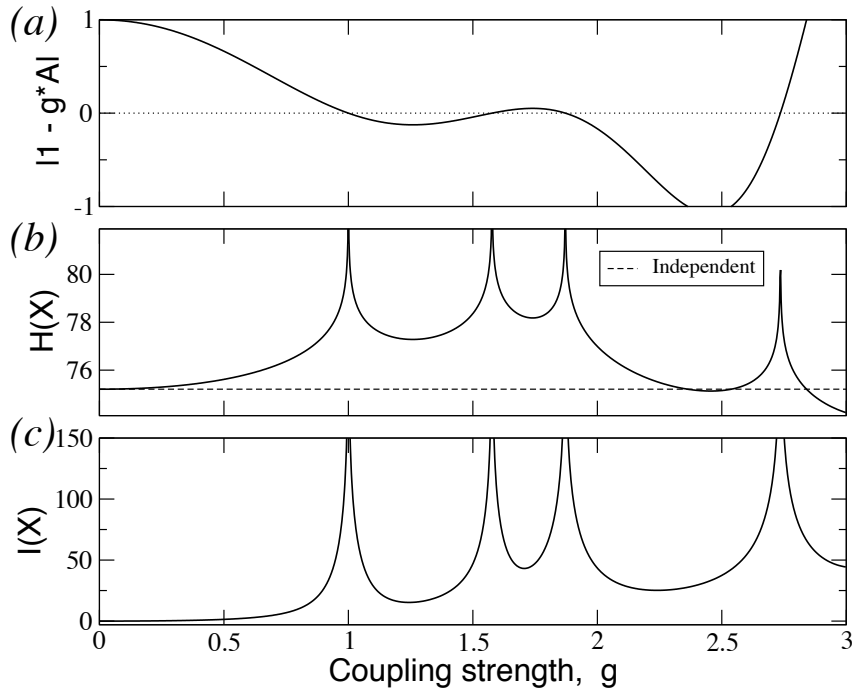
Figure 5.3: Parametric study of the linear system (5.5) using the cortical network of the cat. (a) Integrability range. When the determinant $|1-g\hat{A}| = 0$ the system has a pole. Negative values lead to non-physical solutions. (b) Entropy and (c) Integration diverge around the poles.

subnetwork of 200 neurones. At low coupling regimes the dynamical correlation between areas largely follows the underlying anatomical connectivity, and as the coupling is increased, the V, SM and FL communities *melt* together. Still, there are some differences. For example, in the present case the auditory system dissapears in the strong coupling regime ($g \gtrsim 0.7$). Nevertheless, this result indicates the validity of the simple linear system (5.5) for the exploratory purpouses of this section.

Once the dynamical framework has been established, we can now define segregation and the capacity of integration in dynamical and information theoretical terms.
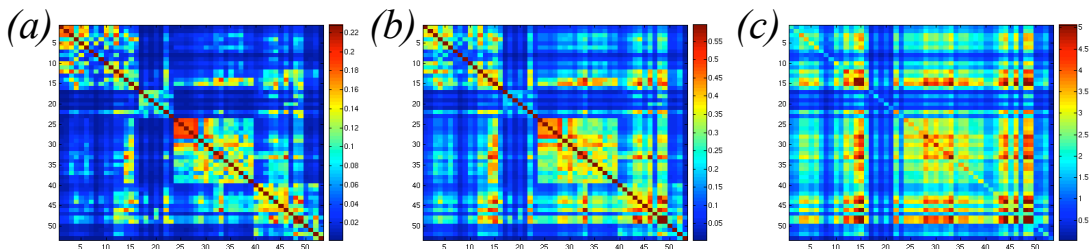
Figure 5.4: Analytically estimated covariance matrices of the cat cortical network. The adjacency matrix has been previously normalized by $1/\lambda_{max}$ and the noise level set to $\xi_i = 1.0$. (a) $g = 0.5$, (b) $g = 0.7$ and (c) $g = 0.9$.

Figure 5.5: Dynamical segregation of the communities V, A, SM and FL after simultaneous lesion of cortical areas. (a) The modular integration $I_{\mathcal{P}_4}(G_S)$ increases for some subsets respecting to $I_{\mathcal{P}_4}(G_{cat})$ of the original system (dashed line). Lesion of other subsets leads to a large independence of the communities (red dots). (b) Co-participation matrix of the areas participating together in the subsets marked by red dots in (a).
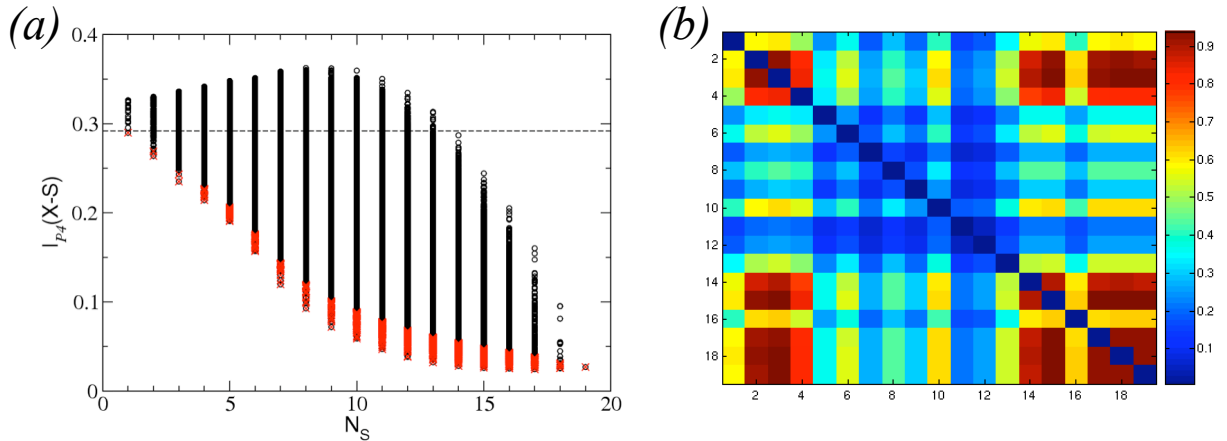
5.2.1. Dynamical segregation after multiple lesions

The measure of integration $I(X)$ is an extension of the mutual information for more than two systems. Defined as it is, $I(X)$ represents the extremal case in which all the elements $x_i \in X$ are considered individually. However, one could also define $I(X)$ for sets of elements and cover different scales of the organisation. Imagine a partition of the vertices $\mathcal{P} = \{S_1, S_2 \dots S_n\}$ such that $X = S_1 \cup S_2 \cup \dots \cup S_n$, then we define the **modular integration** as:

$$I_{\mathcal{P}}(X) = \sum_{j=1}^{n} H(S_j) - H(X). \tag{5.8}$$

When $n = N$, then $I_{\mathcal{P}}(X) = I(X)$. The entropy of a subset $S \subseteq X$ can be obtained by first computing $COV(X)$ of the system and then extracting from it the covariance submatrix $COV(S)$ for the elements $x_i \in S$. Thus, $H(S) = \frac{1}{2} \log \left[(2\pi e)^{N_S} |COV(S)| \right]$.

In order to characterise the dynamical segregation, we measure the statistical dependence between the anatomical communities, $\mathcal{P}_4 = \{\text{V, A, SM, FL}\}$, by use of the modular integration $I_{\mathcal{P}_4}(X - S)$ of the lesioned network $G_S = G_{cat} - S$. If the removal of a subset of areas S leads to a dynamical independence of the communities, then $I_{\mathcal{P}_4}(G_S) = 0$. The results after lesioning all the $524,097$ subsets $S \in \mathcal{S}_{hubs}$ are shown in Figure 5.5. The original network has a modular integration of $I_{\mathcal{P}_4}(G_{cat}) = 0.292$. Even if all areas removed have a large degree, the lesion of some subsets does increase the dynamical dependence between the communities ($I_{\mathcal{P}_4}(G_S) > 0.292$), while the lesion of other subsets leads to relevant dynamical separation of the communities, see Figure 5.5(a). Considering only the subsets whose lesion leads to small values of $I_{\mathcal{P}_4}(G_S)$ (red dots in Figure 5.5(a)), a co-participation matrix has been constructed, Figure 5.5(b). A core of areas is observed $\{7, \text{AES}; \text{EPp}; \text{Ia, Ig, CGp, 35, 36}\}$ whose simultaneous lesion leads to a large dynamical segregation of the communities.
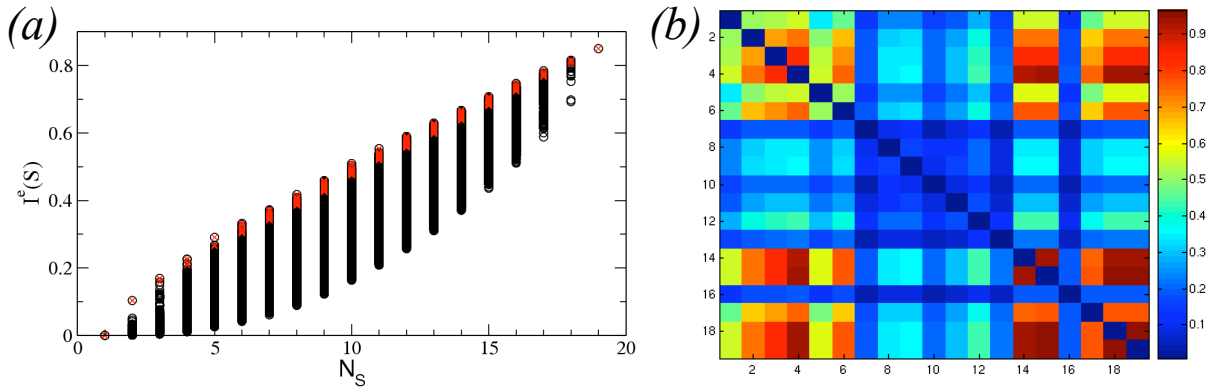
Figure 5.6: Functional capacity of integration of cortical areas under stimulation of the primary sensory areas (visual area 17, auditory area AI and somato-sensory areas 1, 2 and 3b). Stimulated areas are given a larger noise level $\xi_j = 10.0$. (a) Local integration $I(S)$ (considering only subsets of areas). The differences in $I^e(S)$ permit the identification of subsets involved in the integration of multisensory information. (b) Co-participation matrix of cortical areas within the subsets leading to large $I^e(S)$ (red dots).

5.2.2. Integration capacity after sensory stimulation

The solution of the linear System (5.5) when all ξ_i are equal (see Figure 5.4) might be interpreted as the activity of the cortical areas in the *resting-state*, say, when a subject is relaxed and performing no specific mental activity. All areas are driven by a Gaussian noise of small intensity and by the input of their neighbours. In the beginning of the chapter, the following has been stressed:

1) We aim to characterise the capacity of a group of areas to integrate the information present in the system, and

2) integration might be described as the combination of information of *different character*.

To quantify the integration of a subset of areas S, a submatrix $COV(S)$ can be extracted from the $COV(X)$ of the whole system. Then, the local integration $I(S)$ is calculated in an equivalent manner than $I(X)$:

$$I(S) = \sum_{x_j \in S} H(x_j) - H(S) = \frac{1}{2} \, \log \left[\frac{\prod_{j=1}^{N_S} \nu_j}{|COV(S)|} \right]. \tag{5.9}$$

Even if it is unclear how to define the *character* of information, in the case of cortical networks there is an additional fact which helps to overcome this problem. Sensory information of different modalities enters the cortex through specific regions called primary sensory areas: primary visual cortex (area 17), primary auditory cortex (area AI) and primary somato-sensory cortex (areas 1, 2 and 3b[3]). In order to quantify the capacity

---

[3]According to reference [115] the cortical areas identified as 1, 2 and 3b are subregions of the primary sensory area, called by some authors as SI.

of the specific areas to integrate the multisensory information entering the cortex, all primary sensory areas {17, AI, 1, 2, and 3b} have been simultaneously excited and $I(S)$ has been computed for all $S \in \mathcal{S}_{hubs}$. The excited areas are assigned a larger noise level $\xi_j = 10.0$, while for the rest of areas $\xi_i = 1.0$ as before. As the integration is now measured in conditions of excitation, we refer to it as $I^e(S)$.

The results, depicted in Figure 5.6, display similar characteristics to the previous ones observed along this chapter, Figures 5.1, 5.2 and 5.5. For a fixed size N_S, the local integration of subsets in the excited system, $I^e(S)$, largely differs among the subsets. For example, within the subsets of size $N_S = 10$, some of them achieve $I^e(S) \approx 0.5$ while others have only $I^e(S) \approx 0.15$. Initially, 19 cortical areas have been considered to form the subsets $S \in \mathcal{S}_{hubs}$. The differences in $I^e(S)$ permit to discriminate the cortical areas involved in the integration of multisensory information from those which are not. Considering only those subsets S' with local integration among the 10% of largest $I^e(S')$ for each size, red dots in Figure 5.6(a), the co-participation matrix of the cortical areas has been constructed, Figure 5.6(b). The elements of the co-participation matrix correspond to the number of times (given in frequency) that two areas participate together in one of the maximal subsets. As for previous measures, a core of cortical areas is found which participate together in over 75% of all the subsets with 10% largest $I^e(S)$: {7, AES; EPp; 6m; Ia, Ig, CGp, 35, 36}. The next areas to join this core are the visual 21a and the somato-motor 6l, but they co-participate only in 50% of the occasions with those areas in the core.

5.3. Summary and Discussion

In Chapters 3 and 4, the topological organisation of the cortico-cortical network of the cat has been extensively analysed. The relation between the observed structure and its potential function has been justified in the basis of intuition and neuroscientific facts. For example, the observed organisation of cortical areas into modules, which are segregated from each other, can be explained as a functional necessity to keep separated the cortical regions specialised in processing the input of one sensory modality (visual, auditory, ...) After finding that most of the pairwise communications are performed by direct connections or paths of length 2, the coincident inputs and outputs of two cortical areas can be interpreted as a sign of their functional similarity.

The main result of Chapter 4 is the finding that most of the intra-modal communication is centralised, mediated by a set of hubs which are densely connected with each other. While the centrality of the hubs is a sign of their accessibility to the information in the system, it only warranties their role as *transmitters* of information between the sensory systems. The additional observation that the hubs are densely interconnected, strongly suggest that they might be the responsible for integrating the multisensory information in the brain, which is a necessary condition for the emergence of generalised states of perception, e.g. consciousness [30, 108, 121, 135]. In order to construct a more solid bridge between the observed structural organisation and its potential function, in this chapter the concept of integration has been revisited. The *capactiy of integration* of a group of areas has been expressed in terms of: 1) accessibility to the information of different character, 2) the capacity to combine that information and, a weaker condition

3) the inefficacy of the system to integrate information in the absense of key areas. An effort has been done to translate these theoretical conditions into measurable quantities both in topological and in dynamical terms.

From the topological point of view, the *accessibility* to information has been quantified as a modification of the betweenness centrality to account for the collective behaviour of more than one area. The *segregation* of the system after selective lesion of cortical areas has been performed by the simultaneous attack on several areas instead of the typical one-by-one removal of vertices. To quantify the effect of the lesions, the modularity and the average pathlength of the remaining (lesioned) network have been measured. In order to accomplish a statistical analysis, the 19 cortical areas with largest degree have been considered as potential *integrators*, and all their possible combinations, a total of $524,097$ sets. The results permit to discriminate between the hubs whose collective behaviour leads to large integration capacity from those which are not relevant for the integration of multisensory information.

In order to study the capacity of integration in dynamical terms, a simple linear dynamical model has been adopted which has the benefit of being analytically solvable, Equation (5.5). Cortical areas are driven only by Gaussian noise and the input from their neighbours. Modifications of the integration measure $I(X)$ introduced by Tononi and Sporns [136, 138] have been applied. The dynamical separation between the systems (V, A, SM and FL) after lesions of subsets of areas has been quantified by the *modular integration*, a modification of $I(X)$ to account for different scales within the system. Finally, the collective integration capacity of the hubs has been studied by stimulation of the *primary sensory areas*. Sensory information enters the cortex through specific cortical areas, visual primary cortex (area 17), primary auditory cortex (area AI) and primary somatosensory areas (area 1, area 2 and area 3b). It has been observed that simultaneous stimulation of the primary sensory areas in the model, leads to a large dynamical dependence, *local integration* $I^e(S)$, of some hubs but not of others. This collective response to multisensory stimulation confirms the integrative function which has been assigned to the supramodal hubs along chapters 3, 4 and 5 based uniquely on topological properties.

While the concepts and the tools defined in this chapter should still be considered preliminary, the results show their potential use and validity. All the different measures, topological and dynamical, have led to consistent and coincident results. In general, we have been able to statistically discriminate the cortical areas which play a collective role in the integration of multimodal information from those hubs which don't. The dynamical analysis of this chapter has been based in a very simple linear model for which the proposed measures can be analytically calculated. In the future, it would be of interest to define the measures for integration such that they can be applied to the time series of multivariate systems, e.g. the output of electroencephalograms (EEG) or functional magnetic resonance (fMRI). While these experimental techniques do largely contribute to understand the neural basis of cognition and sensory perception, they present several limitations. One of them is that the only dynamical information we obtain is the *activation* of particular brain regions during a behavioural task or as the consequence of sensory stimulation. Still, there is no manner to understand from the data *what* is each activated brain region explicitly doing within the ongoing information processes.

CHAPTER 6:
Summary and Discussion

Traditionally, complex dynamical systems are characterised by a large number of nonlinearly interacting elements. The recent discovery of an intricate and nontrivial interaction topology among the elements in natural systems introduces a new dimension to the spectrum of complexity. A network representation provides the system with a form (topology) which can be mathematically tractable towards uncovering its functional organisation and the underlying design principles. The term *complex* is coined because most real systems have neither a regular nor a completely random topology, they survive in some intermediate state, probably governed by rules of self-organisation.

The mammalian nervous system (NS) is a complex system par excellence. Composed of over 10^{10} neurones, it is the responsible for collecting and processing information, and providing adaptive responses which permit the organism to survive in a constantly changing environment. Despite the large number of neurones and their different forms, they only collect and transmit two kinds of electrical signals: graded potentials and action potentials (spikes). Hence, the capacity of the nervous system to simultaneously process different kinds of information relies, to a large extent, on the circuitry where the stimulus is received and processed. Sensory neurones encode information into electrical signals which propagate in a "bottom-up" manner through different processing stages of increasing complexity. Information of the same modality (visual, auditory, etc.) traverses the body together, and separated from the information paths of other modalities. Even at the cerebral cortex, sensory information is segregated and processed in distinct regions which are specialised in detecting specific features of the signal [19, 80]. Despite the fact that the separation of modal information paths is a relevant characteristic of organisation in the NS, at the highest levels this separation seems to fade away [50, 51, 146]. For example, sensory-motor coordination or the emergence of a general state of awareness (consciousness), require that different sensory information is integrated at some time [42, 45, 122, 144], and at some place [108], i.e. the modal paths of information converge. Even if consciousness might be regarded as the result of a global integrative process of multisensory information to create a comprehensive perception of reality there is currently no evidence for a unique brain region performing such a task. On the contrary, there is increasing evidence that cognitive information might be represented over wide, overlapping and interactive neuronal networks in the cerebral cortex [30, 50, 51]. Our work supports this hypothesis by showing that within the cortex of cats, few cortical areas (the hubs) form a *spatially delocalised cluster* in which multimodal processing paths converge.

In our quest to understand the relationship between the topological organisation of the

mammalian cerebral cortex, the long-range connectivity network between cortical areas in the brain of cats has been analysed by graph theoretical methods. The peculiarities of this network have continuously challenged the existing literature on complex networks, forcing us to reconsider established concepts and to reformulate several graph measures. This dissertation is the result of a bidirectional interaction and mutually feeding motivation between theoretical neuroscience and graph theory. In the following, a more detailed summary of our results in both fields is given.

6.1. Contribution to Graph Theory and Complex Networks

From the technical point of view, we have shown that graph theoretical measures can be applied in a flexible manner in order to overcome data limitations, instead of manipulating the data for analytical or computational convenience. Unfortunately, the latter is a common practice in the complex network literature. For example, directed networks are often artificially converted into non-directed ones.

6.1.1. On the structure-function relationship in complex networks

A major question of complex network research is to understand the relationship between structure, function and dynamics [7, 15, 27, 57, 87, 94, 95, 113, 128, 157]. However, large efforts are still required because of the intricate statistical interdependence between the graph measures. To mention only an example, the synchronisability in networks of coupled oscillators has been reported to depend on many different graph characteristics, the degree homogeneity [93, 98, 155, 156], clustering coefficient [150], degree correlations [34], betweenness centrality [27], degree distributions and so on [73]. As pointed out by Atay and collaborators [13], many statistical network properties do not suffice to determine synchronisability because the spectral properties of networks are simply not derivable from them. In the light of this confusion, it seems that graph theory still lacks of a solid foundation on which theories and models can be constructed *safely*. Only when the complicated statistical interrelation between the graph measures is well understood, will we be able to infer with certainty the causal relations governing the interplay between structure, function and dynamics.

In our work, a step has been taken to bring some order to this confusion by analysing the relationship between the local graph measures: degree distribution, degree-degree correlations and reciprocity. More precisely, we have calculated the expected reciprocity $\langle r \rangle$ of networks with *prescribed degree sequences* and *degree-degree correlations* in the thermodynamical limit. This general result has been simplified to account for the 10 different classes of degree-degree correlations and degree distributions in directed networks. After comparing the measured reciprocity r_{real} to the expected reciprocity $\langle r \rangle$ in a set of 14 real networks, we find that in many cases r_{real} and $\langle r \rangle$ are equal. Hence, in those networks, the degree correlations alone "explains" the observed reciprocity. In other cases, while $\langle r \rangle$ accounts for a large part of r_{real}, deviations between them suggest the presence of further internal structure, e.g. communities or higher order correlations. In order to numerically corroborate our analytical results, we have invented novel algorithms to generate *maximally* random networks with the desired degree distribution and degree correlations.

Some recent works have also tried to uncover the statistical interdependencies between graph measures. In [35, 72] the statistical interplay between degree correlations and the clustering coefficient has been studied, but restricted to the special case of undirected graphs. Very recently, the expected number of cycles (closed paths) of arbitrary length [21] has also been computed conditional on the 1-node degree correlations. Further work in this direction is desirable and the analytical tools presented in paper I can be extended to study other network measures such as the clustering coefficient and motif profiles. When analytical studies become impracticable, the numerical methods proposed in paper II open the door for a new generation of faster algorithms to create ensembles of random networks conditional on degree correlations. No doubt, both theoretical and experimental applications will significantly benefit from the advances in this direction.

6.1.2. Topological roles of vertices in networks with communities

A relevant characteristic of many real networks is their mesoscopic organisation into modules, which often reflect groups of functionally specialised elements. In order to classify individual vertices according to the topological position they occupy within the community structure, Guimerà and Amaral (GA) proposed a quantitative framework consisting of two parameters. One evaluates the *internal importance* of the vertex within its community and the other its *external relation* to other communities [58, 59]. Vertices are catalogued from peripheral vertices (make uniquely internal connections) to kinless hubs (highly connected vertices which span their links equivalently among all the communities).

Practical applications of the GA framework to several empirical networks revealed contradictory results, e.g. it would fail to capture the presence of hubs in some networks. A critical revision uncovered several limitations of the GA framework, which seems to be valid in the limit of sparsely connected, large networks with many communities, all of similar size. From the conceptual point of view, we have shown that if a vertex is a hub within its community, this is no warranty that it is also a global hub of the network. Neither it is the opposite true. Here, the original idea of Guimerà and Amaral has been extended and a normalised framework has been proposed, useful to compare the results from different networks under universal criteria. The key element of our proposal is the definition of *participation vectors* which encode the probability of a vertex to belong to each of the communities. Typical community detection methods partition the vertices of a network into separated modules, but except for trivial cases such a division is never clean. In reality, vertices have a probability to participate in more than one community and thus, the modules overlap with each other [99, 114]. The probabilistic description introduced by the participation vectors opens the door to novel techniques which are capable of specifying both the communities and their overlap. Even if we restrict to considering communities defined as partitions, the ability of participations vectors to identify misclassified nodes, should facilitate the development of intelligent community detection methods which "understand" when the best possible partition has been achieved.

6.2. Contribution to Theoretical Neuroscience

The ubiquitous relationship between the connectional architecture of the nervous system and its function is the central issue of this dissertation and the origin of its results, either technical and biological. Among the different scales of connectivity, we chose the network formed by the cortical areas in the brain of cats and the long-range fibers between them for a few reasons:

1) experimental neuroscience has been very successful at studying detailed mechanisms of sensory processing. However, if we ever aim to understand the anatomical substrate of the mind, we should study the brain as a macroscopic object which is able to combine the sensory information from different modalities, together with emotional responses and memories.

2) the cortico-cortical connectivity network of the cat is, up to date, the most complete dataset of its kind and hence, the most suitable for a detailed graph theoretical analysis with statistical warranties. In the future, when the connectivity of the macaque monkey is completed, or when the human long-range connectivity can be extracted via non-invasive techniques with reliability, it will be extremely interesting to repeat the analysis here performed and compare the results to the data from behavioural experiments.

6.2.1. Cortical organisation

The cortical networks of cat and macaque have been classified as small-world networks due to their large clustering coefficient and their small average pathlength [64, 125, 126]. Additionaly, robustness of cortical networks reveal similarity to scale-free (SF) networks [79]. Using data mining techniques, the connectivity data of the cat has been found to be organised into four communities [64, 115, 117], whose composition coincides with the functional divisions: visual, auditory, somatomotor and frontolimbic. The aim of our work was to go beyond the global average measures, e.g. clustering coefficient and average pathlength, and try to relate the individual topological properties of cortical areas to their function. The graph theoretical analysis has led us to a classification of cortical areas into three categories. Unimodal areas displaying almost uniquely local connections with areas in their modality. Among them we find areas involved in highly specialised sensory functions, e.g. the primary visual area or the primary auditory area. Other areas make some multisensory connections to other communities and have been named multimodal. Within each of the four communities, we found at least one cortical area which is densely connected to all four systems. These areas are difficult to classify into only one of the modal systems and therefore have been classified as supramodal hubs. These hubs have rapid access to information from all the sensory systems, which makes them optimal candidates for being responsible of the large-scale integration.

Restricting to the local connectivity of the areas and to their centrality, it can only be affirmed with certainty that the supramodal hubs play a relevant role in the *transmission* of information between the modal systems. Before assigning them an integrative capacity, further observations are required. By use of structural and dynamical measures, we have found that the supramodal hubs are not independent of each other. Topologically, the

hubs form a densely interconnected cluster, which uncovers a hierarchical organisation in which the highest level (the cluster of hubs) is formed by a centralised overlap of the four communities V, A, SM and FL. The last chapter of this dissertation has been dedicated to revisit the concept of integration of information. All the measures proposed to quantify the *capacity of integration*, either topological and dynamical, support the integrative role of the set of areas composed of the supramodal hubs. Very relevant is the observation that, under the simultaneous stimulation of the of primary sensory areas (primary visual, primary auditory and primary somatosensory areas) the set of supramodal hubs achieve large dynamical dependence between them.

Taking all these observations into account, we now have strong arguments to envision large-scale processing and multisensory integration as the result of the collaborative function of the supramodal hubs, in a similar manner in which the cooperative processing of information by the visual areas gives rise to visual perception [44, 108]. There is a remarkable difference yet. While sensory areas of one modality lie physically close to each other, the supramodal hubs are spatially separated but densely connected through the long-range fibers via the white matter; forming a *spatially delocalised* cluster.

Additional confirmation of the classification here proposed arises from dynamical simulations. In papers III and IV the cortico-cortical network of the cat has been simulated by modelling each cortical with a subnetwork of 200 dynamical neurones (FitzHugh-Nagumo). The dynamical behaviour of this network-of-networks shows that the areas classified as unimodal form the dynamical *cores* of each modality (communities V, A, SM and FL), and the areas classified as supramodal hubs act as "mediators" of the dynamical communication between them.

6.2.2. On the nature of multisensory processing

The nature of cortical areas containing cells responsive to multimodal stimulation has gained a lot of attention in the recent years [39, 108, 146]. Our work has focused in the characterisation of integration and the role of the multisensory connections for that purpose. However, the function of multisensory interactions seems to be far more complex as emphasised by Allman and co-authors in a paper with the suggestive title *"Do cross-modal projections always result in multisensory integration?"* [3]. While integration can be regarded as a bottom-up process, the top-down feedback of multimodal areas over unimodal areas may be a relevant mechanism for the control of selective attention [40]. Indeed, it has been observed that the effect of many multimodal connections is the subthreshold modulation (inhibition or facilitation) of the neuronal activity in other modalities [3, 40, 88]. These cross-modal interferences may be regarded as the anatomical substrate permitting the competition and regulation of the attentional focus between modalities.

Despite the large attention we paid to integration, the graph theoretical analysis can also shed some light about the character of the multisensory connectivity. The hierarchical separation between unimodal areas and supramodal hubs is not perfect. The presence of a third (intermediate) category of *multimodal areas* is the consequence of the existence of different kinds of cross-modal interactions. In our normalised framework to identify the topological roles of the areas, a clear (ascending) linear trend has been observed, indicating that the hierarchical ordering of the areas follows a gradual ordering rather

than a clear-cut separation into two hierarchies. According to the results in Figure 4.7(b), apart from area 6m, no other SM area could be considered as a supramodal hub. Apart from area 1, no other SM area can be clearly classified as unimodal. It appears that the somatosensory-motor cortex plays a general role as an intermediate hierarchy. Most of its areas have some multimodal connections. In speculative terms, this seems very reasonable considering the function of the motor cortex. Movement may arise either as the consequence of (bottom-up) sensory input, e.g. a reflex response, or as the result of a voluntary and planned action (top-down). A more detailed inspection, also reveals a large number of direct connections between motor and visual areas (which are not supramodal hubs), which might reveal the circuitry controlling eye movement and visual attention.

This gradual hierarchical ordering has additional consequences. In Chapter 4 we found that the cortical network displays a very rich communication structure, composed of a mixture of serial and "parallel" processing paths. In reference [8], a method to detect communities has been proposed which is based on the detection of different dynamical scales in the network. Every hierarchy or community has its preferred time-scale. In order to "visualise" the presence of dynamical scales, the authors plotted the eigenvalues of the Laplacian matrix[1] in descending order of magnitude. Characteristic time scales are revealed as plateaus in the plot, indicating the accumulation (or the degeneration) of eigenvalues around specific values. When computed for the cortico-cortical network of the cat, the ordered plot of the eigenvalues (not shown) displays no plateaus, meaning that the network, even if it is composed of some communities and possessing a hierachical organisation, lacks any characteristic time-scales. This is a direct consequence of the rich structure of multimodal communication paths and the gradual hierarchical ordering of the cortical areas.

---

[1]The Laplacian matrix is calculated as: $L = D - A$, where A is the adjacency matrix and D is a diagonal matrix whose elements are $d_{ii} = \sum_{j=0}^{N} A_{ij}$. Hence, the row sums of L are zero. In order to perform dynamical simulations and derive analytical results, the adjacency matrix is often replaced by the Laplacian matrix which has the benefit that all its eigenvalues are positive, $\lambda_i \geq 0$. The case $\lambda_1 = 0$ corresponds to the synchronised state. All the rest correspond to the orthogonal manifold.

APPENDIX A:

Universal Formulation of the Topological Roles

Typical community detection methods partition the vertices of a network into separated modules, but except for trivial cases such a division is never clean. In reality vertices have a probability to participate in more than one community and thus, the modules overlap with each other [99, 114]. In order to classify vertices after the topological position they occupy within the community structure, Guimerà and Amaral (GA) proposed a quantitative framework consisting of two parameters. One evaluates the internal position of the vertex and the other its external connectivity [58, 59]. Assume a network of size N and a partition into n communities. Within a community S of size N_S, its vertices have an internal degree κ_i. The internal parameter, named as within-module degree of a vertex is defined as the z-score of its internal degree:

$$ z_i = \frac{\kappa_i - \langle \kappa \rangle}{\sigma} \tag{A.1} $$

where $\langle \kappa \rangle = \frac{1}{N_S} \sum_{j \in S} \kappa_j$ is the average internal degree within the community, and σ its standard deviation. When $z_i > 2.5$ the node is classified as a hub of the network[1]. The external parameter, named as the participation coefficient, quantifies how distributed are the links of a node among all the communities:

$$ P_i = 1 - \sum_{s=1}^{n} \left(\frac{k_{i,s}}{k_i} \right)^2 \tag{A.2} $$

where k_i is the degree of the node and $k_{i,s}$ the number of links that i makes with nodes of community S. If $i \in S'$ and has only internal links then, $k_{i,s'} = 1$ and $k_{i,s} = 0$ for any $s \neq s'$, hence $P_i = 0$. On the contrary, if the node has its links equally distributed between all the communities, $P_i \to 1$. A Combination of z_i and P_i leads to a diagram of the type in Figure A.1(a). Additionally seven regions have been defined to simplify the orientation and interpretation of the classification: R1, ultra-peripheral nodes; R2, peripheral nodes; R3, non-hub connectors; R4, non-hub kinless nodes; R5, peripheral hubs; R6, connector hubs; R7, kinless hubs.

---

[1]While the division of regions in terms of the participation index have been validated by a simulated annealing analysis of real and artificial networks, the choice of $z = 2.5$ as a valid delimiter between hubs and non-hubs is not justified in any of the references [58, 59, 60].
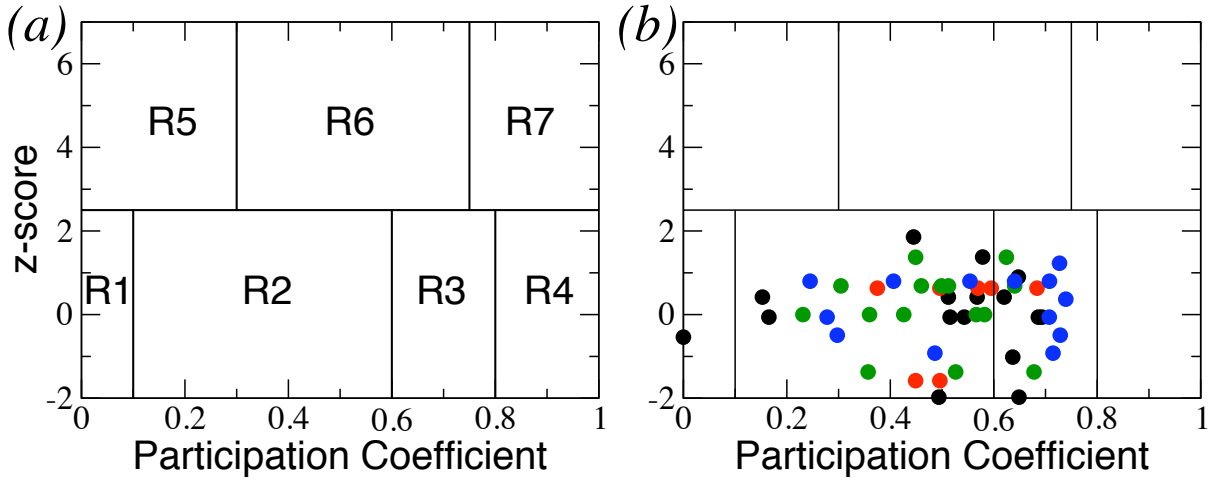
Figure A.1: (a) Two dimensional diagram of Guimerà and Amaral to classify the position of the nodes according to a partition into communities. The diagram is the results of two graph parameters, one describing the internal position of the node within its community, and a external parameter capturing the overlap of the node with other communities. Different regions are defined to help in the interpretation of results. (b) Application of the measures to G_{cat} and its anatomical partition into four anatomical communities (V, A, SM and FL), gives rise to counter-intuitive results.

Limitations of the GA framework

When applying GA's method to different real networks, some counterintuitive results are observed. For example, the GA diagram for the cortical network of the cat (G_{cat}) in Figure A.1(b) does not display any hub (R5, R6 and R7 are empty) even if we know that it contains several. It does neither display kinless nodes (R4 and R7), while some areas heavily connect to all the four communities. A close inspection of z_i and P_i revealed several limitations of the formalism, which seems correct in the thermodynamical limit (large size and sparse connectivity) with all communities of similar size. But for networks of limited size and inhomogeneous communities, a normalised formulation is required. Conceptually speaking, it should be noted that a vertex which is a local hub within its community, is not necessarily a global hub of the network. Neither it is in the opposite case. We list other limitations:

a) *z-score depends on the density of links:* Imagine two communities of the same size N_s, one is sparsely connected and the other is dense. In the sparse community, the average degree is small $\langle \kappa \rangle \ll N_s$ and it is therefore likely to find nodes with $z_i > 2.5$. On the contrary, in the dense community $\langle \kappa \rangle$ is larger and thus it is less likely to find nodes with $z_i > 2.5$. Note that κ_i is bounded by $N_s - 1$. If the nodes of different communities are to be classified after the same threshold, $z = 2.5$, then the z-score requires a normalisation.
b) *Communities of different size:* Inhomogeneous community sizes may lead to critical differences and a normalized framework is desirable. z_i depends also on the size of the community (network) and again, a universal thershold $z = 2.5$ leads to an unfair classification. On the other hand, the formulation of P_i implicitely assumes that all

communities are of the same size. We understand that the probability of a node to connect to a community depends not only on its degree k_i but also on the size of the community N_s.

c) ***Small number of communities:*** The participation coefficient is defined as a quantity ranging from 0 to 1. Unfortunately $P_i \to 1$ only if the number of communities is infinite. A node which spans its links equivalently among all the n communities has $k_{i,s} = \frac{k_i}{n}$ links per community. In this case its participation coefficient is:

$$P_i = 1 - \sum_{s=1}^{n} \left(\frac{k_{i,s}}{k_i} \right)^2 = 1 - \sum_{s=1}^{n} \left(\frac{\frac{k_i}{n}}{k_i} \right)^2 = 1 - n\frac{1}{n^2} = 1 - \frac{1}{n}$$

This means that, according to the current formulation of P_i, finding nodes in the regions $R3$, $R4$ and $R7$ is statistically much more difficult, if not impossible. In our case, the cat cortex is devided into $n = 4$ communities, and thus $P_i^{max} = 0.75$. Notice that in Figure A.1(b) some cortical areas almost achieve $P_i = 0.75$, meaning that they should be classified as kinless nodes. However, they do not fall in the regions R4 or R7.

A.1. Normalisation of the Within-module Degree (z-score)

While the original and general idea of Guimerà and Amaral remains valid, understanding of its limitations has led us to an extension of the formalism and its conceptual interpretation towards a universal framework.

A.1.1. Dependence of z_i on size and density

Let us investigate the effect of the density in the outcome of the z_i. Specially we want to find *the largest possible density of links for which a hub can achieve $z_i < 2.5$*. For that, a series of numerical experiments have been performed. Consider a star graph of size N whose central vertex ($i = 1$) is connected to the rest of vertices by one link. The central node has degree $k_1^* = N - 1$ and the rest have $k_i^* = 1$ for all $i = 2, 3 \dots N$. Notice that, in the space of *connected graphs* (there is no isolated vertices) the central vertex of a star graph has the largest possible z_i. We term it as z_1^*.

Starting from a star graph of size N, at each iteration $N - 1$ links are introduced at random and z_1 is measured. By this process the dependence of z_1 on the density ρ has been plotted for networks of different sizes, Figure A.2(a). There are two lessons from the results:

1) The z_1 decays as the density of links grows, so there exist a critical density for which it is impossible to find a node with $z > 2.5$.

2) z_1 does also depend on the size of the network, which strongly suggests that a proper normalization is required.

For comparison with the cat cortex and its communities, the same process has been repeated with star graphs of sizes $N = 53, 16$ and 7. The results shown in Figure A.2(b) reveal the following conclusions:
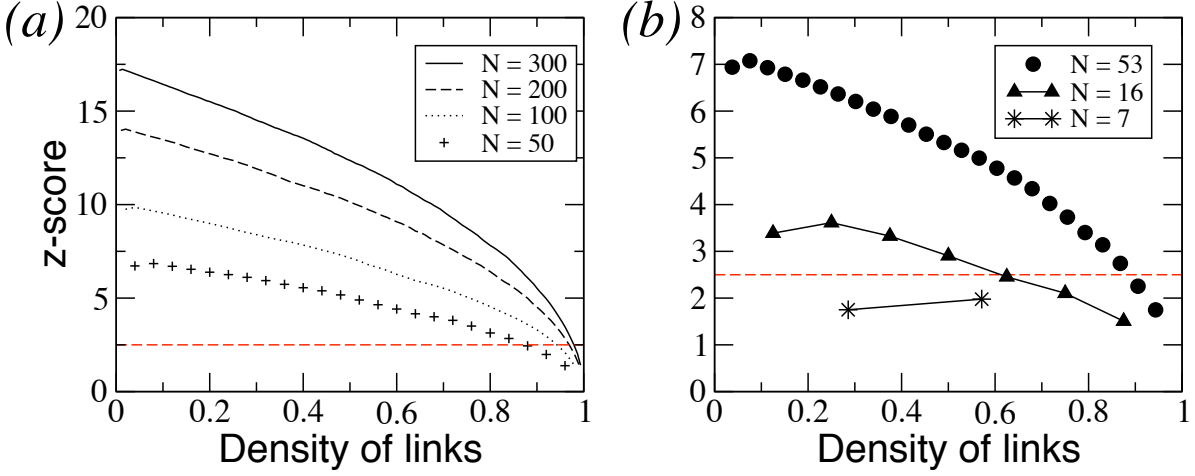
Figure A.2: z-score of the central node in star graphs. Starting from a star graph of N nodes, at each iteration $N - 1$ links are introduced at random and the z-score of the central node is measured.

1) In a star network of $N = 53$ (size of G_{cat}) $z_1 < 2.5$ only when the density of links is larger than $\gtrsim 0.9$, what is extremely large. However, for the smaller networks, $N = 16$, $z_1 > 2.5$ only when $\rho \gtrsim 0.6$. The three equivalent communities in the cat cortex (V, SM and FL) have internal densities of 0.58, 0.74 and 0.65 meaning that it is impossible to find in those communities an area satisfying the condition to be considered as a local hub.

2) For the network of size $N = 7$ (auditory cortex), in no case can the central node have $z_1 > 2.5$, not even in the initial star configuration when $k_1 = 6$ and $k_i = 1$ for $i = 2, 3 \ldots 7$. In this case it is obvious that the central node is a hub, but a resolution limit of the z-score is reached.

Having uncovered the technical reasons for why the GA diagram displays no hubs in the case of the G_{cat} network, we attempt a normalization of z_i to overcome these limitations.

A.1.2. Proposed normalisation

In order to normalize z_i so that all networks and communities of different sizes are comparable under universal criteria, we make the following proposal. As the central vertex has the maximum z-score of connected graphs of size N, then z_i should be normalised by $z_1^*(N)$. The normalised within-module degree is then: $z_i' = \frac{z_i}{z_1^*(N_s)}$. For practical applications an analytical formula of $z_i^*(N)$ is desired. Remind that the average degree is defined as $\langle k \rangle = L/N$ where L is the number of links. In a star graph there are only $L^* = N - 1$ links, thus $\langle k^* \rangle = \frac{N-1}{N}$ and the standard deviation of its degree distribution σ^* can be
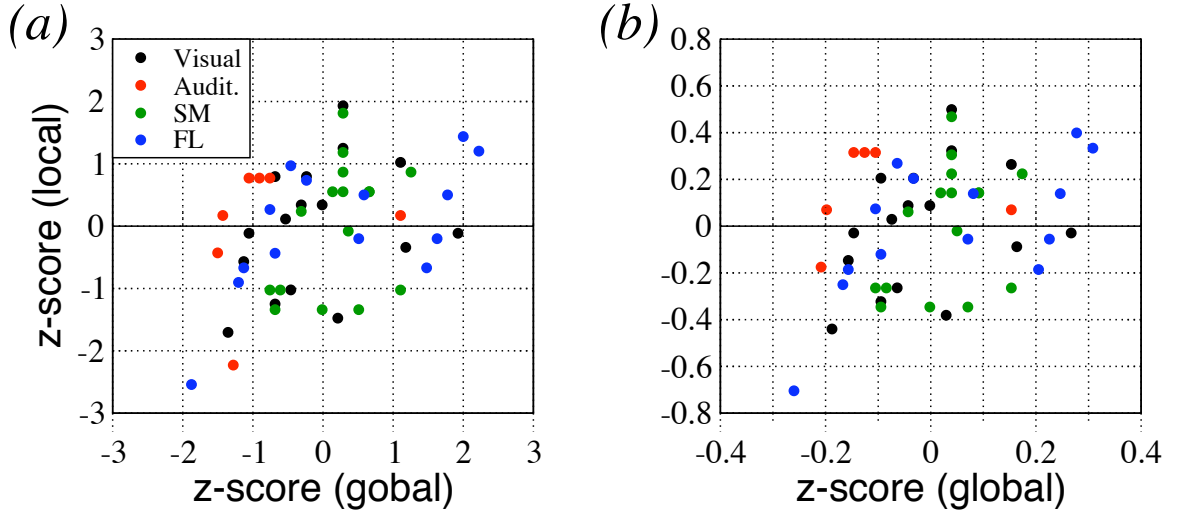
Figure A.3: Comparison of z-global vs. z-local. (a) Original measure, (b) normalised z-scores. The plots show that a local hub within a community is not necessarily a hub of the network, and neither the other way around. Otherwise, the areas would follow a linear relationship in the plot.

calculated as:

$$\sigma^* = \sqrt{\frac{1}{N}\sum_{i=1}^{N}(k_i - \langle k^*\rangle)^2} = \frac{1}{\sqrt{N}}\sqrt{(k_1 - \langle k^*\rangle)^2 + \sum_{i=2}^{N}(k_i - \langle k^*\rangle)^2} =$$

$$= \frac{1}{\sqrt{N}}\sqrt{\left(N - 1 - \frac{N-1}{N}\right)^2 + (N-1)\left(1 - \frac{N-1}{N}\right)^2} = \dots$$

$$= \frac{1}{N}\sqrt{\frac{N-1}{N}}\sqrt{(N-1)^3 + 1}$$

With this result, the z-score of the central node of a star graph of size N is:

$$z_1^* = \frac{k_1 - \langle k^*\rangle}{\sigma^*} = \frac{(N-1) - \frac{N-1}{N}}{\sigma^*} = \sqrt{\frac{N}{N-1}}\frac{(N-1)^2}{\sqrt{(N-1)^3 + 1}} \to \sqrt{N-1}$$

And finally, the normalised within-module degree (z-score) is:

$$z_i' = \frac{z_i}{z_1^*} = \frac{z}{\sqrt{N-1}}. \tag{A.3}$$

With such a normalization a node has $z_i' \to 1$ when it is the only hub of a very sparse network, $z_i' \approx 0$ when the node has a non-relevant degree, and $z_i' \to -1$ when it has very few connections in a highly connected network[2].

In Figure A.3(b) the z-global vs. z-local has been replotted. The z-global of each node is normalized by $\sqrt{N-1}$, while the local z-scores are normalized by the size of the corresponding community $\sqrt{N_s - 1}$. The result is very similar to the one without normalisation (Figure A.3(a)) because the communities V, SM and FL have very similar size ($N_s = 14$ and $N_s = 16$). However, the nodes of the auditory cortex ($N_s = 7$) significantly change their relative position in the diagram.

---

[2]This fact has been proven with "anti-star" networks, say, an almost complete graph where one of the nodes has a unique link. In such a case its $z \approx -\sqrt{N-1}$.

A.2. Alternative Approach to P_i: Participation vectors

In the light of the limitations detected, our goal is twofold. First, P_i should be defined in the range $[0,1]$ independently of the number of communities n. Second, P_i should take on account the inhomogeneous size of communities.

The fraction $\frac{k_{i,s}}{k_i}$ quantifies *how well* is the vertex i connected to the vertices in the community S. However, the random probability of i connecting to S does not only depend on k_i, but also in the size of the community. Just imagine two communities, S' and S'', of distinct size $N_{s'} > N_{s''}$. If the k_i links are assigned at random, then obviously the links fall in S' with larger probability. Let us then define for each vertex a Participation Vector $\overrightarrow{P_i}$, say, a vector of n dimensions (number of communities) whose elements $P_i(s)$ represent the probability that i belongs to S. There is no unique manner of defining such a vector, neither of reducing its information into a scalar value

A.2.1. Defining the participation vectors

A vertex can maximally connect to the N_s vertices of S. If $k_i > N_s$, then i necessarily have neighbours in more than one community. Consequently, let's define the elements of the participation vector as $P_i(s) = \frac{k_{i,s}}{N_s}$, meaning that, i has $k_{i,s}$ neighbours in S, out of all the N_s possible. To be more precise, if $i \in S$, then $P_i(s') = \frac{k_{i,s}}{(N_{s'}-1)}$. Let's illustrate the usefulness of the participation vectors by a few examples from cortical areas. The elements $P_i(s)$ represent the probability that the area belongs to a given system: visual (V), auditory (A), somato-motor (SM) and frontolimbic (FL):

area	(V	A	SM	FL)
17	(0.6	0.0	0.0	0.0)
19	(0.933	0.143	0.313	0.0)
7	(0.667	0.143	0.563	0.571)
AES	(0.667	0.429	0.813	0.429)
6m	(0.438	0.143	0.733	0.714)
Ia	(0.563	0.571	0.625	0.692)

Areas 17 and 19 clearly belong to the visual system. The primary visual cortex (area 17) makes no connections outside the visual cortex. Area 19 has some connections to the auditory and somato-motor systems, although it is very densely connected within the visual system ($P_{19}(V) = 0.933$). In the case of visual area 7, while $P_7(V)$ is the largest element, it is very closely followed by $P_7(SM)$ and $P_7(FL)$. This can be interpreted as area 7 largely overlapping among the three systems and it would be interpreted as a *connector node* or a *connector hub*. Yet a more remarkable example is the vector of the fromtolimbic area Ia. While $P_{Ia}(FL)$ is the largest element, Ia largely overlaps among all the four cotical system and it would be very difficult to classify it any of the communities. After this observation, Ia is a strong candidate to be classified as a *kinless hub*.

As an example of further potential uses of participation vectors, let's pay attention to cortical area AES, which has been placed in the visual system. However, the largest element of its participation vector is $P_{AES}(SM)$, what indicates that, the community detection method applied to the network has misclassified it.

Defining vectors by the expected number of links

Another possibility to define the vectors $\overrightarrow{P_i}$ is by computing the number of expected links that i may have in S. If the k_i links are randomly distributed, then i should have $\langle k_{i,s} \rangle = k_i \frac{N_s}{N}$ links in S. (Again, if $i \in S$ then the factor becomes $N_s - 1$). Now, the elements of the participation vector could be defined as $P_i(s) = \frac{k_{i,s}}{\langle k_{i,s} \rangle}$.

Although this definition of participation vectors might look more elegant, we must say that both approaches are equivalent:

$$P_i^{exp}(s) = \frac{k_{i,s}}{\langle k_{i,s} \rangle} = \frac{k_{i,s}}{k_i \frac{N_s}{N}} = \frac{k_{i,s} N}{k_i N_s} = \frac{N}{k_i} \frac{k_{i,s}}{N_s} = \frac{N}{k_i} P_i^{frac}(s).$$

Since $\frac{N}{k_i}$ is a constant value for the vector, a normalization deletes any difference between the two definitions.

A.2.2. From participation vectors to participation index

The absolute values in the participation vectors obviously depend on the degree of the vertex, but for the purpouses of constructing a participation index, this is irrelevant. For that, the interesting information is the relative differences between the n elements of $\overrightarrow{P_i}$, because by this difference it is possible to quantify how 'closer' is the vertex to one community than to the others. Therefore, we propose to define the participation index by computing the standard deviation of the elements of $\overrightarrow{P_i}$.

The vectors can be normalized by the total sum of their elements. In the case of a perfect kinless vertex, its normalised participation vector is then $\overrightarrow{P_i} = (1/n, 1/n, \dots, 1/n)$. As all elements are equal, $\sigma_i = \sigma(\overrightarrow{P_i}) = 0$. In the opposite situation, if i has all its connections into one single community, its normalised participation vector is, e.g., $\overrightarrow{P_i} = (1, 0, 0 \dots, 0)$. In this case the average value is also $\langle P_i \rangle = 1/n$ and its standard deviation is:

$$\sigma_{max}(n) = \sqrt{\frac{1}{n} \sum_{s=1}^{n} (P_i(s) - \langle P_i \rangle)^2} = \frac{1}{\sqrt{n}} \sqrt{(1 - \langle P_i \rangle)^2 + (n-1) \langle P_i \rangle^2} = \dots = \frac{\sqrt{n-1}}{n}.$$

Finally, to follow the same standards as in the GA framework (peripheral nodes have $P_i \to 0$ and kinless nodes $P_i \to 1$), we define the Participation Index as:

$$P_i' = 1 - \frac{\sigma_i}{\sigma_{max}(n)} = 1 - \frac{n}{\sqrt{n-1}} \sigma_i \quad : \quad \sigma_i = StdDev\left(\overrightarrow{P_i}(s)\right) \tag{A.4}$$

A.3. Summary and Discussion

In order to classify the topological roles that vertices play within a partition of the network with modular structure, Guimerà and Amaral (GA) proposed a method based on two parameters, one quantifying the internal position of the node within its community and another parameter evaluating its external connectivity [58, 59]. Here, the GA framework

has been re-analysed and several limitations have been detected. While the formulation is valid in the thermodynamical limit and for partitions of many communities of similar size, for many real networks it provides contradictory results. A normalised formulation is required in order to compare networks of different characteristics under universal criteria. Understanding of those limitations permitted us to propose alternative and normalised parameters.

The tools presented here, apart from extending the previous framework, have very interesting potential uses. A generalised use of the z-local vs. z-global plots (Figure A.3), might be very useful to understand and classify different types of hierarchies. Community detection methods might largely benefit from the probabilistic characterisation encoded in the participation vectors. On the one hand, they permit to characterise and quantify the overlapping nature of communities. In a similar manner in which the modularity function is useful to evaluate and compare of partitions provided by different methods, participation vectors open the door to novel techiques which are capable of specifying both the communities and their overlap. On the other hand, even if we restrict to communities defined as partitions, the ability of participation vectors to detect misclassified nodes allows for the development of intelligent community detection methods which "understand" when the best possible partition has been achieved. Although it has not been presented, preliminary tests were positive. Starting from approximate modules, a simple algorithm would detect misclassified nodes, move them to another community and recover the best known partition for various real networks.

APPENDIX B:

Table of Cortical Areas

In the following, the 53 cortical areas contained by the cortico-cortical network of the cat are summarised, organised according to the common partition into the four communities adopted in the literature [64, 115, 117]. The ordering (identity number) is the same as in Figure 3.1. Additional notes extracted from [115] have been included. For completeness and to facilitate the reference, the adjacency matrix of the network is also replotted.

id	Area	Notes
VISUAL CORTEX		
1	17	primary visual cortex
2	18	retinotopically organised
3	19	retinotopically organised
4	PLLS	
5	PMLS	
6	AMLS	
7	ALLS	
8	VLS	
9	DLS	
10	21a	
11	21b	
12	20a	retinotopically organised.
13	20b	retinotopically organised.
14	7	multisensory (V, A, SM), involved in oculomotor function.
15	AES	multisensory (V, A, SM), involved in oculomotor function.
16	PS	retinotopically organised.
AUDITORY CORTEX		
17	AI	primary auditory field. Tonotopically organised.
18	AII	secondary auditory field. Weak tonotopical organisation.
19	AAF	tonotopically organised.
20	P	tonotopically organised.
21	VP(ctx)	tonotopically organised.
22	EPp	visual and auditory association area.
23	Tem	

id	Area	Notes
SOMATO-MOTOR CORTEX		
24	3a	somatotopically organised (response to deep stimuli).
25	3b	somatotopically organised (response to cutaneous stimuli).
26	1	somatotopically organised (response to cutaneous stimuli).
27	2	somatotopically organised (response to cutaneous stimuli).
28	SII	has representations of some body regions.
29	SIV	has an orderly representation of the body surface.
30	4g	involved in motor function.
31	4	involved in motor function.
32	6l	in the premotor cortex
33	6m	in the premotor cortex
34	5Am	
35	5Al	
36	5Bm	might be involved in visuomotor integration.
37	5Bl	might be involved in visuomotor integration.
38	SSSAi	polysensory responsivity.
39	SSAo	polysensory responsivity.
FRONTOLIMBIC CORTEX		
40	PFCMil	
41	PFCMd	
42	PFCL	
43	Ia	responds to multimodal stimulation.
44	Ig	responds to multimodal stimulation.
45	CGa	
46	CGp	
47	RS	Retrospenial cortex.
48	35	in the perirhinal cortex
49	36	in the perirhinal cortex
50	pSb	Presubiculum, parasubiculum and postsubicular cortex.
51	Sb	Subiculum.
52	Enr	Entorhinal cortex.
53	Hipp	Hippocampus

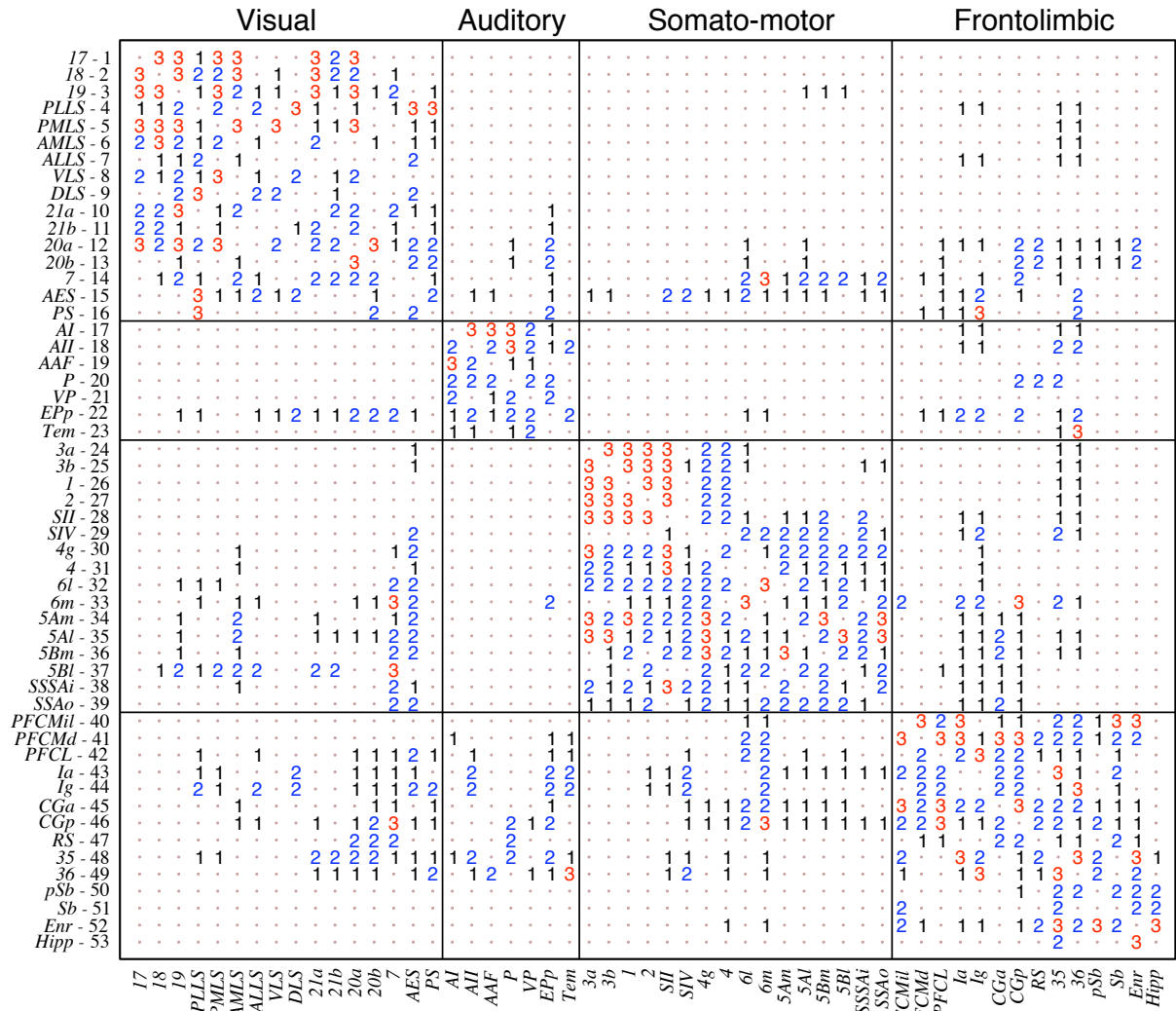**Figure B.1:** Adjacency matrix of the cortico-cortical connectivity of the cat comprising of 826 directed connections between 53 cortical areas. The connections are classified as weak (1, black), intermediate (2, blue) and dense (3, red) according to the axonal densities in the projections between two areas. For visualisation purpouses, the non-existing connections (0) have been replaced by dots.

Acknowledgements

I thank Prof. Jürgen Kurths for giving me the chance to do what I always wanted: dedicate my working life to satisfy the selfish passion for understanding nature. Receive my sincere gratitude for your patient support during these years. I also want to remember the extense number of past and present friends at the Nonlinear Dynamics Group, with whom I spent nice moments either at work and outside. Lucia, the dissertation is dedicated to you because without your determination to start this project, I simply wouldn't be writting these pages.

I feel extremely fortunate because in this time I came accross with colleagues who, apart from being clever and talented scientists, they are also excellent persons. To all of you I owe a beautiful lesson: *that keeping a constructive mind is what makes of this business a pleasure.* Vinko Zlatić, it is thank to your talent that the work on reciprocity became the nice paper that I think it is. I hope we can collaborate soon again and share some beers. To Professors Claus C. Hilgetag and Markus Kaiser, I thank your always kind and friendly attention, and for your disposition to share your experience with us. To Professor Alex Arenas, thank you so much for your interest in my ideas and for always having the time to read and comment them. For your help and hospitality. I am also in debt with Javier Borje for bringing the problem of functional roles to my attention and for our small adventure trying to find a solution. Thank you for the long hours of chattering about everything.

I thank Stefan Schinkel and Zunbeltz Izaola for their help correcting and formatting this document.

At this point of my life I could not forget of my older brother, Iñaki Zamora López. In a family oriented into arts and humanities, it was thank to your books, to the documentaries we watched together on TV and to your desperate attempts to make me understand the infinity of universe, that my curiosity for nature woke up when I was a kid. Your clever explanations when I was struggling with mathematics at the school, made all this possible.

Last but not least. Changsong, I left you for the end because you deserve a very special mention, for being my mentor and my friend. Your elegant attitude to life and science is a beautiful example for all of us. I wish you all the best.

Gorka Zamora López
Berlin, 2nd October, 2008

Bibliography

[1] www.cocomac.org.

[2] W. Aiello, F. Chung, and L. Lu. A random graph model for massive graphs. In *Proceedings of the 32nd Annual ACMSymposium on Theory of Computing*, pages 171–180, New York, 2000. Association of Computing Machinery.

[3] B. L. Allman, R. E. Bittencourt-Navarrete, L. P. Keniston, A. E. Medina, M. Y. Wang, and M. A. Meredith. Do cross-modal projections always result in multisensory integration? *Cereb. Cortex*, 18:2066–2076, 2008.

[4] J. Ignacio Alvarez-Hamelin, Luca Dall'Asta, Alain Barrat, and Alessandro Vespignani. Large scale networks fingerprinting and visualization using the k-core decomposition. In Y. Weiss, B. Schölkopf, and J. Platt, editors, *Advances in Neural Information Processing Systems 18*, pages 41–50. MIT Press, Cambridge, MA, 2006.

[5] L. A. N. Amaral, A. Scala, M. Bathélémy, and H. Stanley. Classes of small-world networks. *Proc. Nat. Acad. Sci.*, 97:21, 2000.

[6] J. M. Anthonisse. The rush in a directed graph. Technical Report BN9/71, Stichting Mathematisch Centrum, 1971.

[7] A. Arenas, A. Diaz-Guilera, J. Kurths, Y. Moreno, and C. Zhou. Synchronization in complex networks. *Physics Reports*, in press, 2008.

[8] A. Arenas, A. Díaz-Guilera, and C. Pérez-Vicente. Synchronization reveals topological scales in complex networks. *Phys. Rev. Lett.*, 96:114102, 2006.

[9] A. Arenas, A. Fernández, and S. Gómez. Analysis of the structure of complex networks at different resolution levels. *New J. Phys.*, 10:05039, 2008.

[10] A. Arenas, A. Fernández, and S. Gómez. Analysis of the structure of complex networks at different resolution levels. arXiv:physics/0703218v2, 2008.

[11] A. Arenas, A. Fernandez, and S. Gomez. *Bio-Inspired Computing and Communication*, chapter A Complex Network Approach to the Determination of Functional Groups in the Neural System of C. Elegans. Lecture Notes in Computational Science. Springer, in press.

[12] Y. Artzy-Randrup, S. J. Fleischman, N. Ben-Tal, and L. Stone. Comment on: "network motifs: simple building blocks of complex networks" and "superfamilies of evolved and designed networks". *Science*, 305:1107c, 2004.

[13] F. Atay, T. Biyikoğlu, and J. Jost. Network synchronization: Spectral versus statistical properties. *Physica D*, 224:35–41, 2006.

[14] D. A. Bader, S. Kintali, K. Madduri, and M. Mihail. Approximating betweenness centrality. In *Algorithms and models for the web graph*, Lecture notes in computer science. Springer Berlin, 2007.

[15] Y. Bar-Yam and I. Epstein. Response of complex networks to stimuli. *Proc. Nat. Acad. Sci.*, 101(13):4341–4345, 2004.

[16] A. L. Barabási and R. Albert. Emergence of scaling in random networks. *Science*, 286:509–512, 1999.

[17] M. Barbosa and et al. *Lectures in supercomputational neuroscience*, chapter Parallel computation of large neuronal networks with structured connectivity, pages 343–367. Springer-Verlag, Berlin, 2007.

[18] M. Barthélemy, A. Barrat, R. Pastor-Satorras, and A. Vespignani. Velocity and hierarchical spread of epidemic outbreaks in scale-free networks. *Phys. Rev. Lett.*, 92(17):178701, 2004.

[19] M. F. Bear, B. W. Connors, M. A. Paradiso, B. Connors, and M. Paradiso. *Neuroscience: Exploring the brain*. Lippincott Williams and Wilkins, 2006.

[20] A. Bekessy, P. Bekessy, and J. Komolos. Asymptotic enumeration of regular matrices. *Stud. Sci. Math. Hung.*, 7:343–353, 1972.

[21] G. Bianconi, N. Gulbahce, and A. E. Motter. Local structure of directed networks. *Phys. Rev. Lett.*, 100:118701, 2008.

[22] T. Binzegger, R. J. Douglas, and K. A. C. Martin. A quantitative map of the circuit of cat primary visual cortex. *J. Neurosci.*, 24(39):8441–8453, 2004.

[23] S. Boccaletti and M. Ivanchenko et al. Detecting complex network modularity by dynamical clustering. *Phys. Rev. E*, 75:045102(R), 2007.

[24] M. Boguñá, R. Pastor-Satorras, and A. Vespignani. Cut-offs and finite size effects in scale-free networks. *Eur. Phys. J. B*, 38:205, 2004.

[25] V. Braitenberg and A. Schüz. *Anatomy of the cortex: statistics and geometry*. Springer, Berlin, 1991.

[26] U. Brandes. A faster algorithm for betweenness centrality. *J. of Math. Soc.*, 25(2):163–177, 2001.

[27] M. Chavez, D.-U. Hwang, A. Amann, and S. Boccaletti. Synchornizing weighted complex networks. *CHAOS*, 16:015106, 2006.

[28] R. Cohen, K. Erez, D. ben Avraham, and S. Havlin. Resilience of the internet to random breakdowns. *Phys. Rev. Lett.*, 85:4626–4628, 2000.

[29] T. M. Cover and J. A. Thomas. *Elements of information theory*. Wiley, New York, 1991.

[30] A. R. Damasio. Time-locked multiregional retroactivation: A systems-level proposal for the neuronal substrates of recall and recognition. *Cognition*, 33:25–62, 1989.

[31] L. Danon, A. Díaz-Guilera, J. Duch, and A. Arenas. Comparing community structure identification. *J. Stat. Mech.*, P09008, 2005.

[32] D. J. de Solla Price. Networks of scientific papers. *Science*, 149:510–515, 1965.

[33] D. J. de Solla Price. A general theory of bibliometric and other cumulative advantage processes. *J. Amer. Soc. Inform. Sci.*, 27:292–306, 1976.

[34] M. di Bernardo, F. Garofalo, and F. Sorrentino. Effects of degree correlation on the synchronizability of networks of nonlinear oscillators. Proc. 44th IEEE Conference on Decision and Control, and the European Control Conference WeA14.1, 2005.

[35] S. N. Dorogovtsev. Clustering of correlated networks. *Phys. Rev. E*, 69:027104, 2004.

[36] S. N. Dorogovtsev, A. V. Goltsev, and J. F. F. Mendes. k-core organization of complex networks. *Phys. Rev. Lett.*, 96:040601, 2006.

[37] S. N. Dorogovtsev and J. F. F. Mendes. Evolution of network. *Advances in Physics*, 51(4):1079 – 1187, 2002.

[38] S. N. Dorogovtsev, J. F. F. Mendes, and A. N. Samukhin. Size-dependent degree distribution of a scale-free growing network. *Phys. Rev. E*, 63(6):062101, 2001.

[39] J. Driver and T. Noesselt. Multisensory interplay reveals crossmodal influences of 'sensory-specific' brain regions, neural responses and judgments. *Neuron Rev.*, 57:11–23, 2008.

[40] J. Driver and C. Spence. Multisensory perception: Beyond modularity and convergence. *Curr. Biol.*, 10:R731–R735, 2000.

[41] R. M. Durban. *Studies on the developmnet and organisation of the nervous system of* Caernorhabditis Elegans. PhD thesis, King's College, Oxford, 1987.

[42] A. K. Engel and W. Singer. Temporal binding and neural correlates of sensory awareness. *Trends Cogn. Sci.*, 5(1):16–25, 2001.

[43] P. Erdős and E. Rényi. On random graphs i. *Publ. Math. Debrecen*, 6:290–297, 1959.

[44] D. C. Van Essen, C. H. Anderson, and D. J. Felleman. Information processing in the primate visual system: an integrated systems perspective. *Science*, 255:419–423, 1992.

[45] M. Fahle. Figure-ground discrimination from temporal information. *Proc. R. Soc. Lond. B*, 254:199–203, 1993.

[46] A. M. Faser and H. L. Swinney. Independent coordinates for strange attractors from mutual information. *Phys. Rev. A*, 33:2318–2321, 1986.

[47] D. J. Felleman and D. C. van Essen. Distributed hierarchical processing in the primate cerebral cortex. *Cereb. Cortex*, 1:1–47, 1991.

[48] S. Fortunato and M. Barthélemy. Resolution limit in community detection. *Proc. Nat. Acad. Sci.*, 104:36–41, 2006.

[49] L. C. Freeman. A set of measures of centrality based upon betweenness. *Sociometry*, 40:35–41, 1977.

[50] J. M. Fuster. *Cortex and Mind: unifying cognition*. Oxford University Press, New York, 2003.

[51] J. M. Fuster. The cognit: A network model of cortical representation. *Int. J. Psychophysiology*, 60:125–132, 2006.

[52] D. Garlaschelli and M. I. Loffredo. Patterns of link reciprocity in directed networks. *Phys. Rev. Lett.*, 93:268701, 2004.

[53] K.-I. Goh, B. Kahng, and D. Kim. Universal behaviour of load distribution in scale-free networks. *Phys. Rev. Lett.*, 87:27, 2001.

[54] M. L. Goldstein, S. A. Morris, and G. G. Yen. Problems with fitting to the power-law distribution. *The European Physical Journal B*, 41(2):255–258, 2004.

[55] D. M. Gordon. Threshold models of collective behavior. *Am. J. Sociol.*, 83:1420–1443, 1978.

[56] D. M. Gordon. The organization of work in social insect colonies: Task allocation as an ad hoc, dynamical network. *Complexity*, 8:43–46, 2003.

[57] T. Gross and B. Blasius. Adaptive coevolutionary networks: a review. *J. Royal Soc.*, 5(20):259–271, 2008.

[58] R. Guimerà and L. A. N. Amaral. Cartography of complex networks: modules and universal roles. *J. Stat. Mechs.*, P02001, 2005.

[59] R. Guimerà and L. A. N. Amaral. Functional cartography of complex metabolic networks. *Nature*, 433:895, 2005.

[60] R. Guimerà, M. Sales-Pardo, and L. A. N. Amaral. Classes of complex networks defined by role-to-role connectivity patterns. *Nature Physics*, 3:63 – 69, 2007.

[61] E. D. Gundelfinger, C. Seidenbecher, and B. Schraven, editors. *Cell Communication in Nervous and Immune System*, volume 43 of *Results and Problems in Cell Differentiation*. Springer, 2006.

[62] M. Gustafsson. *Large-scale Topology, Stability and Biology of Gene Networks*. PhD thesis, LiU-Tryck, Linköpings Universitet, 2006.

[63] M. Gustafsson, M. Hörnquist, and A. Lombardi. Comparison and validation of community structures in complex networks. *Physica A*, 367:55976, 2006.

[64] C. C. Hilgetag, G. A. P. C. Burns, M. A. O'neill, J. W. Scannell, and M. P. Young. Anatomical connectivity defines the organization of clusters of cortical areas in the macaque monkey and the cat. *Phil. Trans. R. Soc. Lond. B*, 355:91–110, 2000.

[65] C. C. Hilgetag and M. Kaiser. Clustered organisation of cortical connectivity. *Neuroinf.*, 2:353–360, 2004.

[66] C. C. Hilgetag and M. Kaiser. *Lectures in supercomputational neuroscience: Complex networks in brain dynamics*, chapter Organization and function of complex cortical networks. Springer, Berlin, 2008.

[67] C. C. Hilgetag, R. Kötter, K. E. Stephan, and O. Sporns. *Computational Neuroanatomy*, chapter Computational methods for the analysis of brain connectivity. Humana Press, Totowa, NJ, 2002.

[68] C. C. Hilgetag, M. A. Oeill, and M. P. Young. Hierarchical organization of macaque and cat cortical sensory systems explored with a novel network processor. *Phil. Trans. R. Soc. Lond. B*, 355:71–89, 2000.

[69] P W. Holland and S. Leinhardt. *Sociological Methodology*, chapter The statistical analysis of local structure in social networks, pages 1–45. Jossey-Bass, San Francisco, 1975.

[70] P. Holme. *Form and Function of Complex Networks*. PhD thesis, Umeå University, 2004.

[71] P. Holme and B. J. Kim. Growing scale-free networks with tunable clustering. *Phys Rev. E*, 65:026107, 2002.

[72] P. Holme and J. Zhao. Exploring the assortativity-clustering space of a network's degree sequence. *Phys. Rev. E*, 75:046111, 2007.

[73] H. Hong, B. J. Kim, M. Y. Choi, and H. Park. Factors that predict better synchronizability on complex networks. *Phys. Rev. E*, 65:067105, 2002.

[74] M. Huss and P. Holme. Currency and commodity metabolites: their identification and relation to the modularity of metabolic networks. *IET Syst. Biol.*, 1(5):280–285, 2007.

[75] S. Itzkovitz, R. Milo, N. Kashtan, G. Ziv, and U. Alon. Subgraphs in random networks. *Phys. Rev. E*, 68(2):026127, 2003.

[76] R. Jana and S. Bandyopadhyay. A markov chain monte carlo method for generating random (0,1)-matrices with given marginals. *Sankhya A*, 58:225–242, 1996.

[77] M. Kaiser and C. C. Hilgetag. Modelling the development of cortical systems networks. *Neurocomputing*, 58–60:297–302, 2004.

[78] M. Kaiser and C. C. Hilgetag. Nonoptimal component placement, but short processing paths, due to long-distance projections in neural systems. *PLoS Comp. Biol.*, 2(7):e95, (2006).

[79] M. Kaiser, R. Martin, P. Andras, and M. P. Young. Simulation of robustness against lesions of cortical networks. *Eur. J. Neurosc.*, 25:3185–3192, 2007.

[80] E. R. Kandel, J. H. Schwartz, and T. M. Jessell. *Principles of Neural Science.* McGraw-Hill, 2000.

[81] L. Katz and J. H. Powell. Probability distributions of random variables associated with a structure of the sample space of sociometric investigations. *Ann. Math. Stat.*, 28:442–448, 1957.

[82] K. Klemm and V. M Eguíluz. Highly clustered scale-free networks. *Phys. Rev. E*, 65:036123, 2002.

[83] R. Kötter and F. T. Sommer. Global relationship between anatomical connectivity and activity propagation in the cerebral cortex. *Phil. Trans. R. Soc. London B*, 355:127–134, 2000.

[84] T. I. Lee and N. J. Rinaldi et al. Transcriptional regulatory networks in *Saccharomyces cerevisiae. Science*, 298:799–804, 2002.

[85] F. Liljeros, C. R. Edling, L. A. N. Amaral, H. E. Stanley, and Y. Aberg. The web of human sexual contacts. *Nature*, 411:907, 2001.

[86] S. F. Maier and L. R. Watkins. Immune-to-central nervous system communication and its role in modulating pain and cognition: Implications for cancer and cancer treatment. *Brain, Behavior, and Immunity*, 7(1)1:125–131, 2003.

[87] C. Marr and M.-T. Hütt. Topology regulates pattern formation capacity of binary cellular automata on graphs. *Physica A*, 345:641–662, 2005.

[88] M. A. Meredith, L. R. Keniston, L. R. Dehner, and H. R. Clemo. Crossmodal projections from somatosensory area SIV to the auditory field of the anterior ectosysvian sulcus (FAES) in cat: further evidence for subthreshold forms of multisensory processing. *Exp. Brain Res.*, 172:472–484, 2006.

[89] S. Milgram. The small world problem. *Psychol. Today*, 2:60–67, 1967.

[90] R. Milo, S. Shen-Orr, S. Itzkovitz, N. Kashtan, D. Chklovskii, and U. Alon. Network motifs: Simple building blocks of complex networks. *Science*, 298:824 – 827, 2002.

[91] M. Molloy and B. Reed. A critical point for random graphs with given degree sequence. *Random Structures and Algorithms*, 6(2-3):161–179, 1995.

[92] I. Morgado, editor. *Emoción y conocimiento.* Tusquets Editores, Barcelona, 2002.

[93] A. E. Motter, C. S. Zhou, and J. Kurths. Enhancing complex-network synchronization. *Europhys. Lett.*, 69:334–340, 2005.

[94] M. Müller-Linow and M.-T. Hütt. Topology regulates the distribution pattern of excitation in excitable dynamics on graphs. *Phys. Rev. E*, 74:016112, 2006.

[95] M. E. J. Newman. The structure and function of complex networks. *SIAM Review*, 45(2):167–256, 2003.

[96] M. E. J. Newman and M. Girvan. Finding and evaluating community structure in networks. *Phys. Rev. E*, 69:026113, 2004.

[97] M. E. J. Newman, S. H. Strogatz, and D. J. Watts. Random graphs with arbitrary degree distributions and their applications. *Phys. Rev. E*, 64:026118, 1972.

[98] T. Nishikawa, A. E. Motter, Y.-C. Lai, and F. C. Hoppensteadt. Heterogeneity in oscillator networks: Are smaller worlds easier to synchronize? *Phys. Rev. Lett.*, 91:014101, 2003.

[99] G. Palla, I. Derényi, I. Farkas, and T. Vicksek. Uncovering the overlapping structure of complex networks in nature and society. *Nature*, 435:814, 2005.

[100] A. Papoulis. *Probability, random variables and stochastic processes.* McGraw-Hill, New York, 3rd edition, 1991.

[101] R. E. Passingham, K. E. Stephan, and R. Kötter. The anatomical basis of functional localization in the cortex. *Nature Reviews*, 3:606, 2002.

[102] R. Pastor-Satorras, A. Vázquez, and A. Vespignani. Dynamical and correlation properties of the internet. *Phys. Rev. Lett.*, 87:258701, 2001.

[103] A. Peters and B. R. Payne. Numerical relationships between geniculocortical afferents and pyramidal cell modules in cat primary visual cortex. *Cereb. Cortex*, 3:69–78, 1993.

[104] A. Pikovsky, M. Rosenblum, and J. Kurths. *Synchronization: a universal concept in nonlinear science.* Cambridge nonlinear science series. Cambridge University Press, 2003.

[105] E. Ravasz and A.-L. Barabási. Hierarchical organization in complex networks. *Phys. Rev. E*, 67:026112, 2003.

[106] H. Rheingold. *Smart mobs: The next social revolution.* Perseus, Cambridge, MA, 2002.

[107] J. M. Roberts. Simple methods for simulating sociomatrices with given marginal totals. *Social Networks*, 22:273–283, 2000.

[108] L. C. Robertson. Binding, spatial attention and perceptrual awareness. *Nat. Reviews*, 4:93–102, 2003.

[109] K. S. Rockland and N. Ichinohe. Some thoughts on cortical minicolumns. *Exp Brain Res.*, 158:265–277, 2004.

[110] J. G. Röderer. On the concept of information and its role in nature. *Entropy*, 3:3–33, 2005.

[111] D. Rodney and M. Kevan. *The Synaptic Organization of the Brain*, chapter Neocortex, pages 459–509. 1991.

[112] P. R. Roelfsema, V. A. F. Lamme, and H. Spekreijse. Synchrony and covariation of firing rates in the primary visual cortex during contour grouping. *Nature. Neurosc.*, 7(9):982–991, 2004.

[113] A. Roxin, H. Riecke1, and S. A. Solla. Self-sustained activity in a small-world network of excitable neurons. *Phys. Rev. Lett.*, 92:198101, 2004.

[114] J. Ruan and W. Zhang. Identifying network communities with a high resolution. *Phys. Rev. E*, 77:016104, 2008.

[115] J. W. Scannell, C. Blakemore, and M. P. Young. Analysis of connectivity in the cat cerebral cortex. *J. Neurosci.*, 15(2):1463–1483, 1995.

[116] J. W. Scannell, G. A. P. C. Burns, C. C. Hilgetag, M. A. O'Neil, and M. P. Young. The connectional organization of the cortico-thalamic system of the cat. *Cereb. Cortex*, 9:277–299, 1999.

[117] J. W. Scannell and M. P. Young. The connectional organization of neural systems in the cat cerebral cortex. *Curr. Biol.*, 3(4):191–200, 1993.

[118] S. Seidman. Network structure and minimum degree. *Social Networks*, 5:269–287, 1983.

[119] C. E. Shannon. A mathematical theory of communication. *Bell System Tech. J.*, 27:379–423, 1948.

[120] S. S. Shen-Orr, R. Milo, S. Mangan, and U. Alon. Network motifs in the transcriptional regulation network of *escherichia coli*. *Nature Genetics*, 31:64 – 68, 2002.

[121] W. Singer. Consciousness and the binding problem. *Ann. N.Y. Acad. Sci.*, 929:123–146, 2001.

[122] W. Singer and C. M. Gray. Visual feature integration and the temporal correlation hypothesis. *Annu. Rev. Neurosc.*, 18:555–586, 1995.

[123] T. A. B. Snijders. Enumeration and simulation methods for 0-1 matrices with given marginals. *Psychometrika*, 56:397, 1991.

[124] R. Solomonoff and A. Rapoport. Connectivity of random networks. *Bull. Math. Biol.*, 13(2):107–117, 1951.

[125] O. Sporns. *Neuroscience databases*, chapter Graph theory methods for the analysis of neural connectivity patterns, pages 169–183. Kluwer Academic, Dordrecht, 2002.

[126] O. Sporns, G. Tononi, and G. M. Edelman. Theoretical neuroanatomy: Relating anatomical and functional connectivity in graphs and cortical connection matrices. *Cereb. Cortex*, 10:127–141, 2000.

[127] O. Sporns, G. Tononi, and R. Kötter. The human connectome: a structural description of the human brain. *PLoS Comput. Biol.*, 1(4):0245–0251, 2005.

[128] O. Sporns and G. M. Tononi. Classes of network connectivity and dynamics. *Complexity*, 7(1):28–38, 2001.

[129] O. Sporns and J. D. Zwi. The small world of the cerebral cortex. *Neuroinformatics*, 2:145–162, 2004.

[130] K. E. Stephan, L. Kamper, and et. al. Advance database methodology for the collation of connectivity data on the macaque brain. *Phil. Trans. R. Soc. London B*, 356:1159–1186, 2001.

[131] R. Steuer, J. Kurths, C. O. Daub, J. Weise, and J. Selbig. The mutual information: Detecting and evaluating dependencies between variables. *Bioinf.*, 18(2):231–240, 2002.

[132] S. H. Strogatz. *Nonlinear dynamics and chaos: with applications to physics, biology, chemistry, and engineering.* Westview Press, Cambridge, Mass, 2000.

[133] S. H. Strogatz. *Sync: the emerging science of spontaneous order.* Theia, New York, 2003.

[134] L. Tian, P. Kilgannon, and et al. Binding of t lymphocytes to hippocampal neurons through icam-5 (telencephalin) and characterization of its interaction with the leukocyte integrin cd11a / cd18. *Eur. J. Inmunol.*, 30(3):810–818, 2000.

[135] G. Tononi. An information integration theory of consciousness. *BMC Neurosc.*, 5:42, 2004.

[136] G. Tononi, G. M. Edelman, and O. Sporns. Complexity and coherency: integrating information in the brain. *Trends Cog. Sci.*, 2:12, 1998.

[137] G. Tononi, A. R. McIntosh, and et al. Functional clustering: identiying strongly interactive brain regions in neuroimaging data. *Neuroimage*, 7:133, 1998.

[138] G. Tononi and O. Sporns. A measure for brain complexity: relating functional segregation and integration in the nervous system. *Proc. Nat. Acad. Sci.*, 91:5033, 1994.

[139] G. Tononi, O. Sporns, and G. M. Edelman. A complexity measure for selective matching of signals by the brain. *Proc. Nat. Acad. Sci.*, 93:3422, 1996.

[140] J.-N. Tournier and A. Q. Hellmann. Neuro-immune connections: evidence for a neuro-immunological synapse. *Trends in Inmunol.*, 24(3):114–115, 2003.

[141] A. Trautmann and E. Vivier. Agrin–a bridge between the nervous and immune systems. *Science*, 292:1667–1668, 2001.

[142] J. Travers and S. Milgram. An experimental study of the small world problem. *Sociometry*, 32:425–443, 1969.

[143] L. Ungerleider and M. Mischkin. *Analysis of Visual Behavior*, chapter Two cortical visual systems. MIT Press, Cambridge, MA, 1982.

[144] M. Usher and N. Donnelly. Visual synchrony affects binding and segmentation in perception. *Nature*, 394:179–203, 1993.

[145] P. R. Villas-Boas, F. A. Rodrigues, G. Travieso, and L. da F. Costa. Border trees of complex netowrks. *J. Phys. A*, 41:224005, 2008.

[146] M. T. Wallace. The development of multisensory processes. *Cogn. Processes*, 5:69–83, 2004.

[147] S. Wasserman and K. Faust. *Social Network Analysis*. Cambridge University Press, Cambridge, 1994.

[148] D. J. Watts and S. H. Strogatz. Collective dynamics of 'small-world' networks. *Nature*, 393:440, 1998.

[149] J. G. White, E. Southgate, J. N. Thomson, and S. Brenner. The structure of the nervous system of the nematode *Caenorhabditis elegans*. *Phil. Trans. Roy. Soc. London B*, 314:1–340, 1986.

[150] X. Wu, B. Wang, T. Zhou, W. Wang, M. Zhao, and H. Yang. Synchronizability of highly clustered scale-free networks. *Chinese Phys. Lett.*, 23 (4):1046–1049, 2006.

[151] M. P. Young. Objective analysis of the topological organization of the primate cortical visual system. *Nature*, 358(6382):152–155, 1992.

[152] M. P. Young, C.-C. Hilgetag, and J. W. Scannell. On imputing function to strcuture from the behavioural effects of brain lesions. *Phil. Trans. R. Soc. Lond. B*, 355:147–161, 2000.

[153] G. Zamora-López, V. Zlatić, C. S. Zhou, H. Štefančić, and J. Kurths. Reciprocity of networks with degree correlations and arbitrary degree sequences. *Phys. Rev. E*, 77:016061, 2008.

[154] L. Zemanová, C. S. Zhou, and J. Kurths. Structural and functional clusters of complex brain networks. *Physica D*, 224:202–212, 2006.

[155] C. S. Zhou and J. Kurths. Hierarchical synchronization in networks of oscillators with heterogeneous degrees. *Chaos*, 16:015104, 2006.

[156] C. S. Zhou, A. E. Motter, and J. Kurths. Universality in the synchronization of weighted random networks. *Phys. Rev. Lett.*, 96:034101, 2006.

[157] C. S. Zhou, L. Zemanová, G. Zamora-López, C. C. Hilgetag, and J. Kurths. Hierarchical organization unveiled by functional connectivity in complex brain networks. *Phys. Rev. Lett.*, 97:238103, 2006.

[158] C. S. Zhou, L. Zemanová, G. Zamora-López, C. C. Hilgetag, and J. Kurths. Structure-function relationship in complex brain networks expressed by hierarchical synchronization. *New J. Phys.*, 9:178, 2007.

[159] V. Zlatić, G. Bianconi, A. Díaz-Guilera, D. Garlaschelli, F. Rao, and G. Caldarelli. On the rich-club effect in dense and weighted networks, 2008.